Multi-omics in Precision Medicine

Maria Murach
Pila, Poland

Bc. Poznan University of Technology, 2017
M.S. Poznan University of Technology, 2021
M.S. University of Virginia, 2022

A Dissertation presented to the Graduate Faculty of the
University of Virginia in Candidacy for the
Degree of Doctor of Philosophy

Department of Biochemistry & Molecular Genetics
University of Virginia
July, 2024

Abstract

Cardiovascular disease (CVD), including atherosclerosis, is a leading global cause of death. Atherosclerosis, characterized by plaque accumulation in arteries, can lead to myocardial infarctions (MI) or strokes. Imaging techniques like computed tomography angiography (CTA) are crucial for diagnosing and assessing the disease. The coronary artery calcification (CAC) score calculated from CTA images is a prognostic tool for atherosclerosis, with high scores correlating with increased risks of major adverse cardiovascular events (MACE) and all-cause mortality. Despite the emerging efforts and existing therapies, the residual risk and the onset of coronary events remains high.

Immune cells, including T cells and B cells, play complex roles in atherosclerosis and their precise function is dependent on the cell subtype. T cells in plaques can promote or inhibit disease progression, while B cells produce antibodies affecting lipid uptake and foam cell formation. Loss of TET2 in immune cells is linked to higher risk of CVD and hematological malignancies.

Precision medicine sought to better stratify patients and identify biomarkers that can help design therapies suitable for patients' individual profiles. Given the complex nature of the immune system and its role in the progression of atherosclerosis, the motivation for this work is to demonstrate how multi-omics can enhance our understanding of CVD and underlying genetic conditions, guiding the development of more precise and effective treatments

Here, I present a study, where we investigated TET2's role in regulating B1 cell numbers and functions. TET2 loss increased B cell subtypes in the peritoneal cavity, bone marrow, and spleen. B1a cells from TET2-KO mice showed fewer unique CDR3 sequences, indicating reduced antigen diversity. The TRUST4 algorithm enabled accurate detection of BCR and TCR repertoires from bulk RNASeq data, providing insights into immune cell receptor diversity.

In a pilot study, I analyzed phosphorylation states of effector molecules in IL-1β and IL-6 signaling pathways in patients with no CAC and high CAC. T cells were the primary immune cells activated by both cytokines. T regulatory cells showed lower phosphorylation of STAT5 in patients with high coronary calcification. Additionally, Subjects with high CAC showed a lower response to IL-1β and IL-6 stimulation, a phenomenon, to our knowledge, never reported before. The study provides interesting findings but is limited by sample size. Identifying specific T cell subpopulations responsive to IL-1β and IL-6 presents new research opportunities and potential therapeutic targets.

Understanding immune cell dynamics in atherosclerosis could improve disease prognosis and treatment response, aligning with precision medicine's goals. Further studies are needed to elucidate the biological significance of these findings and their clinical applications in managing cardiovascular disease.

Signatures

_____

Stefan Bekiranov, PhD

_____

Coleen McNamara, MD

_____

Ani Manichaikul, PhD

_____

Aakrosh Ratan, PhD

_____

Greg Medlock, PhD

Dedications

I dedicate this dissertation to 3 people.

First, to my Grandma Maria Polańska, who passed away in 2022 when I was a second-year PhD student. She was my greatest cheerleader and supporter, my best friend from the day I was born. Although born in rural Poland, without any financial means or educational infrastructure, struggling with Rheumatoid arthritis, she was the first person to get a college degree in our family. She received her master's degree in mathematics from Adam Mickiewicz University in Poland in 1962, 10 years before UVA started admitting female students. She was a woman of the sharpest mind I have ever seen, a natural wordsmith, and the kindest heart. She had a passion for education and rejected an offer to pursue a PhD to become a teacher. She strived to give her students the opportunities she didn't have. She patiently tried to answer all my questions and fed my craving for knowledge, for which I will always be thankful. I hope one day I learn to perceive the world the way she did. I know she would be proud.

Secondly, to my nephews, Józef and Jacek Murach, who both came to the world shortly before or during my PhD. I hope they remember that "impossible" is just a word. Godspeed.

Acknowledgments

"It takes a village to raise a child" – I believe it also applies to graduate students. I am incredibly lucky to have the best village around me.

First, I want to thank my advisor, Stefan Bekiranov. Thank you for opening the door of opportunities, for allowing me to be a part of many diverse projects that allowing me to learn from multiple people and multiple perspectives. Thank you for creating a highly collaborative environment that fostered multiple friendships that go beyond the lab. Thank you for your continuous support and confidence in me and sense of humor that kept me going through the grad school struggles. I greatly appreciate your passion for mathematics and ability to build a bridge between different fields, the skill to explain complex issues to scientist from different backgrounds, and your commitment to filling the gap between informatics and biology. But most importantly, thank you for giving me freedom to make my own mistakes and learn from them, the freedom to pursue research routes that were not always successful. "Keep cranking!"

I would like to thank Coleen McNamara, my unofficial second mentor. Thank you for giving me a chance to work with your group and experience the most inviting and warm lab atmosphere one can ever imagine. Thank you for including me in collaborations with great scientists across the world. I will forever be grateful for the opportunity to learn from you, to witness your incredible scientific and medical ethics, commitment to be the best researcher and supervisor, but most importantly, a good person. Although at times hard to hear, thank you for all the constructive criticism and making sure I was always on the right track. I guess it's the right time to confess that all the above reasons led me to create a well-deserved nickname for you, "the Queen", that evolved from Chantel's "the boss".

As my PhD path was not as straightforward as I expected, I would like to thank my two other PhD mentors, Greg Medlock and Sean Moore. Thank you for allowing me to be a part of your

groups, for fostering my ideas, for all the advice and the chance to get my hands dirty in the lab without any prior experience. If not for the hands-on experience, I would never be a bioinformatician I am today.

Thank you to my thesis committee, Ani Manichaikul, Aakrosh Ratan, Greg Medlock, Coleen McNamara and Stefan Bekiranov. Thank you for the thoughtful insights and the encouragement to leave my comfort zone.

The first thing you hear when you join a PhD program is that you need to find mentors outside of your lab, as they bring new perspectives and new points of view. I was again incredibly lucky to encounter the best bonus mentors I could ever ask for. Special thanks to Ani Manichaikul, Casey Hoffman, Carrie Cowardin and Jessica Allen for all their words of scientific (and life) wisdom, support and advice, a push when I needed it.

Thank you to my lab village, Antony, Brett, Cassidy, Chantel, Christine, Corey, Emily, Jesse, Katie, Megan, Melissa, Micah, Myles, Patrick, Sydney, Vicky for being perfect lab mates. Thank you for giving me the reasons to laugh until I couldn't breathe anymore, thank you for always having time for me, thank you for all the life and research support, thank you for making the lab feel like home. Thank you for all the outside lab shenanigans. Thank you for appreciating my love for animals and letting me hang out with your puppies (Beckett and Gracie) to ease my nerves. Thank you for your friendship, which goes way beyond graduate school. Special thanks to Corey and Myles, as we spent endless hours in our little cubicles and talked about anything and everything.

Thank you to ALL my graduate school friends and other friends I made along the way. You all made the grad school a blast and made sure I was busy and happy outside of the lab. But special thank you for my three Charlottesville best friends, Iza, Ola, Patryk, for being there for me through all the good and all the bad. Thank you to my best polish community, Jeremi, Ola, Kasia, Marysia, Alek, Daria and Michał for being my family. To my friends in Poland, thank you for your commitment to keeping our friendships alive even through video chats. Special thank you to my

best friend of 15 years, Monika, for being the sister I never had, her parents, Magda and Piotr, for being my second family, and Marysia, for being my true friend, believing in me and constant support for 13 years and counting.

I was extremely privileged to be born into a family where education was always a priority. I wouldn't be who I am and where I am without you. Thank you to my grandma, Maria, whom I dedicate this thesis, for paving the way. To my brother, Jan, his wife, Ola and their sons, Józef and Jacek, for their friendship, support and confidence in me. Special mention for my fury friend Rudi, who undoubtedly helped me through the pandemic. To my extended family, especially my aunt Ewa, her husband and sons, for never making me feel left out even though I live on the other side of the world. Dziękuję.

And most importantly, thank you to my parents, Alina and Adam, for all their support in EVERY way possible from across the ocean. For their continuous readiness to help, endless hours spent on the phone with me, unconditional love and all the plane tickets home. For supporting all my ideas, even when I wanted to quit and open a bakery. For making sure home always feels like home, no matter how far away I am. Dziękuję.

Attributions

The work presented in this dissertation is an outcome of the collaborative efforts of multiple individuals. Additionally, much of the text is adapted from published work. Here I highlight the major contributions of other scientists to the work presented in this dissertation and the relevant publications.

Chapter 2

This chapter is based on work described in the following publication:

> Dennis Emily*, **Maria Murach*,** Cassidy M.R. Blackburn, Melissa Marshall, Katherine Root, Tanyaporn Pattarabanjird, Justine Deroissart, et al. "Loss of TET2 Increases B-1 Cell Number and IgM Production While Limiting CDR3 Diversity." Frontiers in Immunology 15 (2024).
>
> https://www.frontiersin.org/journals/immunology/articles/10.3389/fimmu.2024.1380641.
>
> *authors contributed equally
>
>

The study was conceptualized and designed by Coleen McNamara and Emily Dennis. The analysis and visualization of RNASeq data as well as data curation was led by me and Stefan Bekiranov. The main contributors to the individual elements are listed in the methods section of Chapter 2. I, Emily Dennis and Maria Murach wrote the publication with contributions from the rest of the authors. I and Emily Dennis made the figures and tables presented in this chapter, and those created by Emily Dennis have attributions stated in the figure/table legends.

Chapter 3

This chapter is based on work of following authors:

Jesse Cochran, † James McParland, † **Maria Murach,**† Chantel McSkimming, Hema Kothari, Christine Flora, Antony Haider, Corey Williams, Brett Ransegnola, Nisha Hosadurg, Toral Patel, Todd Villines, Angela Taylor, Stefan Bekiranov, Coleen McNamara

†authors contributed equally

J.M. and C.M. designed experiments. J.M., J.C, C. McSkimming, and A.H. conducted experiments. C.F. collected and compiled clinical data. M.M., B.R., C.W., and J.C. analyzed data. M.M. and J.C. generated figures. T.C.V, N.H. and T.P. performed the cardiac CT interpretations. H.K., A.T., and S.B. provided advice and technical support for the overall study. M.M., J.M., J.C., and C. McNamara wrote the manuscript. T.C.V., N.H., T.P, C.W., and S.B. edited the manuscript. McNamara acquired funding to support this research.

Contents

List of figures

List of tables

Chapter 1

Introduction

1.1 Precision Medicine

1.1.1 Defining precision medicine

Despite extensive global efforts to deliver novel therapies to all patients in need, the design of a universal therapy for everyone remains a challenge. This issue led to the creation of the medical notion of precision medicine, which is defined as P4 medicine - participatory, personalized, predictive, and preventative medicine (Hood & Friend, 2011). Precision medicine is targeted at individual patients, aiming to optimize drugs, therapies, and diagnostics to deliver the best results

Figure 1.1 Precision medicine model is as venn diagram made up of the person(s), markers, exposome and behavioral health.
Figure and caption from UC Davis Health.

in the treatment of various diseases. It integrates behavioral health, environmental exposures, personal medical profile, and assessment of known disease markers to tailor the therapy to individual patient's needs, as presented in Figure 1.1. Integration of exposome (environmental influences), behavioral health, specific markers, and knowledge about an individual can increase the chances of choosing medical care that's most likely to be effective. Stratifying patients based on their medical profiles, as seen in clinical trials, can help identify populations that would benefit the most from treatments, leading to more efficient health care. Furthermore, investigating unresponsive populations and researching candidate factors responsible for treatment failure can result in identifying new drug targets and novel insights into disease pathogenesis (Svensson et al., 2022).

1.1.2 Precision medicine in the clinic

The value of personalized approaches was recognized early in the cancer field. In 2005, *Piccart-Gebhart et al.* reported that Trastuzumab and Chemotherapy improve disease-free survival, specifically in patients with HER2-positive breast cancer. Another mutation influencing treatment choices in breast cancer is BRCA1/2 (Quek & Mardekian, 2019) and EGFR in lung cancer (Chu, 2014). All these findings are now standard-of-care practices in oncology when choosing therapies for cancer patients.

Several clinical trials have demonstrated the need to understand patient populations better. One example is the CANTOS trial (Libby, 2017; Ridker et al., 2018) , where Canakinumab was administered to patients with a history of myocardial infarctions (MI) and elevated high-sensitivity C-reactive protein (hs-CRP) levels to assess whether reducing inflammation could lower cardiovascular event incidence. Only 25% of patients responded to the tested medication. The post-trial stratification of patients reported variation in patients' response to the drug based on the

baseline levels of inflammation markers other than hs-CRP. The re-analysis of the trial's results and efforts to uncover genetic and molecular factors enabling differentiation between responsive and not responsive groups are hoped to reveal more detail into the biology of the disease and the drug's mechanism of action and its effects on studied patients (Ridker et al., 2017, 2018).

Currently, the efforts focus on individual's genetic, epigenetic, proteomic, and demographic factors that can determine the efficacy of medical interventions (Auffray et al., 2010). The inclusion of additional tests, as well as reanalyzing the data from published clinical trials, provide deeper insights into patient populations and their diversity. The high costs of diagnostic tools for determining individual medical profiles limit the clinical feasibility of many approaches. There is an ongoing need for more affordable solutions, together with integrating large datasets with artificial intelligence and machine learning, to predict individual treatment needs with greater accuracy.

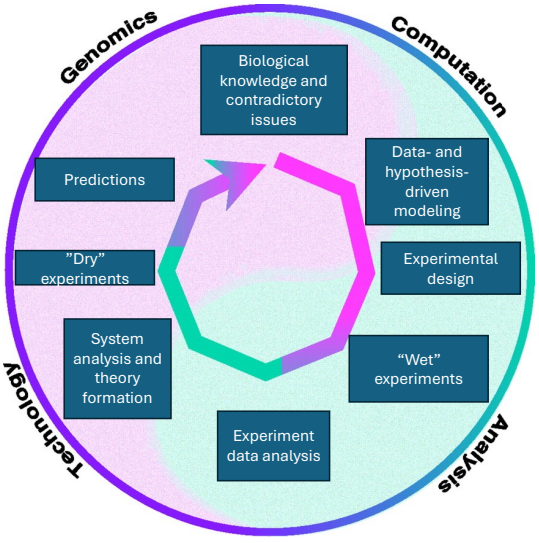

Figure 1.2 The cycle of basic research
The cycle begins at the hypotheses, experiments in the laboratory to data simulation and complex data analysis and finally to predictions.

Figure adapted from (Kitano 2002)

1.1.3 Basic research and precision medicine

Precision medicine focuses on delivering the most effective health care to patients in the clinic, but it all begins in research laboratories. As depicted in

Figure 1.2, every finding begins with hypotheses followed by experiments in the laboratory, complex data analysis, integration with current knowledge on the topic, and finally, predictions that can be useful in the clinic. Basic science influences medicine in many forms: from model studies in animal models to discovering the mechanisms of the disease, analyzing large-scale datasets and identifying hypotheses-generating patterns (Hulsen et al., 2019), detecting genetic variants influencing drug metabolism and efficacy (Ahmed et al., 2016), creating computational models to predict disease progression (Gardiner et al., 2022), through data-driven machine-based

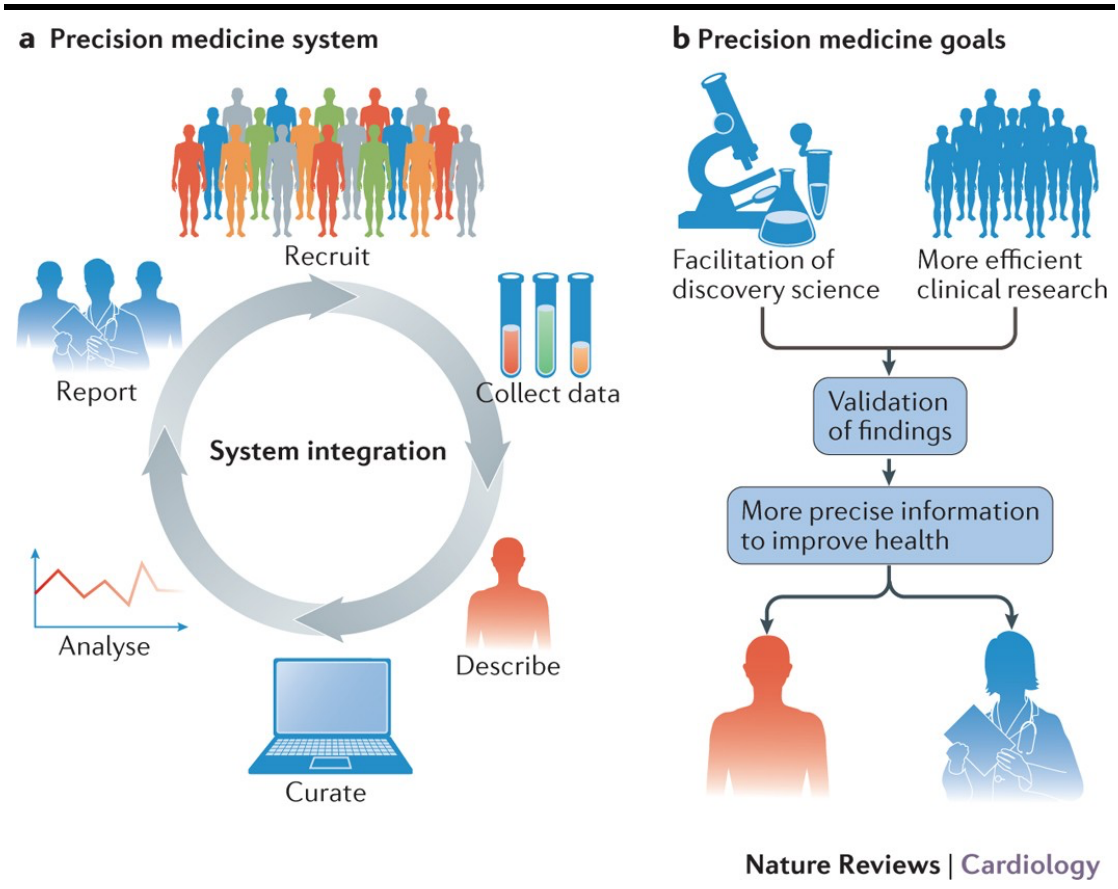

Figure 1.3 Essential features and goals of a precision medicine system.
Figure adapted from (Antman and Loscalzo 2016)

diagnostic tools (Kale Satish & Shinde Sandeep, 2023). Translational science laid the foundation for novel therapies and diagnostic tests in many diseases, including Alzheimer's, Inflammatory bowel disease, epilepsy, pulmonary arterial hypertension, and many more (Forloni, 2020; Gardiner et al., 2022; Kelly & Chan, 2022; Nabbout & Kuchenbuch, 2020).

By leveraging the newest findings in genomic, bioinformatic, molecular biology, and proteomics, we can tailor medical care to match patients' genetic and molecular profiles to ensure the most effective treatments. Figure 1.3a-b presents how collecting detailed patient data, their standardization and reanalysis, and the integration of novel scientific findings can benefit medical care. The collection and proper curation of medical information can be valuable in the future when validation of new discoveries is needed. With an emerging understanding of the biological basics of many diseases and constantly evolving research technologies, the relationship between research laboratories and medical clinics strengthens, offering hope for future medical interventions tailored to each patient's needs.

1.2 Introduction to multi-omics

1.2.1 Multi-omics

Considering the growing number of complex datasets spanning all types of hierarchical biological and medical data, there's a need for systemized approaches to accelerate the analysis without compromising its quality. Multi-omics refers to the integrated analysis of multiple 'omes,' such as the genome, proteome, transcriptome, and metabolome, to provide a comprehensive view of biological processes. Computational biology, which includes multi-omics, leverages large-scale biological data to explore the relationships between molecules in different disease contexts. It focuses on studying biological systems as opposed to studying their individual components.

Computational biology utilizes advanced computational methods to answer biological questions.

Recent advances in high-throughput technologies in genomics and proteomics have enabled the integration of biological data from multiple sources to uncover pathways involved in pathogenesis and homeostasis (Kidd et al., 2014). Efforts to uncover the dynamics of biological interactions and cell crosstalk can enhance our understanding of how diseases impact human bodies.

Figure 1.2 illustrates the research cycle from the laboratory experiments that utilize biological samples and novel technologies to data analysis and the expansion of current knowledge. Results from these experiments can be used to create computational models that drive hypothesis generation and support system analysis.

A deeper understanding of molecular complexities and regulatory networks offers hope for uncovering mechanisms of regulation and biological interaction that, after experimental confirmation, could be leveraged as novel potential drug targets. These insights could also form the

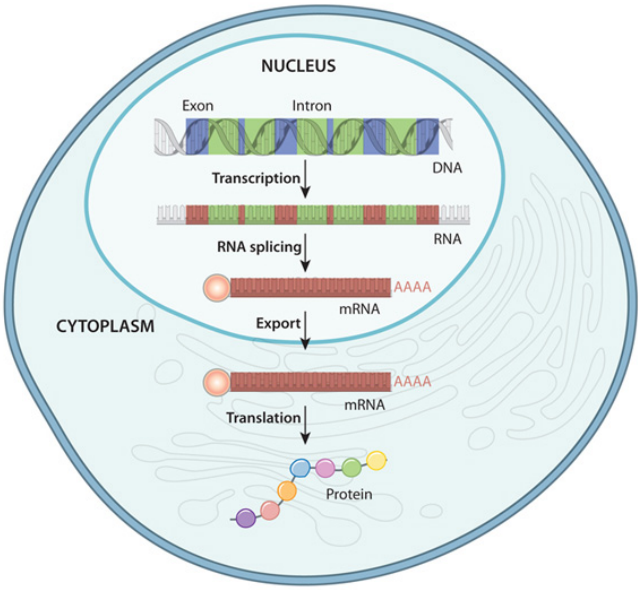

Figure 1.4 An overview of the flow of information from DNA to protein in a eukaryote
First, both coding and noncoding regions of DNA are transcribed into mRNA. Some regions are removed (introns) during initial mRNA processing. The remaining exons are then spliced together, and the spliced mRNA molecule (red) is prepared for export out of the nucleus through addition of an endcap (sphere) and a polyA tail. Once in the cytoplasm, the mRNA can be used to construct a protein. Figure and caption from Nature Education.

basis for diagnostic tools to potentially detect diseases before the onset of symptoms.

1.2.2 The Central Dogma of Molecular Biology

DNA encodes information that directs cell function and protein expression. Together with transcriptional and translational regulators, DNA dictates which genes will be expressed, and which proteins will be synthesized. These proteins perform essential cellular functions such as molecule transport, cell signaling, and maintaining cellular structure.

Figure 1.4 presents a central dogma of molecular biology, where DNA is transcribed into RNA, which is then translated into proteins. Genes are coded in DNA by a set of sequences (exons) that will be a part of the mature mRNA (messenger RNA) and by introns which will be removed from the mature mRNA sequence. Transcription, the process responsible for creating mRNA, a molecule encoding a “recipe” for protein synthesis, begins with the binding of RNA polymerase to the promoter sequence present almost always at the 5’ end of the DNA. RNA splicing is the process responsible for connecting exons and further modification before the RNA is ready to leave the nucleus to be later translated into proteins. Proteins are functional molecules that participate in multiple cellular processes such as replication and DNA transcription, secretion of other proteins, cell division, metabolism, transport, and cellular and intercellular signaling.

1.2.3 Transcriptomics

Measuring mRNA levels is a tool to estimate the degree to which genes are expressed. The gene expression landscape reveals cell states in tissues, making it a powerful tool for studying diseases. Comparing gene expression levels between healthy and diseased tissues can identify

differentially expressed genes (DEGs). Further analysis of DEGs can reveal affected cell functions and pathways involved in the disease state.

Methods like qPCR and expression microarrays can be used to determine mRNA levels. Yet, they are usually targeted at specific gene subsets and cannot provide a full gene expression profile of a sample, providing a biased measurement (San Segundo-Val & Sanz-Lozano, 2016). With the development of high-throughput sequencing methods, it's now possible to sequence RNA at low costs, at high resolution, and high capacity (Stark et al., 2019).

Figure 1.5 depicts the flow of a sequencing experiment. The process usually begins with isolating RNA from the tissue of interest, followed by reverse transcription of RNA to cDNA (coding DNA), ligation of adapters, and PCR amplification of the cDNA. Then samples are sequenced using short-read instruments like Illumina or long-read technologies like PacBio or OxfordNanopore. The choice of short- or long-read technology depends on the study context. The short reads generally provide more accurate readings, while long-reads better capture repeated sequences, a known short-read caveat.

The processing of sequencing reads which are the output of the sequencers begins with mapping to reference genome using tools like STAR (Dobin et al., 2013), bowtie (Langmead et al., 2009) , or BWA (H. Li & Durbin, 2009). Subsequently, the reads mapped to the genes are quantified for each sample using tools like featureCounts (Liao et al., 2014) , and the number of reads mapped to a gene reflects the level at which the gene is expressed. To assess the differences in gene expression between samples (differential expression), read counts are analyzed using DESeq2 (Love et al., 2014) or edgeR (Robinson et al., 2010). After filtering and normalization to exclude outliers and adjust for different levels of expression between genes, a more direct comparison between conditions can be performed. The output of the differential expression analysis consists of a list of genes log2(fold change) of counts between analyzed conditions and p-value to assess the significance of the observed difference.

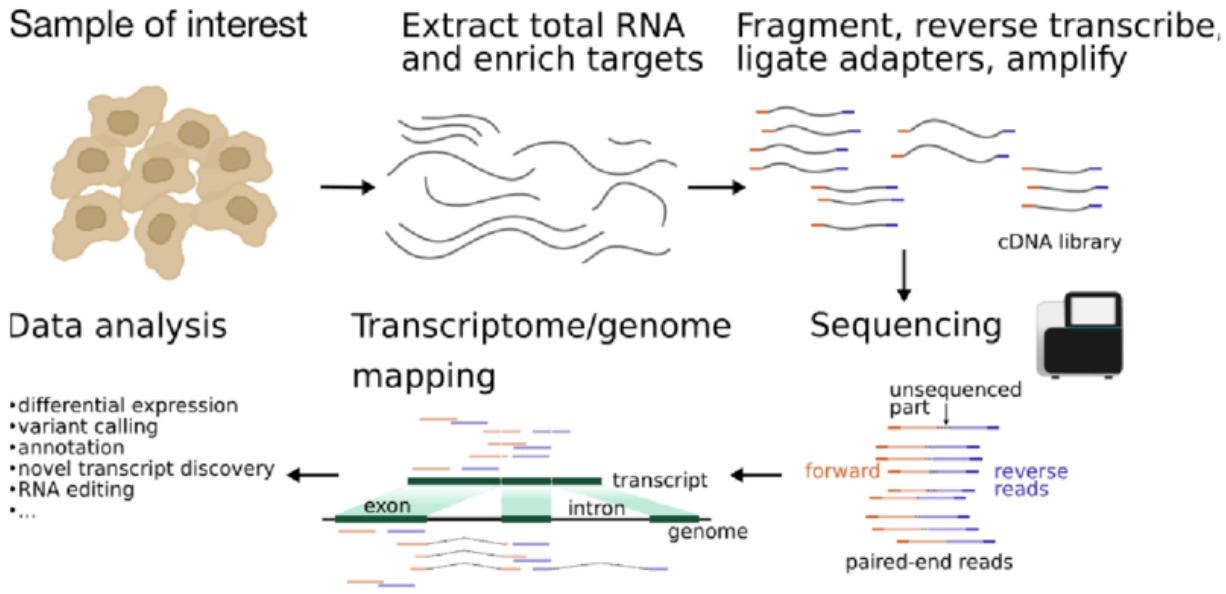

Figure 1.5 The flow of a sequencing experiment.
Each sequencing experiment consists of sample collection, extraction of RNA from the sample, fragmenting of the RNA, reverse transcription to cDNA, adapter ligation, amplification, sequencing and then following bioinformatics analysis of the resulting sequencing reads.

The list of differentially expressed genes between the conditions can be then subjected to pathway analysis tools like gene ontology (GO) enrichment analysis which is based on hypergeometric testing (Thomas et al., 2022), Metascape (Zhou et al., 2019), or Gene set enrichment analysis (GSEA), which uses enrichment score on a ranked list of genes (Subramanian et al., 2005). The output of the analysis is a set of molecular, functional, or signaling pathways containing the differentially expressed genes. Understanding the processes involving differentially expressed genes gives a broader view of the potential cellular changes induced by the analyzed condition. Enriched pathways can also guide research in directions not covered by the initial hypotheses, allowing for the exploration of alternative and novel hypotheses, highlighting the strength of the unbiased nature of RNASeq compared to other methods measuring mRNA levels.

1.2.4 Proteomics

To understand cellular function and changes beyond transcription, scientists have developed approaches to quantify and identify proteins in various samples. Although both proteomics and transcriptomics are used to identify cell types in single-cell technologies, recent studies have shown that the correlation between RNA and protein expression is highly variable and rarely high for some cells, such as immune cells. This demonstrates the superiority of using protein expression assays for cell type annotation and measuring functional protein levels as opposed to mRNA (Franks et al., 2017; Y. Liu et al., 2016; Prabahar et al., 2024; Raj & Oudenaarden, 2008; Reimegård et al., 2021; Specht et al., 2021).

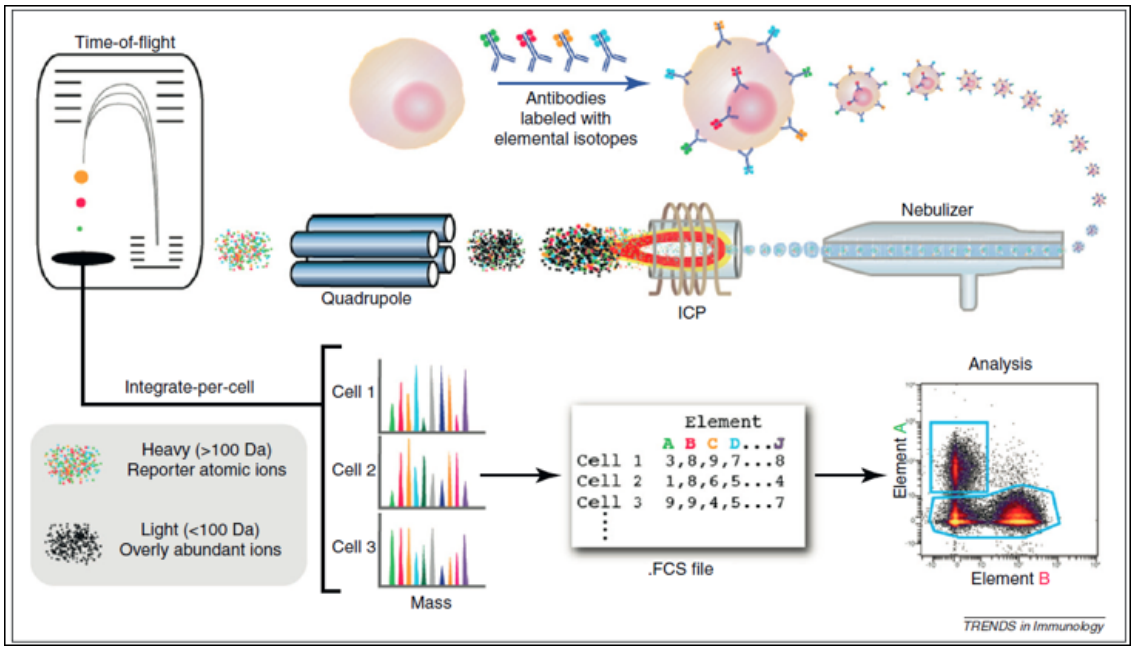

Figure 1.6 The CyTOF process, from Bendall et al. (2012).
Mass cytometry allows single-cell atomic mass spectrometry of heavy elemental (>100 Da) reporters. Schematic of ICP-MS-based analysis of cellular markers. An affinity product (e.g. antibody) tagged with a specific element binds to the cellular epitope. The cell is introduced into the ICP by droplet nebulization. Each cell is atomized, ionized, overly abundant ions removed, and the elemental composition of remaining heavy elements (reporters) is determined. Signals corresponding to each elemental tag are then correlated with the presence of the respective marker and analyzed using conventional cytometry platforms. (Figure and caption from Sean C. Bendall et al. 2012)

Common methods used to study proteins include Mass Spectrometry (MS), Two-Dimensional Gel Electrophoresis (2-DE), and protein microarrays. In recent years, several single-cell-based approaches emerged, allowing for the identification of protein landscapes at single-cell resolution. Flow Cytometry (FC) and Mass Cytometry, also known as Cytometry by Time-of-Flight (CyTOF), are two antibody-based methods. They detect surface and internal proteins by using antibodies tagged with either fluorophores (FC) or metals (CyTOF) to bind target proteins, followed by analysis of their intensities or masses on a cell-to-cell basis (Spitzer & Nolan, 2016).

The typical CyTOF experiment begins with the staining of cells with antibodies that are conjugated to metal isotopes. Next, the cells are fixed to ensure intact cell structure and permeabilized to allow for intracellular penetration by antibodies. Then, inside the cyTOF experiment, samples are nebulized, ionized, and accelerated to allow for later detection and quantification of the metal isotopes. Then, the output .fcs files need to be processed, normalized, and debarcoded using tools like bead-normalization (Finck et al., 2013) and single-cell-debarcoder (Zunder et al., 2015). There is a substantial number of programs and libraries available for the analysis of cyTOF data including Flowsom (Van Gassen et al., 2015), CATALYST (Nowicka et al., 2019), and cyCombine (Pedersen et al., 2022).

The process usually consists of:

- **Normalization:** Adjusting the data to account for technical variations and ensuring comparability across samples.
- **Batch Correction:** Correcting for differences that arise from processing samples in different batches, thus minimizing batch effects.
- **Clustering:** Grouping cells with similar protein expression profiles to identify distinct cell populations.
- **Dimensionality Reduction:** Reducing the complexity of the data while retaining essential information, often using techniques like t-SNE (t-distributed stochastic neighbor

embedding) or UMAP (Uniform Manifold Approximation and Projection).

- **Cell Type Annotation:** Assigning labels to cell clusters based on known markers or protein expression patterns to identify cell types.
- **Quantification and Differential Analysis Between Conditions:** Measuring protein levels across different conditions and identifying significant changes to understand the effects of experimental treatments or disease states.

Assessing the differences in protein levels between different conditions gives a broad view of the influence of analyzed conditions on cellular state and function. It also allows for the assessment of the tissue state by assessing the frequencies of different cell types based on their surface marker expression. Other single cell methods, like CITEseq and REAPseq, allow for simultaneously measuring both protein levels and mRNA levels (Peterson et al., 2017; Stoeckius et al., 2017). However, their inability to stain intracellular proteins, inability to sequence a full transcriptome, and very high cost are a limiting factor in many studies.

1.2.5 Multi-omics in Precision Medicine

Both transcriptomics and proteomics are used in clinical research to gain more insight into patients' characteristics, laying the ground for a better understanding of differences between people. Multi-omics data provides an invaluable asset to get a detailed inside into disease and its characteristics in individual patients (Sethi et al., 2023). Those data types and advanced data analysis approaches differ from standard clinical testing (Sohag et al., 2021). Their extensive utilization, including artificial intelligence, as seen in Figure 1.7, could identify patients at higher risk, capture the disease onset early, or inform about various genetic predispositions for the disease.

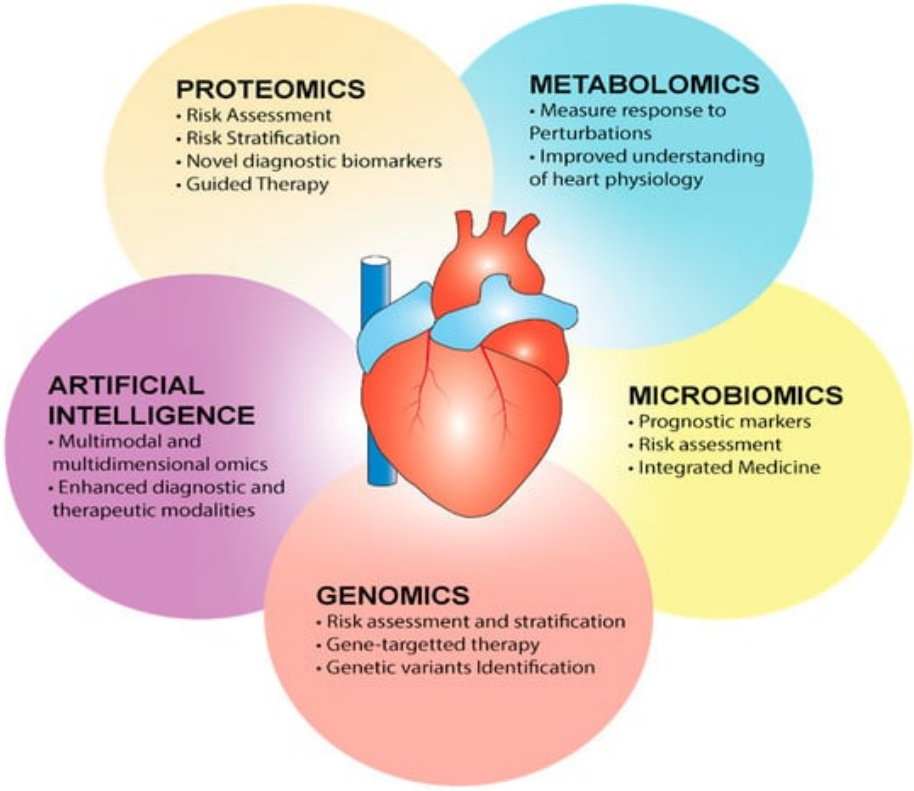

Figure 1.7 Domains of precision medicine in cardiology.
Figure and caption from (Sethi et al., 2023)

1.3 Cardiovascular Disease

1.3.1 Atherosclerosis as an inflammatory disease

Heart disease remains the leading cause of death in the United States killing 610,000 people every year (1 in 4 deaths)(Figure 1.8). Atherosclerosis or coronary artery disease (CAD) is a major form of heart disease causing 370,000 deaths in the US yearly (Pahwa & Jialal, 2024). The disease is caused by the accumulation of plaques inside arteries, limiting the amount of oxygen passed to the heart. These plaques, consisting of lipids, smooth muscle cells, and immune cells, induce an

inflammatory response and when ruptured can form a thrombus causing myocardial infractions (MI) or strokes (Bentzon et al., 2014).

The risk of developing atherosclerosis is influenced by many genetic, environmental, and lifestyle factors like age, sex, high cholesterol, diet, hypertension, diabetes, obesity, physical inactivity, and tobacco usage.

There are several stages of atherosclerotic plaque development (Bentzon et al., 2014). Plaques form when the intima (innermost layer of the artery) thickens and changes in gene expression and endothelial turnover occur (Figure 1.9 A). Next, accumulating low density lipids (LDLs) and their oxidized forms induce the innate and adaptive immune response. Endothelial cells begin to express genes inducing monocytes to differentiate into macrophages (adhesion molecules, chemoattractants, and macrophage colony-stimulating growth factors) (Figure 1.9B). LDL binds to proteoglycans present on the intima, and with time, endothelium starts to express more of the lipoprotein-binding proteins causing further retention of the LDLs in plaques. Then, extracellular lipid pools form inside the intima (Figure 1.9 C). Macrophages recruited to plaque sites express more proinflammatory cytokines and accumulate oxidized LDL due to dysregulated lipid metabolism, leading to foam cell formation. Note that smooth muscle cells (SMCs) and dendritic cells (DCs) can also accumulate lipids and form foam cells (Bentzon et al., 2014; Clarke & Bennett, 2009; Moore & Tabas, 2011).

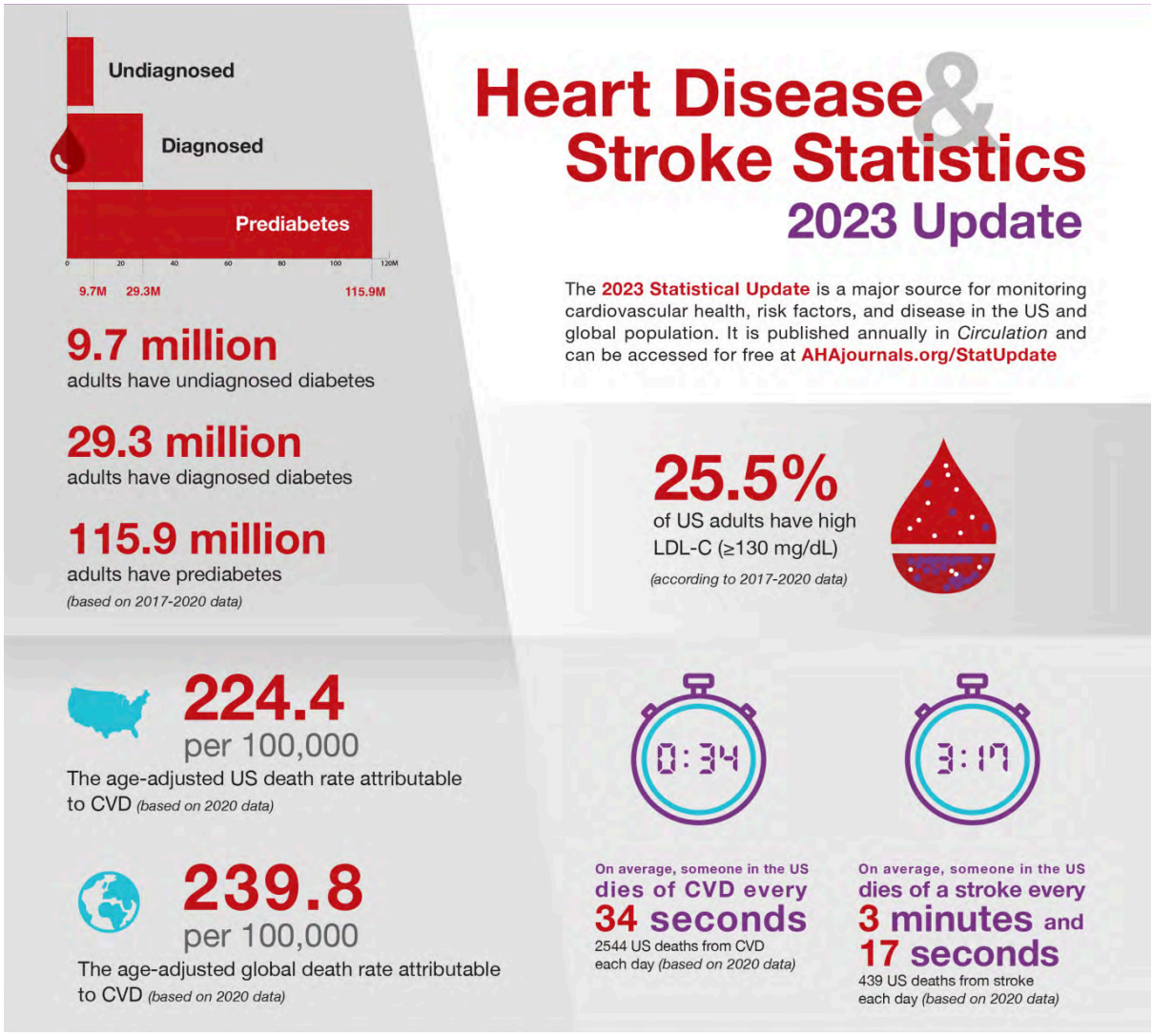

Figure 1.8 Heart disease & Stroke Statistics by American Heart Association
Heart disease remains the leading cause of death in the United States causing 224.4 per 100 000 deaths. Figure and caption from American Heart Association (Tsao et al. 2023).

The next stage of the development of atherosclerotic plaques is a formation of a necrotic core. The accumulation of lipids inside the intima causes the thickening of the tissue. The invasion of the macrophages disrupts the intima with the presence of cell debris, causing lipid pools to grow into a necrotic core (Figure 1.9D). Another cause of the formation of necrotic core is apoptosis and necrosis of foam cells and SMCs. The presence of lipid pools, apoptotic macrophages, and SMCs

at the margin of the necrotic core becomes detectable simultaneously and suggests an impaired efferocytosis inside the plaques (Schrijvers et al., 2005; Tabas, 2010). Neovessels can grow into the lesions allowing for subsequent intra-plaque bleeding, triggering further inflammatory response (Kolodgie Frank D. et al., 2003; Kumamoto et al., 1995). With time, the tissue inside the plaque loses the properties of a normal arterial intima and becomes rich in collagen forming a fibrous cap. Atherosclerotic lesions can also calcify with age and those calcifications can take up the whole volume of the plaque (Figure 1.9E).(Kragel et al., 1989). The autopsies of patients after thrombi events suggested that the thinning of the fibrous cap could be associated with plaque rupture (Burke Allen P. et al., 1997), indicating that high calcification may suggest greater stability.

The presence of those plaques can obstruct the flow of blood in the arteries (Bentzon et al., 2014). The rapture of an atherosclerotic lesion can cause thrombosis and subsequent myocardial infractions (MI) or strokes. The efficacy of statin treatments in patients with atherosclerosis implies that the inflammatory response is at least partially triggered by the lipid burden.

While the pathogenesis of atherosclerosis remains a complex issue, treatments are needed to address different stages of disease development to ensure the ability to target all patients in need.

1.3.2 Imaging of atherosclerotic plaques

The most common way of diagnosing atherosclerosis or assessing the progression of the disease is imaging. Various imaging methods allow for the detection of stenosis, measuring the plaque burden and the extent of their calcification, and identification of necrotic core and segments with arterial remodeling. Two commonly used methods include Intravascular ultrasound (IVUS) and Computed tomography angiography (CTA) (Guimarães et al., 2024; Owen et al., 2011). Using a dedicated catheter with ultrasound-based technology, IVUS delivers cross-sectional images from the inside of the artery, providing a 360-degree view of the vessel. Yet, the application of IVUS is

invasive and associated with low but nonnegligible risk which is higher in patients with advanced disease (Hausmann et al., 1995). The complications include dissection, perforation, arrhythmia, thrombosis, and vasospasm. In this work, I will focus on CTA.

Compared to IVUS, CTA assesses the vessel areas accurately and provide quality images of arteries to diagnose CAD (M. Kruk et al., 2014, Budoff et al., 2008; Khamis, 2016). CTA made its way into the clinic in 1995 and has since become a standard of care procedure in many medical facilities. The National Institute for Health and Care Excellence recommends using CTA as an

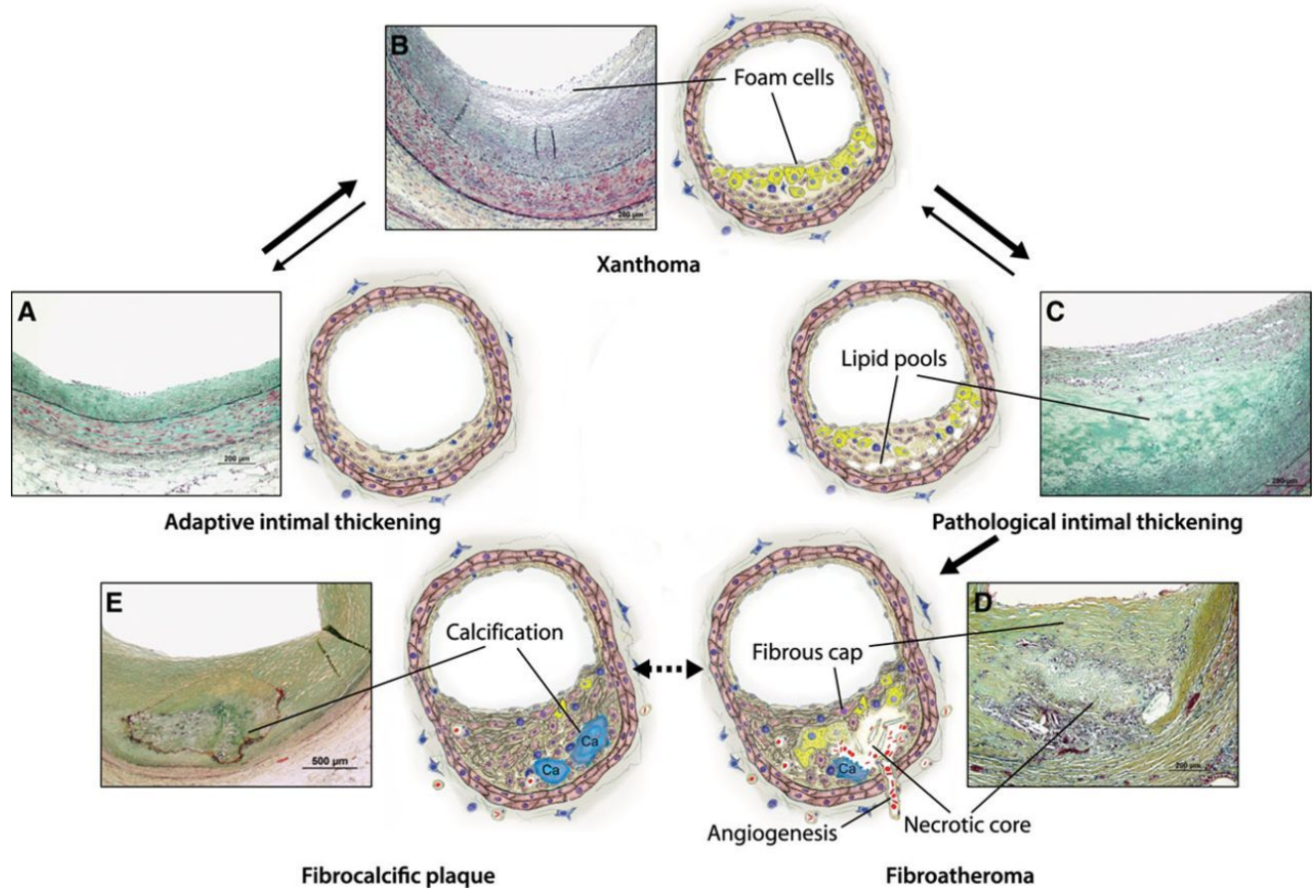

Figure 1.9 Stages of plaque development

A, Adaptive intimal thickening characterized by smooth muscle cell accumulation within the intima. **B**, Intimal xanthoma corresponding to the accumulation of foam cell macrophages within the intima. Pathological intimal thickening in **C** denotes the accumulation of extracellular lipid pools in the absence of apparent necrosis. **D**, Fibroatheroma indicating the presence of a necrotic core. The necrotic core and surrounding tissue may eventually be calcified, which forms fibrocalcific plaque shown in **E**. Because some of the advanced lesion types (fibroatheromas and fibrocalcific plaques) evolve simultaneously in life, their interrelationships are difficult to resolve in autopsy studies. (Figure and caption from Bentzon et al. 2014)

initial test if patients present with stable chest pain with no prior history of CAD (Timmis & Roobottom, 2017). Figure 1.10 presents different stages of atherosclerosis and plaque burden detected by CTA and the associated risk. The technique requires intravenous contrast administration, and to obtain diastolic images, the subject needs to hold their breath for approximately 10 seconds. The total duration of the procedure is about 15 minutes, and it delivers complete, 2 or 3-dimensional images of the heart and surrounding arteries (Budoff et al., 2006, 2022). Furthermore, the radiation dose emitted during the examination by computed tomography can be as low as 1mSv, which is significantly lower than other techniques for the imaging of coronary arteries (Budoff et al., 2022; Hausleiter et al., 2009; Trattner et al., 2018).

1.3.3 Coronary Artery Calcification

Studies have shown that plaque characteristics like plaque number and extent, location, and composition can be used as prognostics and have been associated with clinical outcomes in extensive cohort studies (Armin Imhof et al., 2015; Ayoub et al., 2017, 2017; Motoyama et al., 2015; van Werkhoven et al., 2009). Coronary artery calcification (CAC) score is a method to quantify the amount of calcified plaque burden in coronary arteries (Mohlenkamp et al., 2011) (Agatston et al., 1990). CAC is quantified based on the density of the calcified tissue multiplied by the lesion area and then summed across regions. This score was established in 1990 and has been widely used in clinics since then. CAC score value of 0 means no calcified plaque detected (low risk of CAD), 1-10 means calcium was detected in minimal levels (risk of CAD less than 10%), 11-100 means mild levels of calcified plaques were detected, 101-300 means moderate levels of calcium were detected and corresponded to moderate risk of CVD events and score of 300 and higher corresponds to extensive levels of plaques and high risk of CVD events.

Multiple studies investigated the score's prognostic value. High CAC was also associated with a higher risk of MACE (Biavati et al., 2024, Budoff et al., 2023) and all-cause mortality (Mohlenkamp et al., 2011). Interestingly, in subjects with no CAC, hs-CRP (high-sensitivity C-

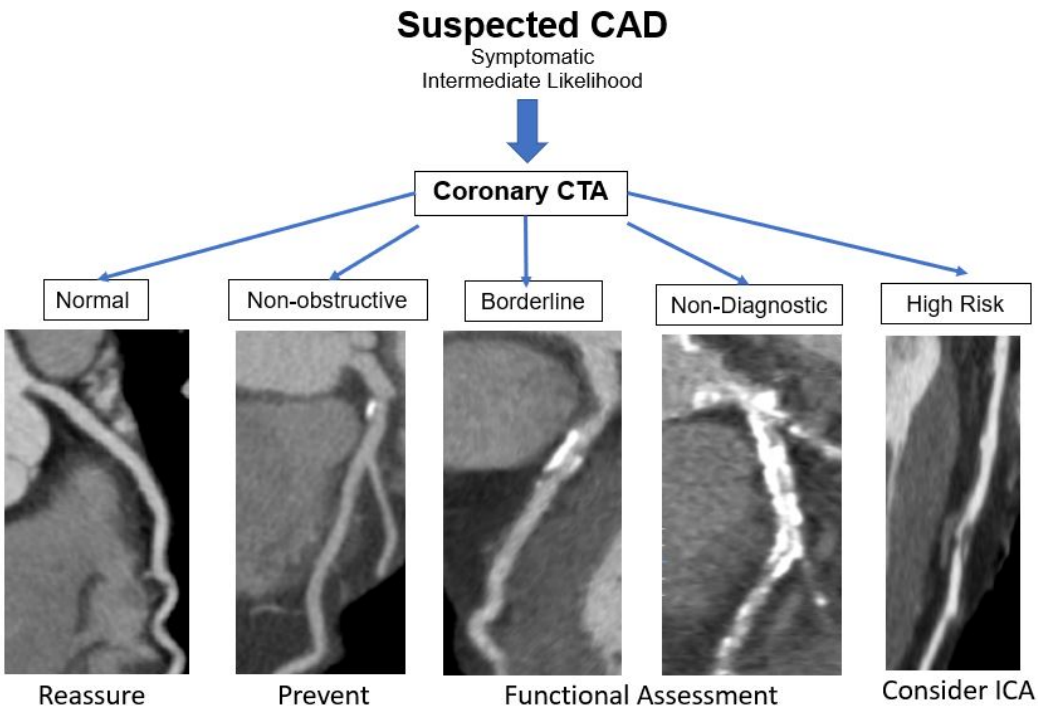

Figure 1.10 Coronary CTA approach to diagnosis and management of CAD in symptomatic patients with an intermediate pre-test likelihood of CAD.
(Figure and caption from *Anatomic and Functional Assessment With CTA*, n.d.)

reactive protein), a marker of inflammation, was associated with an increase in coronary risk. Yet, based on other research, hs-CRP itself was not able to predict CAC incidence and progression in a larger population (Tajani et al., 2024).

1.4 Immune system in atherosclerosis

1.4.1 T cells in atherosclerosis

In addition to monocytes and macrophages, atherosclerosis includes a complex interplay of several other immune cell types: T cells, B cells, Neutrophils, Dendritic cells, and natural killer (NK) cells (Ali et al., 2020; Kobiyama & Ley, 2018; Saigusa et al., 2020; Tabas & Lichtman, 2017; Vallejo et al., 2021; van Kuijk et al., 2019; Winkels & Wolf, 2021). For this dissertation, I will focus on B Cells and T Cells.

T cells are commonly identified in atherosclerotic plaques, mainly in the region of the fibrous cap, but they have also been found in adventitia. T cell development starts in bone marrow. Lymphoid progenitors migrate from bone marrow to the thymus, where they acquire markers typical for T cells and start to express pre-T cell receptors. Two major subtypes of T cells, $CD4^+$ T cells and $CD8^+$ T cells induce immune response upon recognizing peptides on major histocompatibility complex I (MHC I) on Antigen-presenting cells (APC) while $CD4^+$ T cells recognize peptides on MHC II on all nucleated cells. The ability to bind to those peptides is encoded by the T cell receptor (TCR). The TCR binding with pro-inflammatory molecules can activate T cells and trigger clonal proliferation. Common disease antigens known to induce an immune response in T cells are LDL and its oxidized subspecies, as well as apolipoprotein B (apoB), which is a component of LDL (Colantonio et al., 2016). Based on in vitro studies, it's known that some of the CD4+ T cells present in plaques recognize oxidized LDL (Stemme et al., 1995).

The pro- or anti-atherogenic properties of T cells depend on the cell subtype and the cellular context. For example, regulatory T cells are believed to have atheroprotective functions, but CD4+ CD4+ Type 1 helper cells and NK T Cells have been shown to contribute to disease progression in animal models.

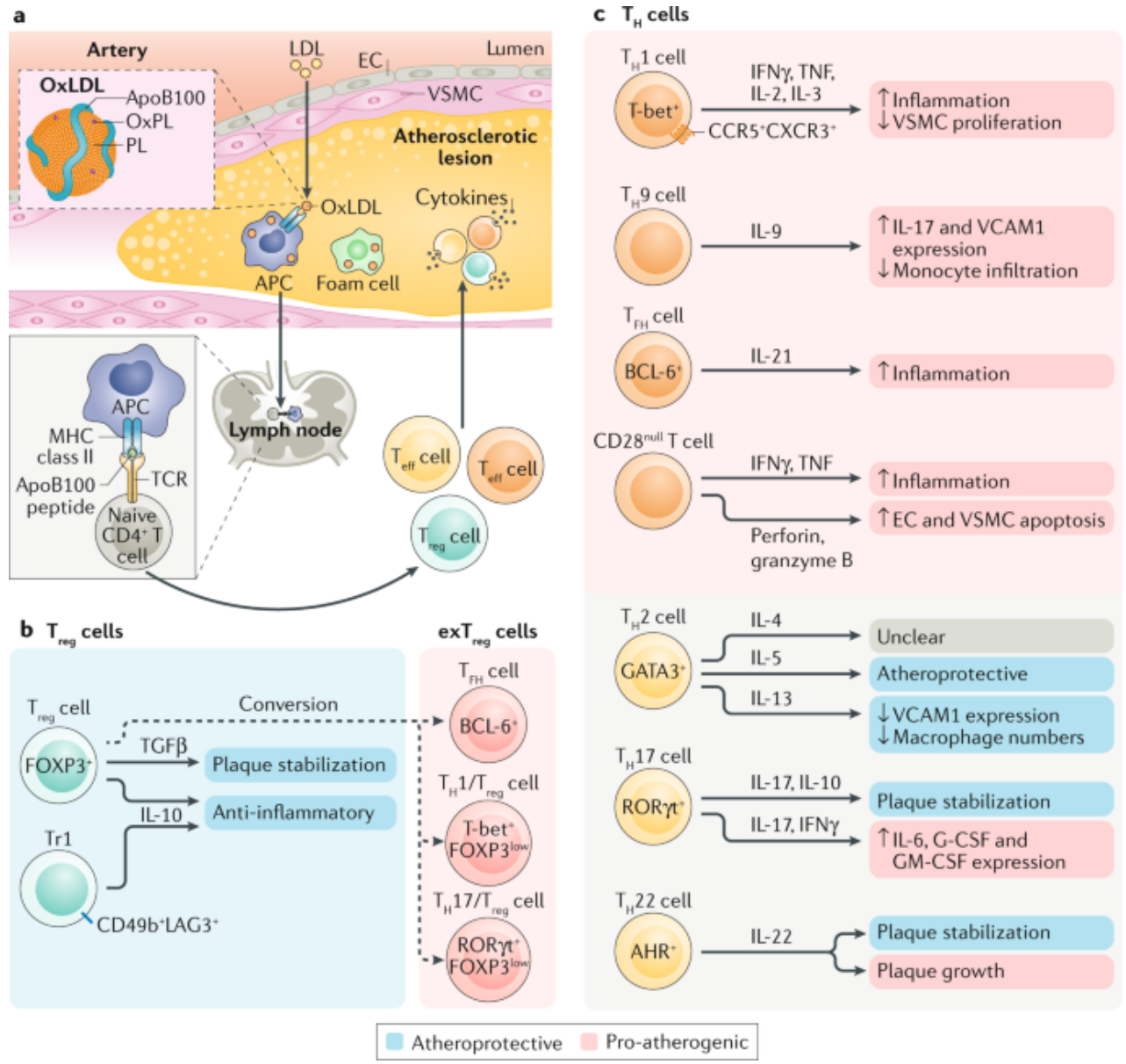

Figure 1.11 Role of T helper cells and regulatory T cells in the pathogenesis of atherosclerosis.

a | Naive CD4⁺ T helper (T_H) cells are primed in secondary lymphoid organs. T_H cells acquire the complete phenotype of effector T (T_{eff}) cells or regulatory T (T_{reg}) cells after encountering antigenic peptides from apolipoprotein B (ApoB) presented by antigen-presenting cells (APCs). APCs take up and process oxidized LDL (OxLDL), migrate to the draining lymph node and present peptides from ApoB on major histocompatibility complex (MHC) class II molecules. Naive T cells recognize this complex through their specific T cell receptors (TCRs). Co-stimulatory molecules induce T cells to express transcription factors that favour the differentiation into distinct T_H phenotypes. Homing receptors promote T cell migration to atherosclerotic lesions, where they secrete effector cytokines. **b**,**c** | CD4⁺ T cells can act in a pro-atherogenic or atheroprotective manner. Atherosclerotic lesions contain T_H1, T_H2, T_H9, T_H17, T_H22, T_{reg}, type 1 regulatory T (Tr1) cells and follicular helper T (T_{FH}) cells. T_{reg} cells can convert to 'exT_{reg} cells' (dashed arrows), losing expression of CD25 and forkhead box protein P3 (FOXP3) and acquiring properties of other T_H cell phenotypes such as T_H1, T_H17 and T_{FH}. Instability of FOXP3 expression triggers the formation of antigen-specific, but dysfunctional, partially non-protective exT_{reg} cells. (Figure and caption from Saigusa, Winkels, and Ley 2020)

However, in the study published in 2023 by Tomas et al., (Tomas et al., 2023) the authors show that the animal model findings may not translate into human populations, and iNKT cells (Invariant Natural Killer T cells) are not associated with the incidence of coronary events (CE) based on their case-control study in 416 patients.

1.4.2 CD4+ T cells

$CD4^+$ T cells are characterized by the expression of CD4 surface protein can be further divided into T helper cells and T regulatory cells as presented in Figure 1.11.

T helper cells relevant in the pathogenesis of atherosclerosis involve:

- **Th1** characterized by expression of T-box (T-box transcription factor TBX21), CXCR3 (CXC-chemokine receptor 3), and CCR5 (C-C chemokine receptor type 5). Patients with recent CE showed an increased number of Th1 in plaques when compared to patients with atherosclerosis but no symptoms. Plaque Th1 produces several cytokines associated with atherosclerosis, like IFNγ (Interferon gamma), IL-2, Il-3, and TNF (tumor necrosis factor) α. Yet, Th1 cells can also contribute to the attenuation of atherosclerosis by increasing VSMC (vascular smooth muscle cells) proliferation via IFNγ (Amento et al., 1991; Buono et al., 2003, 2005; Butcher et al., 2016; Fernandez et al., 2019; Frostegård et al., 1999; Gupta et al., 1997; J. Li et al., 2016; Niwa et al., 2004; Orecchioni et al., 2019; Rocha et al., 2008; Saigusa et al., 2020; Tellides et al., 2000; Vergnes et al., 2003; Y. Wang, 2007; Whitman et al., 2000)
- **Th2** are characterized by expression of GATA3 transcription factor and secretion of IL-4, IL-5, IL-10, IL-13and IL-33. Th2 cells are present in atherosclerotic plaques. Th2 cells in the PBMCs have been found to associate with lower atherosclerosis burden, and IL-4 has been negatively correlated with the disease in humans, but the finding was not confirmed in

murine studies, and the potential mechanism of protection remains unknown. There's evidence of dual protective and atherogenic function of other cytokines produced by Th2, but the mechanisms and precise effects remain unknown. (Davenport & Tipping, 2003; Engelbertsen et al., 2013, 2014; King et al., 2007; Tracy et al., 2013).

- **Th9** produce IL-9, cytokine increased in plasma from patients with atherosclerosis compared to healthy population. IL-9 has been shown to influence the production of IL-17, a pro-inflammatory cytokine associated with atherosclerosis. However, the role of Th9 cells in the disease progression is understudied (Gregersen et al., 2013; Kaplan, 2013; Lin, 2013; W. Zhang, Tang, et al., 2015).
- **Th17** are distinguished by the expression of RORγt (Retinoic acid receptor-related orphan receptor gamma t) and CCR6 (C-C chemokine receptor type 6) and secrete IL-17. IL-17 enhances the immune response by inducing the secretion of proinflammatory molecules: IL-6, G-CSF, and GM-CSF. Th17 can also produce atheroprotective IL-10. Studies suggest that patients with unstable plaques have increased numbers of Th17 and IL-17 in plasma, but other studies could not confirm this finding. Studies have shown both the stabilizing effects of IL-17 in carotid atherosclerotic plaques and its pro-inflammatory effects on VSMCs in coronary artery plaques (X. Cheng et al., 2008; Eid et al., 2009; Gisterå et al., 2013; Hashmi & Zeng, 2006; Taleb et al., 2009).
- **Th22** cells can be characterized by unique expression of IL-22, but not IFNγ and IL-17. Higher numbers of Th22 cells in circulation correlate with acute coronary syndrome compared with the healthy population. Studies in mice suggest that IL-22 is involved in both plaque stabilization and plaque growth. (Fatkhullina et al., 2018; Lin, 2013; Rattik et al., 2015; Xia et al., 2012; L. Zhang et al., 2013)
- **Tfh** (T follicular helper cells) expresses BCL-6 (the defining transcription factor B cell lymphoma 6) and, with B cells, forms and maintains germinal centers where B cells mature

after the activation of follicular B cells by antigen presentation on T cells. Tfh has been associated with atherosclerosis in mice. Studies suggest that TFH are proatherogenic. (Clement et al., 2015; Crotty, 2019; Gaddis et al., 2018; Nus et al., 2017; Ryu et al., 2018)

- CD28null T cells don't express CD28, the main receptor on $CD4^+$ T cells. Those cells are cytotoxic and pro-inflammatory. They naturally occur in humans but not in mice. The number of CD28null T cells is higher in the blood of patients with acute coronary syndrome than in healthy individuals, and those cells are immune to apoptosis and can invade human plaques. (Dumitriu, 2012; Kovalcsik et al., 2015; Liuzzo, 2000; Téo, 2013; Weng et al., 2009)

T regulatory Cells (Treg) are another group of $CD4^+$ T cells important in atherosclerosis. Classic Treg cells express FOXP3 (the transcription factor forkhead box protein P), IL-2 receptor subunit-α (IL-2RA or CD25), CTLA4 but don't express CD127. Data suggests that Tregs provide protection against atherosclerosis in both mice and humans. Tregs can produce IL-10 and TGFβ, cytokines that are considered atheroprotective. IL-10, a cytokine secreted by Tregs, and Tregs cell numbers are higher in patients with stable plaques and healthy individuals compared to patients who experienced MI. Yet, other studies suggest no significantly decreased risk of MI in patients with high Tregs and IL-10 levels and found no differences in Tregs frequencies in patients with carotid or coronary atherosclerosis. Studies showed that the lack of antigen presentation via MHC II worsens atherosclerosis and lowers Treg numbers. High numbers of Tregs in blood from patients with subclinical atherosclerosis were associated with elevated levels of LDL. This indicates that there are different Treg subsets; some can recognize antigens related to the disease and contribute to increased inflammation (Ait-Oufella, 2006; Barth, 2016; Björkbacka, 2016; Caligiuri et al., 2003; George, 2012; Guasti, 2016; Kita et al., 2014; Mailer, 2017; Mor et al., 2006; Roncarolo & Gregori, 2008; Wigren, 2012, 2019). Yet, it's been shown that Treg cells lose their phenotype and

their protective abilities with the progression of the disease (Butcher et al., 2016; J. Li, 2016; Maganto-García et al., 2011). The loss of their function has been associated with unstable

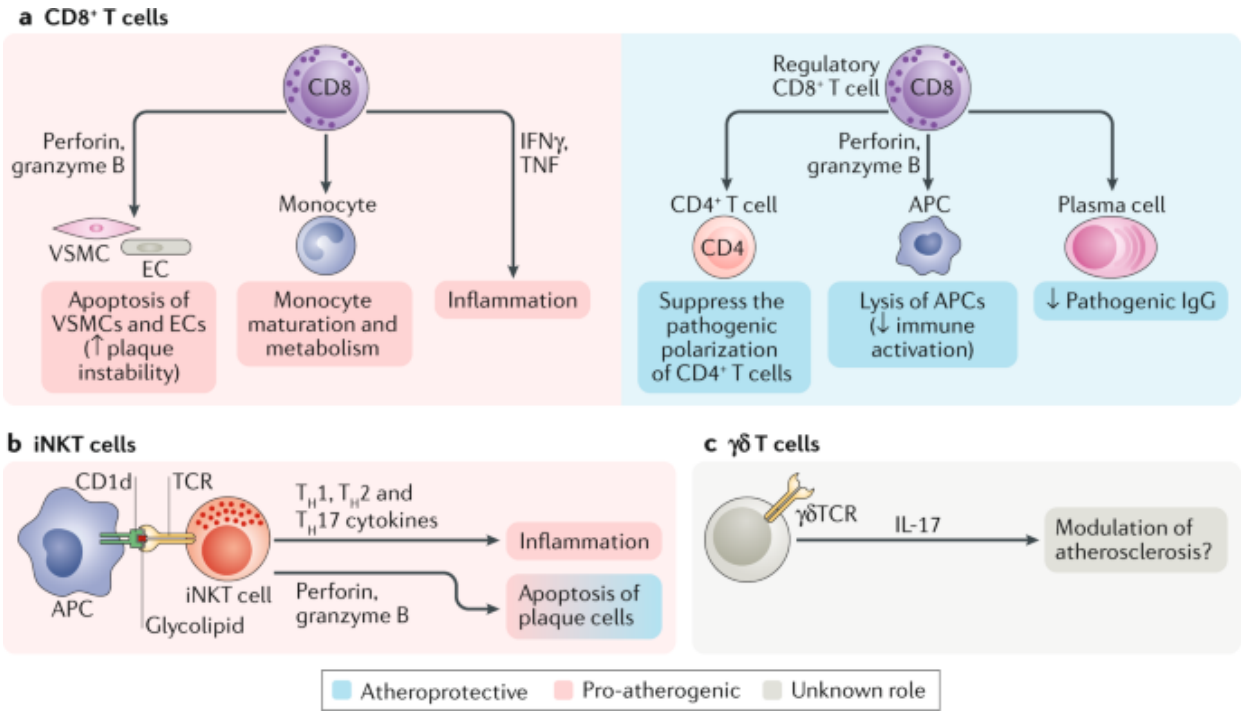

Figure 1.12 Overview of atheroprotective and pro-atherogenic functions of CD8⁺ T cells.
The cytotoxic activity of CD8⁺ T cells towards atherosclerotic lesion-stabilizing cells, such as vascular smooth muscle cells (VSMCs) and endothelial cells (ECs), and the secretion of interferon-γ (IFNγ), tumour necrosis factor (TNF) and other pro-inflammatory cytokines exacerbates the inflammatory response and drives the progression and destabilization of atherosclerotic lesions. Regulatory CD8⁺ T cell subsets can have atheroprotective effects, with high cytotoxic activity towards antigen-presenting cells (APCs) and inhibition of CD4⁺ T cell polarization into pro-atherogenic phenotypes. **b** | Invariant natural killer T (iNKT) cells can be activated by the interaction of the T cell receptor (TCR) with CD1d molecules containing antigenic glycolipids present on APCs. iNKT cells can also be activated in a CD1d-independent manner by Toll-like receptor stimulation and by the activation of APCs, which in turn secrete cytokines that activate iNKT cells, such as IL-12 and IL-18. Activation of iNKT cells results in the rapid release of cytokines associated with T helper 1 (T_H1), T_H2 and T_H17 cells, which activate other immune cells in the atherosclerotic lesion. iNKT cells can also promote atherosclerosis by the induction of apoptosis of plaque cells through the release of cytotoxic proteins such as perforin and granzyme B. **c** | γδ T cells are among the T cell subsets described in mouse atherosclerotic lesions. The intracellular cholesterol content in γδ T cells regulates their activation, proliferation and effector functions. In addition, γδ T cells are an abundant source of IL-17; therefore, these cells could modulate atherosclerosis via IL-17 production. However, the exact role of γδ T cells in atherosclerosis is unclear. (Figure and caption from Saigusa, Winkels, and Ley 2020)

expression of FOXP3, causing the origination of dysfunctional, antigen-specific Tregs cells called ex-Treg (Bailey-Bucktrout, 2013; Komatsu, 2014; Korn, 2007).

Another subtype of T regulatory cells is Tr1 cells, which lack the expression of FOXP3 but express CD49b and lymphocyte activation gene 3. They secrete IL-10, and experiments in Apoe-deficient mice suggest Tr1 cells are atheroprotective. Their frequency is lower in patients with CVD compared to healthy controls (Gagliani, 2013; Mallat, 2003; Zhu, 2018).

1.4.3 CD8+ T cells

$CD8^+$ T cells (Figure 1.12) are increased in the blood of patients with CAD compared to healthy individuals. Those T cells are also present in plaques in both human and murine models (Gewaltig et al., 2008, 2008; Kolbus et al., 2010; Wal et al., 1989). They are present in atherosclerotic plaques in higher frequencies than $CD4^+$ T cells, and studies analyzing their TCR suggest their clonal expansion in the plaque (Fernandez et al., 2019; Paul, 2016).

Similarly to $CD4^+$ cells, studies show their dual protective and atherogenic nature. They can contribute to plaque inflammation and the formation of a necrotic core. Cytokines secreted by $CD8^+$ T cells can have cytotoxic activity directed at VSMCs and worsen the inflammation in lesions. In mice, data suggest that they promote atherosclerosis by secreting IFNγ and granzyme B and impacting peripheral monocytes, yet the evidence is conflicting (Cochain, 2015; Dimayuga, 2017; Kyaw, 2013; Seijkens, 2019).

Atheroprotective properties have been attributed to $CD8^+$ cells based on immunization studies, where they mediated reduced atherosclerosis after immunization with p210 in *Apoe*$^{-/-}$ deficient mice (Chyu, 2012). Furthermore, genetic knockout of $CD8^+$ cells in Ldlr$^{-/-}$ mice led to the development of less stable plaques than in the control group, which had higher numbers of macrophages, reduced collagen content, and increased necrotic core area. (van Duijn et al., 2018)

1.4.4 NKT Cells

Another subset of T cells that plays a significant role in atherosclerosis are Natural killer T cells (NKTs). They can express CD4, CD8, or both or lack expression of CD4 and CD8. NKT is characterized by the expression of surface markers commonly associated with NK cells like CD161 or CD56 (Aslanian et al., 2005; Braun et al., 2010). They can be divided into invariant NKT (iNKT) with restricted TCR pool and type II NKT cells with more variable TCR. They are capable of recognizing lipids, glycolipids and phospholipid antigens presented on CD1d molecules. High numbers of iNKT have been associated with attenuated atherosclerosis in mice; however, human studies suggest an inverse correlation where higher iNKT frequency was correlated with reduced risk of coronary events (Major et al., 2004; Nakai, 2004; Tomas et al., 2023; Tupin et al., 2004; van Puijvelde et al., 2009).

1.4.5 $\gamma\delta$ T cells

$\gamma\delta$ T cells don't recognize specific antigens, and very limited research has been done on those cells in mice (H.-Y. Cheng et al., 2013, 2013; Nielsen et al., 2017; Vu, 2014). They can be found in atherosclerotic lesions (Kleindienst, 1993; Vu, 2014). Cholesterol is present inside $\gamma\delta$ T cells and has been shown to regulate their effector functions and proliferation. Those T cells are a producer of IL-17 in mice. The exact role of those cells in the development of atherosclerosis is unknown.

1.4.6 B Cells

B cells have a unique ability to produce antibodies capable of binding to specific antigens like viruses, bacteria, and toxins. Specific antigens in atherosclerosis consist of various types of highly immunogenic oxidation-specific epitopes (OSEs), including oxidized phospholipids (OxPLs) and malondialdehyde (MDA)--modified amino groups, which have been previously identified on the surface of apoptotic cells, microvessels and LDL (ox-LDL) (Binder et al., 2016; M.-K. Chang et al., 2004; Chou et al., 2008, 2009; Miller et al., 2011; Sage et al., 2019).

B cell receptors (BCR) are immunoglobulins (antibodies) on the surface of B cells responsible for recognizing and binding antigens. They consist of 3 variable genes – V(variable), D (diversity), and J (joining). The specific VDJ sequence formation process is called VDJ

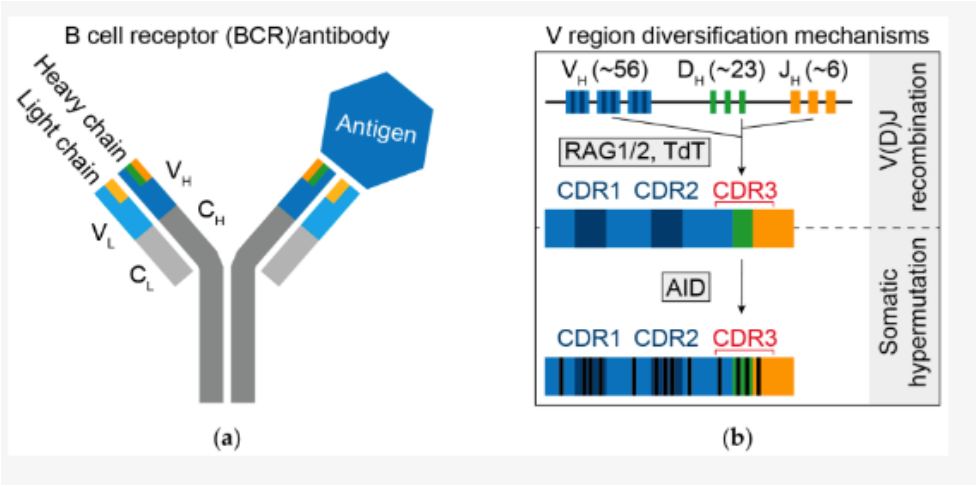

Figure 1.13. Structure and generation of B cell receptors (BCRs)/antibodies.
(a) Schematic representation of an antibody. BCRs are composed of heavy (H) and light (L) chains, which can be separated into variable (V) and constant (C) regions. Heavy and light chain variable regions make contact with the antigen. Light chain constant regions come in two different isotypes (kappa and lambda) and heavy chain constant regions in five (IgM, IgD, IgG1-4, IgA1-2, and IgE; not depicted). (b) V region diversification mechanisms. V(D)J recombination forms the CDR3s of the naïve B cell receptors. During the process of affinity maturation, somatic hypermutation mediated by activation-induced deaminase (AID) results in the development of mutations within B cell receptors/antibodies. RAG1/2: Recombination-activating gene 1/2, TdT: terminal deoxynucleotidyl transferase, CDR1/2/3: complementarity determining region 1/2/3. (Figure and caption from Kreer et al., 2020)

recombination in bone marrow during their hematopoietic development. This process creates a large, diverse set of unique BCRs capable of recognizing a wide range of antigens (David G. Schatz et al., 2011). Heavy and light chain polypeptides form BCR. There are 3 complementarity-determining regions responsible for the binding of the antigen: CDR1, CDR2, and CDR3, where CDR3 is the most variable of the 3 (Figure 1.13 A and B) (Kreer et al., 2020).

Activated B cells proliferate rapidly as plasma blasts and secrete antibodies. Based on the different heavy chain gene usage, there are five classes of antibodies: IgA, IgD, IgE, IgG, and IgM (Falk Nimmerjahn et al., 2005). All those classes have different structures and properties and can be secreted by various types of B cells. In mice, there are two major B cell subtypes differentiated by the expression of different surface markers – B1 cells and B2 cells. B2 cell subtypes can be further divided into marginal zone (MZ) B cells and follicular (FO) B cells. In

mice, B1 cells consist of B1a and B1b subsets. It needs to be noted that B cell subsets are largely studied in mice, and there is a controversy about whether the same B cell subsets are present in humans.

The main function of B1 cells is to provide rapid defense and antigen binding, and they are known to move between different niches. B1 cells secrete large amounts of antibodies that reside in the bone marrow, peritoneal cavity, and spleen. Other B1 cells can be found in serosal cavities (Pattarabanjird et al., 2021). B1 cells are a source of naturally occurring antibodies, which are expressed without infection or immunization and can bind to self-antigens and microbial components. Literature suggests that B1a cells are the main source of naturally occurring antibodies without prior stimulation (Prohaska et al., 2018), and B1b requires minimal activation for Ig production (Baumgarth, 2016; Choi et al., 2012). B1a and B1b cells can be distinguished by the expression of CD5: B1a cells are CD5+, and B1b cells are CD5- (Berland & Wortis, 2002).

B2 cells are considered conventional B cells. They produce antibodies in a T-cell-dependent manner to fight different kinds of pathogens. The majority of B2 cells are FO B cells.

They mature in BM and go to the spleen and can later travel to circulation. FO B cells together with Tfh they form germinal centers (GC) where they become activated via antigen stimulation (Pattarabanjird et al., 2021). In GC, B cells undergo maturation, class switching, and somatic hypermutation to produce highly specific IgG, IgA, and IgE. GC B cells express AID (single-stranded DNA cytosine deaminase), a DNA-altering enzyme responsible for the presence of somatic hypermutation in the BCR region, allowing for the dynamic production of a wide spectrum of unique BCRs (Jeroen M. J. Tas et al., 2016).

MZ B-2 cells are static and located in the marginal zone of the spleen. They show similar characteristics to B1 cells. Their primary function is to guard against blood-borne pathogens. They rapidly respond to antigens, producing antibodies at high capacity.

1.4.7 B Cells in Atherosclerosis

Antibodies were identified in atherosclerotic plaques over three decades ago (Dinah V. Parums et al., 1981; Göran K. Hansson et al., 1980; William Hollander et al., 1979, 1979) . It's also been shown that both plasma and plaques contain antibodies specific to different OSEs (Seppo Ylä-Herttuala et al., 1994). Additionally, IgA and IgG have been found in the vascular wall of lesions, solidifying the hypotheses about the potential role of B cells in CVD progression. However, the presence of B cells in plaques is low compared to other peripheral blood mononuclear cells (PBMCs) (Holger Winkels et al., 2018; Horstmann et al., 2020; Winkels & Wolf, 2021).

Genome-wide association studies have previously indicated the role of B cells in atherosclerosis (Huan et al., 2013). IgM specific to OSEs has been investigated as a potential target for drug development. The binding of IgM to OSEs that accumulate during atherosclerosis, such as malondialdehyde (MDA) and oxidized phospholipids on oxLDL, can reduce macrophage lipid uptake. This reduction prevents the formation of foam cells and the subsequent production of

inflammatory cytokines (Amir Ravandi et al., 2011; M. K. Chang, 1999; Daniel O. Griffin et al., 2011; Horkko, 1999; Lewis, 2009) . A study by the McNamara group at UVA suggests that IgM to OSEs produced by B1b cells offer protection against atherosclerosis in Apoe-deficient mice fed a high-fat diet (Rosenfeld, 2015). Additionally, levels of plasma IgM to MDA-LDL were able to predict 15-year outcomes, offering a new way of assessing CVD risk (Anand Prasad et al., 2017a, 2017b; Khamis, 2016; VJ et al., 2018). In clinical studies, MZ-like B cells (unswitched IgM memory B cells) have also been negatively correlated with the risk of CVD (Meeuwsen et al., 2017).

Proatherogenic properties of B cells have also been investigated. Numerous studies have examined the association of different immunoglobulins with various CVD-related outcomes. High serum IgA levels have been correlated with severe atherosclerosis (Antonio Muscari et al., 1988),

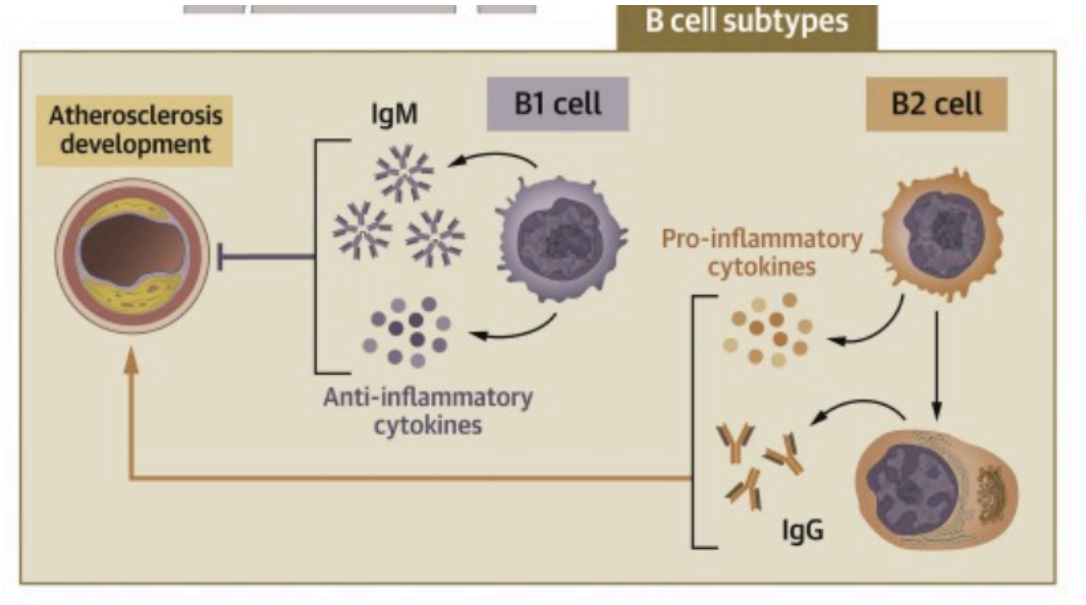

Figure 1.14 Roles of B Cells in Atherosclerosis and Implications of B-Cell–Targeted Therapies for Cardiovascular Disease

Human B cell subsets and their role in atherosclerosis. Figure and caption adapted from (Pattarabanjird et al., 2021)

and high serum IgG were moderately associated with incident ACVD (Khan et al., 2023). In a cohort of 1,496 adults aged over 50, those with high IgE levels exhibited a more than 3 fold increased risk of cardiovascular mortality compared to adults with low IgE levels. The mortality risk escalated with rising IgE serum levels, regardless of the initial baseline values (K.-B. Min & Min, 2019).

The role of B cells in atherosclerosis involves a complex interplay of protective and proatherogenic properties. Identifying antibodies specific to oxidation-specific epitopes within atherosclerotic plaques highlights the potential involvement of B cells in the development and progression of cardiovascular diseases. Additionally, exploring IgM and IgG levels in the context of atherosclerosis risk provides valuable insights into the potential use of B cell-related markers as predictive tools for assessing cardiovascular disease outcomes or as potential drug targets. Yet, further investigation into B cell-mediated immune responses and their impact on atherosclerosis is needed to understand their clinical significance and therapeutic potential fully.

1.5 TET2 mutation

Loss-of-function in TET2 gene and its molecular and physiological consequences has gained more interest among researchers when a study in 2017 established its connection with CVD (Jaiswal, 2017). TET2 emerged as one of the DNA methylation is a crucial epigenetic modification that regulates various cellular processes, including differentiation and proliferation. Its dysregulation can lead to impaired stem cell function and cellular transformation. The ten-eleven translocation (TET) gene family, first identified as a chromosomal translocation partner in leukemia, has emerged as a key enzyme in DNA demethylation. TET genes hydroxylate 5-methylcytosine to 5-hydroxymethylcytosine through multistep process. Somatic mutations in the TET2 gene have been reported in various human hematological malignancies, such as leukemia, myelodysplastic syndrome, malignant lymphoma, and atherosclerosis, underscoring TET2's critical

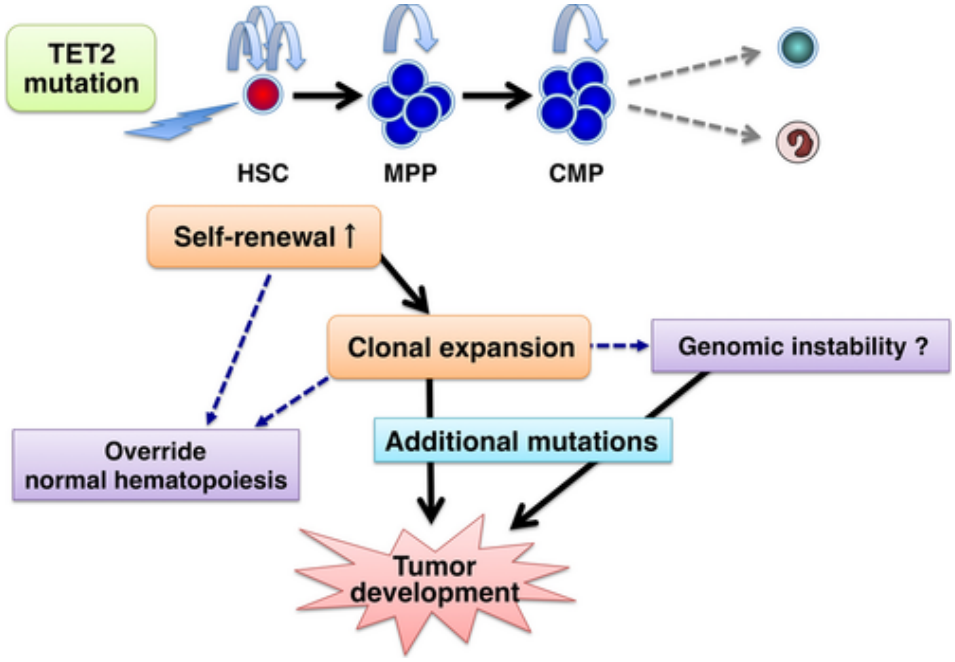

Figure 1.15 Schematic model for development of hematological malignancies induced by *TET2* mutation

role in hematopoiesis (Figure 1.15).

1.5.1 Molecular function and regulation of TET2

DNA methyltransferase (DNMT) mediated cytosine residue methylation is a crucial step in epigenetic regulation (Baylin et al., 2011; Walsh et al., 2006; H. Wu et al., 2014). The stretches of cytosine and guanine on DNA called CpG are frequently the sites of methylation. If the methylation happens at the promoter region of genes, the transcription gets suppressed. Irregular methylation of gene promoter regions has been detected in hematological malignancies in tumor suppressor genes (Das et al., 2004; Leone et al., 2002; Qu et al., 2013).

TET genes hydroxylate 5-methylcytosine (5-mC) to 5-hydroxymethylcytosine (5-hmC), which is converted back to unmodified cytosine. The 5-hmC is further processed back to

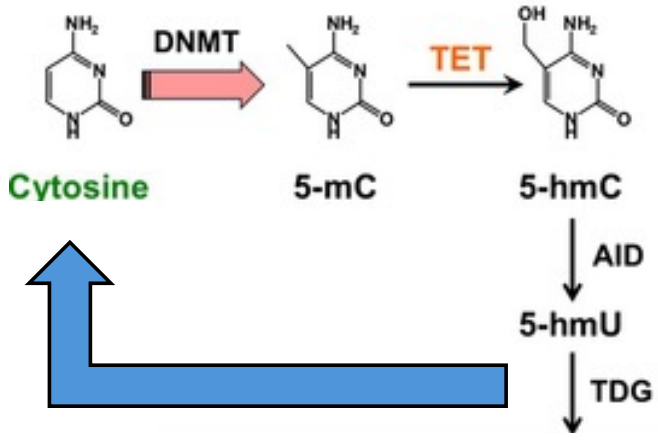

Figure 1.16 Pathway of cytosine demethylation mediated by ten-eleven translocation 2 (TET2) protein
(Figure and caption adapted from Nakajima & Kunimoto, 2014)

unmodified cytosine, removing the transcription suppressing mark from DNA and promoting the expression of genes. (Guo et al., 2011; Nakajima & Kunimoto, 2014; Tahiliani et al., 2009).

1.5.2 TET2 and hematopoiesis

Recent studies discovered that TET2 mutations play a significant role in hematological malignancy, indicating its role in homeostatic hematopoiesis. Several studies using TET2-mutant mice sought to discover its function in the hematopoietic processes (Ko et al., 2011, 2011; Kunimoto et al., 2012; Moran-Crusio et al., 2011; Quivoron, 2011; Roche-Lestienne et al., 2011, 2011). In the BM of adult TET2-deficient mice lineage, negative Sca-1^+ c-Kit^+ hematopoietic stem cells (LSK) and multipotent progenitors (MPP) were significantly expanded compared to WT. Common myeloid progenitors (CMPs) were also higher in frequency in the TET2-mutated mice, and HSCs from those mice had enhanced self-renewal. A study analyzing the consequences of the deletion of TET2 in mice discovered that the white blood cell (WBC) count was elevated in the double TET2-deficient mice compared to WT controls, solidifying the hypothesis about TET2's role in controlling the hematopoietic processes (Z. Li, 2011).

1.5.3 TET2 in Clonal hematopoiesis of indeterminate potential mutations.

Human hematopoietic stem and progenitor cells (HSPCs) have been estimated to accumulate 0.13 ± 0.02 exonic mutations per year. Therefore, by age 50, an individual is expected to have an average of 5 coding gene mutations in each HSPC (Evans et al., 2020; Fuster, 2017). Those genes often drive clonal hematopoiesis. Clonal hematopoiesis is defined as a single HSPC gaining selective advantage over other HSPCs (J. McClatchy et al., 2023).

Clonal hematopoiesis of indeterminate potential (CHIP) is a somatic mutation in hematopoietic stem cells occurring in people without hematological malignancies (Genovese, 2014). CHIP is estimated to be present in 10% of individuals aged 60 years or over. A somatic mutation in the myeloid malignancy-associated gene to be classified as CHIP has to have a variant allele frequency of $> 2\%$ in the peripheral blood. CHIP mutations accumulate with age (Amoros-Perez & Fuster, 2020; Evans et al., 2020; Jaiswal, 2014; Jaiswal & Libby, 2020; Jung et al., 2020; Kumar, 2020; Paramo Fernandez, 2018). CHIP mutations have been associated with an elevated risk of cardiovascular disease, pulmonary disease, type 2 diabetes and hematological malignancies (Buscarlet, 2017; Jaiswal, 2014, 2017a; Sano et al., 2018).

1.5.4 TET2 mutations in atherosclerosis

The discovery of the association between CHIP mutations and atherosclerotic cardiovascular disease was published in 2017 (Jaiswal, 2017). Since then, it's been widely studied in the context of inflammation, obesity, and increased disease risks. Clonal hematopoiesis induced by the loss-of-function TET2 mutation in the hematopoietic system aggravates age- and obesity-related insulin resistance (Fuster et al., 2020). Individuals with TET2 CHIP mutation have a higher mortality rate attributed to an increased risk of CVD (Libby & Ebert, 2018). A study by the Walsh group at UVA investigated how TET2 loss-of-function mutation-related clonal hematopoiesis can contribute to heart failure and identified that IL-1β production by macrophages was increased in an NLRP3-inflammasome-mediated manner in TET2 deficient mice (Sano et al., 2018). Later research found that exogenous IL-1β drives the expansion of TET2-KO HSCs in vitro and in vivo (J. McClatchy et al., 2023). The finding emphasized the role of TET2 in inflammation.

Considering the relationship between TET2, IL-1β, and cardiovascular disease, Ken Walsh's group investigated the results of the CANTOS trial and the response to Canakinumab therapy

among patients with CHIP. CANTOS trial subjects were found to have the prevalence and age dependence of CHIP mutations similar to incident coronary disease populations, and TET2 was the most common CHIP variant (Svensson et al., 2022). The association between subjects with CHIP and the occurrence of heart failure in CHIP is concordant with previous studies (Bing Yu et al., 2021). The study found that Canakinumab-treated patients with TET2 CHIP had a lower incidence of major adverse cardiovascular events (MACE) compared with patients with no TET2 CHIP mutations treated with the mediation and to TET2 CHIP patients treated with placebo (Bing Yu et al., 2021).

1.6 Motivation for this thesis

The motivation for this work is to demonstrate how multi-omics can enhance our understanding of CVD and underlying genetic conditions, guiding the development of more precise and effective treatments

Cardiovascular disease (CVD) affects millions worldwide annually. In the USA, death related to CVD occurs every 34 seconds (Figure 1.8). Despite advancements in treatment and diagnostics, not all patients respond equally to LDL-lowering therapies, which are crucial in managing atherosclerosis. Recent clinical trials and extensive research underscores the inflammatory nature of CVD. The CANTOS trial highlighted the significance of patient inflammation status in assessing risks and selecting appropriate treatments.

The patient-to-patient differences in CVD present an opportunity to leverage multi-omics approaches in clinical studies and basic science and to lay the basics for potential future use in precision medicine.

In Chapter 2, I and colleagues explored the effects of TET2 knockout (KO) in B cell subsets. The association of TET2 with increased CVD risk and the atheroprotective nature of

antibodies produced by B cells, we sought to understand the consequences of the loss-of-function mutation in this cell type. This chapter emphasizes the importance of understanding the homeostatic functions of genes before investigating their roles in disease. We focused on examining the differences in cell numbers in different niches, changes in gene expression, and the B cell receptor (BCR) to better understand immunoglobulin production and how alterations in the TET2 gene could impact BCR diversity, potentially causing immune system dysfunction.

In Chapter 3, together with collaborators, I investigated the association between different immune cell types from PBMCs and their activation states with the coronary artery calcium (CAC) score. This research aimed to uncover differences among patients at various stages of coronary artery disease, helping to enhance the understanding the dynamic changes in the immune system during disease progression. Identifying specific immune cell subsets that play crucial roles could offer new drug targets and direct future research toward previously unexplored cell types. Additionally, further work on potential correlation of immune cell signatures from PBMCs with CAC score could reveal0 novel markers and allow the development of a diagnostic test based on a blood test.

These chapters collectively illustrate how integrating multi-omics approaches can deepen our insight into cardiovascular diseases and the genetic factors contributing to them, paving the way for the creation of more targeted and effective therapies.

Chapter 2

Chapter 3 Loss of TET2 Increases B-1 Cell Number and IgM Production While Limiting CDR3 Diversity

This chapter is adapted from:

Dennis Emily*, **Maria Murach*,** Cassidy M.R. Blackburn, Melissa Marshall, Katherine Root, Tanyaporn Pattarabanjird, Justine Deroissart, et al. “Loss of TET2 Increases B-1 Cell Number and IgM Production While Limiting CDR3 Diversity.”

Frontiers in Immunology 15 (2024).

*authors contributed equally

List of supplementary files associated with this chapter:

- Supplement 3.1: Supplementary figures (S1-S6) and supplementary tables (S2-S3).
- Supplement 3.2: Supplementary table S1

3.1 Introduction

B cells participate in both innate and adaptive immunity through the secretion of antibodies. B cells are broadly divided into B-1 and B-2 subtypes. B-2 cells are derived from hematopoietic progenitor cells in the bone marrow (BM) and function predominantly in T cell-dependent responses for antibody production (McHeyzer-Williams & McHeyzer-Williams, 2005; Y. Wang et al., 2020). B-1 cells originate during early fetal life, are long-lived, and self-renew ((Baumgarth, 2011; Holodick et al., 2014a; Montecino-Rodriguez et al., 2006; Montecino-Rodriguez & Dorshkind, 2012). B-1 cells can be found predominantly in serosal spaces such as the peritoneal cavity (PerC) or the pleural cavity but can also be found in secondary lymphoid organs such as the spleen, lymph nodes, and the BM (Kawahara et al., 2003). B-1 cells are further subtyped into B1a or B-1b cells depending on the expression of CD5 (B1a are CD5+). B-1 cells produce

about 80% of circulating serum IgM (immunoglobulin M). A low level of IgM is produced by B-1 cells in serosal cavities, and the majority of circulating serum IgM is produced by B-1 cells in the spleen and BM (Choi et al., 2012; Holodick et al., 2010, 2014b). IgM antibodies produced by B1a cells are thought to be naturally occurring (i.e., present at birth, in gnotobiotic mice, and without antigen exposure) (Baumgarth et al., 1999; Chou et al., 2009; Hooijkaas et al., 1984). These natural antibodies provide rapid protection from infections and maintain tissue homeostasis through apoptotic cell clearance (Baumgarth et al., 1999; Chou et al., 2009; Holodick et al., 2014b; Hooijkaas et al., 1984). However, recent evidence identified the VDJ region in B1a cells as having N additions (Holodick et al., 2014a; Holodick, Vizconde, et al., 2016; Prohaska et al., 2018; Srikakulapu et al., 2022; Upadhye et al., 2019), an event due to the action of the DNA polymerase TdT, which is only expressed after birth. This suggests more complexity to the regulation of the CDR3 in B1a cells than previously thought.

The TET family of proteins act enzymatically as α-ketoglutarate-dependent cytosine dioxygenases that promote DNA demethylation by oxidizing the methyl group of 5-methylcytosine (5mC) to 5-hydroxymethylcytosine (5hmC) (Nakajima & Kunimoto, 2014; Pan et al., 2015; Rasmussen & Helin, 2016)potent epigenetic modulators. TET2 is involved in hematopoietic cell development and differentiation (Ko et al., 2011; Kunimoto et al., 2012; Moran-Crusio et al., 2011). Dysfunction in TET2 is well characterized in hematological malignancies including acute myeloid leukemia (AML) (L. Chen et al., 2020; Z. Li et al., 2011; Rasmussen et al., 2015; H. Zhao et al., 2018) and myelodysplastic syndrome (MDS) (Z. Li et al., 2011; Sun et al., 2018; W. Zhang, Fu, et al., 2012; W. Zhang, Shao, et al., 2012, 2015). TET2 loss can affect inflammatory responses via altered cytokine secretion (Fuster et al., 2017; Sano et al., 2018) and other biological processes in myeloid cells (Cull et al., 2017; Garcia-Gomez et al., 2017; R. Li et al., 2018; Z. Li et al., 2011; Moran-Crusio et al., 2011; Z. Zhao et al., 2016). TET2 has also been implicated in B cell lymphomas (Dominguez et al., 2018; Jiao et al., 2019; Kubuki et al., 2017; C. J. Lio et al., 2019;

Mouly et al., 2018; Rosikiewicz et al., 2020; Schoeler et al., 2019; Z. Zhao et al., 2015). Most studies of TET2 in B cells primarily focused on B-2 cells and suggested reduced production of high-affinity IgG (Dominguez et al., 2018; Rosikiewicz et al., 2020; Schoeler et al., 2019). Only one study to date has briefly investigated TET2 loss in B-1 cells, and that was with a focus on diffuse large B cell lymphoma and chronic lymphocytic leukemia development (Mouly et al., 2018). In contrast, our study focuses on B-1 cells in young mice without evidence of tumor, allowing for the identification of key homeostatic processes that may be altered by loss of TET2.

Our novel findings characterize the impact of global loss of TET2 on B-1 cell biology at homeostasis, revealing that global TET2 loss leads to increased B-1 cell number, IgM production, and the number of replicated complementarity-determining region 3 (CDR3) sequences, which could impact diseases that are modulated by IgM antibodies to specific antigens.

3.2 Results

3.2.1 Global loss of TET2 results in increased numbers of all B cell subtypes in the peritoneal cavity compared to WT

To determine the impact of the loss of TET2 on major immune cell subtypes in the peritoneal cavity, BM, and spleen of TET2-KO and littermate control mice, spectral flow cytometry was performed (Figure 3.1). B cells were defined as CD45+ CD19+; T cells were defined as CD45+ CD5+ CD19-; Macrophages (Macs) were defined as CD45+ CD5- CD19- F4-80+ CD11b+; and NK cells were defined as CD45+ CD5- CD19- NK1.1+ (Supplemental Figure 1). We found that there was a higher B cell frequency and number in the peritoneal cavity (Figure 3.1&D), but not in the BM (Figure 3.1&E) or spleen (Figure 3.1&F) of TET2-KO mice compared to controls. Numbers of T cells (p-value = 0.0043), and NK cells (p-value = 0.0152) from TET2-KO mice in the peritoneal cavity (Figure 3.1D) were also greater than controls. There were no significant

differences in immune cell numbers from TET2-KO mice in the bone marrow (Figure 3.1E), while in the spleen there was a trending increase in B cells (p-value = 0.0649) with a significant increase in T cells (p-value = 0.0260) and a trending increase in NK cells (p-value = 0.0649) compared to WT (Figure 3.1F).

Upon examination of B cell subsets specifically, we found that in the peritoneal cavity, all B cell subsets were significantly increased in frequency (B1a p-value = 0.0152, B-1b p-value = 0.0411, B-2 p-value = 0.0260) and in number (B1a p-value = 0.0022, B-1b p-value = 0.0043, B-2 p-value = 0.0022) in TET2-KO mice compared to WT (Figure 3.1G, 1J). However, in the BM

Marker	**Fluorophore**	**Clone**	**Vendor**
CD45	PerCP	30-F11	BD
B220	APC	RA3-6B2	eBioscience
CD19	APCefl780	1D3	eBioscience
IgM	PECF594	R6-60.2	BD
IgD	efl450	11-26	eBioscience
CD8	BV510	53-6.7	BioLegend
CD4	PECy5.5	GK1.5	SouthernBiotech
CD44	BV785	IM7	BioLegend
CD62L	BV570	MEL-14	BioLegend
CD25	BB515	PC61	BD
F4/80	PECy7	BM8	eBioscience
CD11b	PerCPCy5.5	M1/70	BD
CD11c	AF647	N418	BioLegend
CD138	PE	281-2	BD
Ly6c	BV711	HK1.4	BioLegend
NK1.1	BV480	PK136	BD
CD5	BV605	53-7.3	BD
CD21	FITC	4E3	eBioscience
CD23	BUV737	B3B4	BD
Zombie NIR Fixable Viability Dye			BioLegend

Table 3.1 The immunophenotyping panel used for flow cytometry results presented in Figure 1.

(Figure 3.1H, 1K) only the B1a cell subset frequency was significantly increased in TET2-KO compared to WT mice (p-value = 0.0260). In the spleen (Figure 3.1I, 1L) B-1b cells but not B1a cells were elevated in both frequency and number (p-value = 0.0173, 0.0043, respectively). There was no difference in TET2-KO B-2 cell frequency in the spleen, although the total number of B-2 cells was significantly increased (p-value = 0.0260).

3.2.2 Peritoneal B1a cells from TET2-KO mice have lower expression of immunoglobulin genes compared to WT

To identify genes differentially expressed in B cell subtypes in mice with TET2-KO compared to WT control, we performed RNA-sequencing (RNASeq) on sort-purified peritoneal B1a and B-1b cells from TET2-KO and WT mice (Figure 3.2A-B, Supplemental Figure 2). We utilized peritoneal B-1 cells due to their abundance in this specific niche, as well as due to the phenotypic changes we observed in Figure 3.1. We found that the global knockout of TET2 had a more significant impact on gene expression within B1a cells compared to B-1b cells. Specifically, we observed a downregulation in the expression of several immunoglobulin genes in B1a cells (and to a lesser extent in B-1b cells) from TET2-KO mice compared to their WT counterparts (Figure 3.2C-D, Supplemental Figure 3). Consistent with this finding, Gene Set Enrichment Analysis (GSEA) revealed that TET2 loss markedly affects pathways linked to immunoglobulin production and immune response activation, primarily within B1a cells. Indeed, the expression of numerous V genes (from both heavy and light chains) was decreased in B1a cells from TET2-KO mice (Figure 3.3B-C). Similarly, the expression of genes involved in the activation of molecular mediators of the immune response was also decreased in these cells (Supplemental Figure 3, 5).

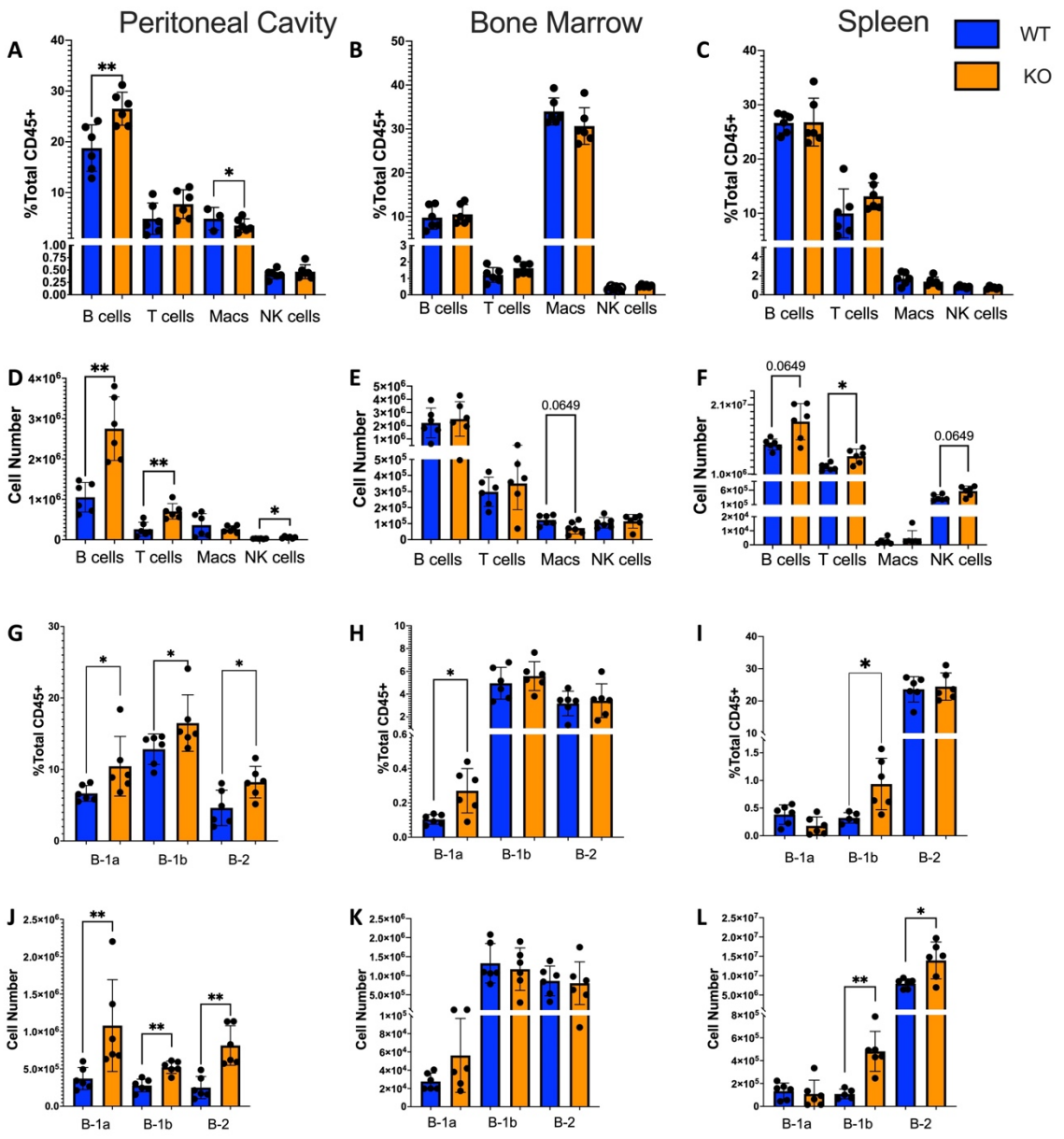

Figure 3.1. Immune subtypes in TET2-KO compared to WT mice.

(A - L) Flow cytometry characterization of the number and frequency of immune cell types in the (A, D) peritoneal cavity; (B, E) bone marrow; (C, F) spleen. Deeper gating into B cell subset frequency and number in the (G, J) peritoneal cavity; (H, K) bone marrow; (I, L) spleen, respectively, from TET2-KO (n = 6) and WT (n = 6) mice. Blue and orange represent WT and TET2-KO mice, respectively. Data are representative of four independent experiments. Significance was determined with two-tailed Mann-Whitney U-tests (* $p < 0.05$, ** $p < 0.01$).

both B1a and B-1b cells from the TET2-KO animals compared to the control animals (Supplemental Figure 3B, These GSEA results provide potential avenues for further hypothesis-driven studies of the role of TET2 in sensory-neural control of B cells, an emerging area of potential significance, recently also connected to cardiovascular disease development via other immune cells (Giudicelli et al., 2005; Song et al., 2021; J. L. Xu & Davis, 2000). Notably, while there are too many differentially expressed genes (DEGs) to test all at the protein level, one of the proteins encoded by our DEG, Sell, also known as CD62L, was also in our flow panel, allowing us to determine if the change in gene expression was also accompanied by changes in the protein level. Indeed, consistent with the decrease in CD62L RNA, we also saw a decrease in CD62L on the surface B1a and B-1b cells in TET2-KO mice (Figure 3.3C-D).

Marker	**Fluorophore**	**Clone**	**Vendor**
IgD	FITC	11-26	eBioscience
CD5	PE	53-7.3	eBioscience
CD23	PE-CY7	B3B4	eBioscience
B220	APC	RA3-6B2	eBioscience
CD19	APC-EF780	1D3	eBioscience
DAPI Staining Solution			Miltenyi Biotec

Table 3.2 The FACS panel used for sorting B cell subsets from the peritoneal cavity presented in Figure 2.

3.2.3 Global loss of TET2 results in higher expression of IgM antibody isotype in peritoneal B1a cells compared to WT

Using TRUST4, a tool for analyzing the B cell receptor (BCR) using bulk RNASeq (Song et al., 2021) and the IMGT (Giudicelli et al., 2005) database, we were able to identify Ig isotype transcripts present in sequencing data and their distribution across B1a and B-1b cells from TET2-KO and WT mice (Figure 3.4A). We found that there was a statistically significant increase in the

expression of IgM in the B1a cells from TET2-KO mice, but we do not see that effect in B1-b cells which is in accordance with the increase expression of *AIDCA*, a gene involved in class-switch recombination (Figure 3.4B, Supplemental Figure 5). In contrast, there was not a significant change in the distribution of IgD, IgG, or IgA isotypes expressed by the different B-1 cells in TET2-KO and WT mice (Figure 3.4A). Consistent with the increase in B-1 cells that we observed in niches that support antibody production, such as the spleen and BM (Figure 3.1E, 1F), and the increase in the IgM transcript in B1a cells, the circulating plasma IgM levels were higher in the TET2-KO compared to WT mice (p-value = 0.0075) (Figure 3.4C). Marginal zone B-2 cells (MZB) are another source of IgM and we did observe an increase in MZB cell number in TET2-KO mice compared to controls, which could contribute to the overall increase in circulating IgM (Supplemental Figure 6). We observed no change in circulating IgG levels.

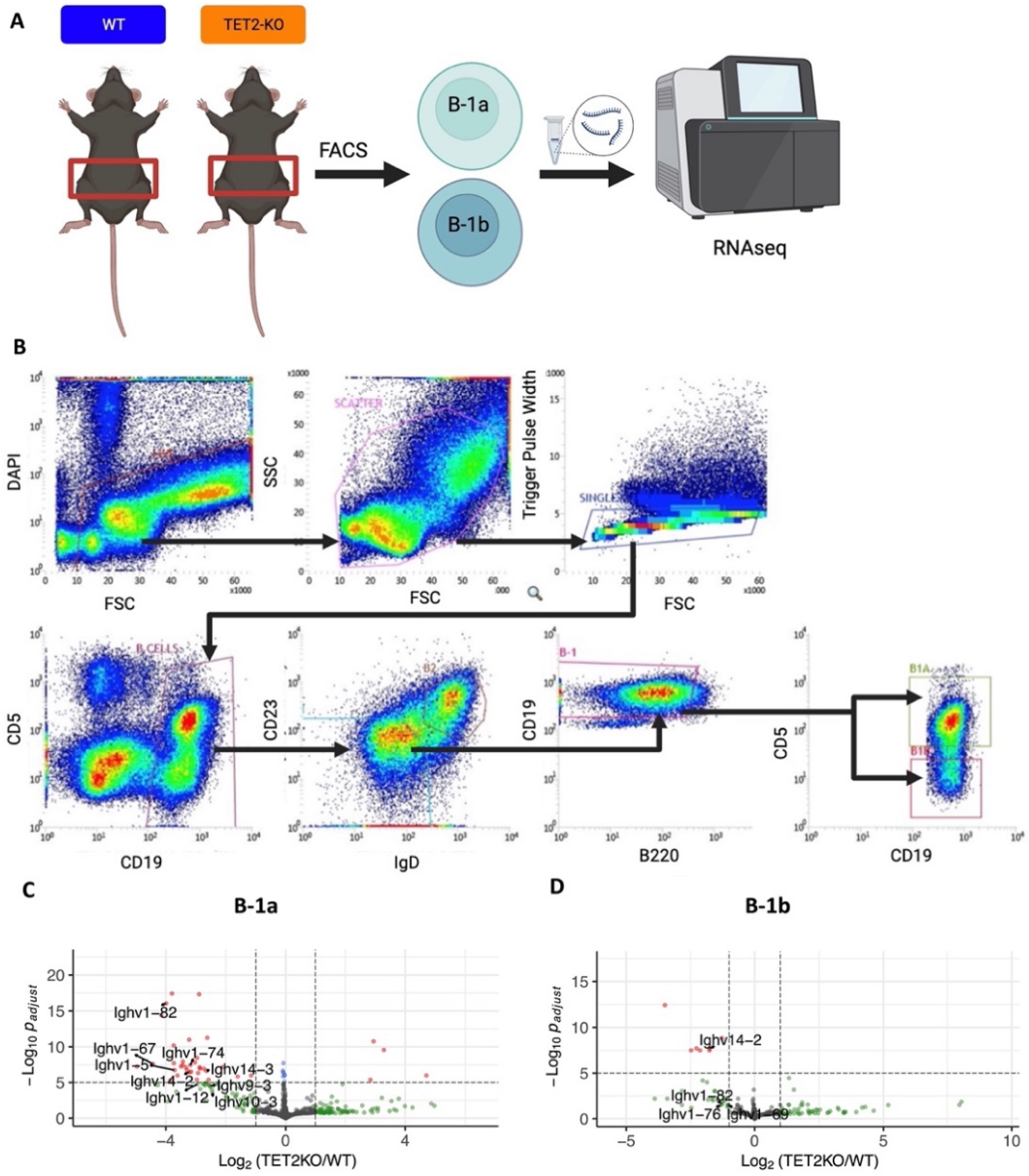

Figure 3.2. RNASeq analysis of differentially expressed genes in peritoneal B-1a and B-1b cells from TET2-KO and WT mice.

(**A**) Schematic of experimental design. B-1a and B-1b cells from the peritoneal cavity of TET2-KO and WT mice were sort-purified and RNA-extracted for RNASeq. (**B**) Gating strategy for sort. B-1a cells are CD19+, IgD-lo, CD23-lo, B220-lo, CD5+ while B-1b cells are CD19+, IgD-lo, CD23-lo, B220-lo, CD5-. (**C, D**) Differentially expressed genes are visualized with volcano plots of the B-1a (**C**) and B-1b (**D**) cells from TET2-KO mice compared to WT. Color legend for volcano plots: Grey – NS, Green: log2FC > 1, Blue: p-value < 0.05 and log2FC < 1, Red: p-value < 0.05 and log2FC > 1. n: B-1a: WT = 4, KO = 4, B-1b: WT = 4, KO = 3. All p-values are False Discovery Rate (FDR)-adjusted. Figure schematic made with BioRender. Panel A and B made by ED.

3.2.4 Global loss of TET2 results in a reduced number of unique heavy chain CDR3 sequences and an increased number of replicated heavy chain CDR3 sequences in peritoneal cavity B1a cells compared to WT

To assess differences in the heavy chain BCR repertoire in B-1 cells from TET2-KO and WT mice, we performed an analysis of the CDR3 sequences using our bulk RNASeq data and TRUST4 (Song et al., 2021). Results demonstrated that in both B1a and B-1b cells from TET2-KO mice, CDR3 diversity was reduced compared to WT mice (Figure 3.5A). The reduction in CDR3 sequence diversity in the B1a cells from TET2-KO mice compared to WT was statistically significant (p-value = 0.02857) (Figure 3.5A), while the reduction in unique CDR3 sequences in TET2-KO B-1b cells compared to WT was trending (p-value = 0.05714) (Figure 3.5A). It is not feasible to establish the presence of clonal expansion based on bulk RNASeq data, due to the inability to determine the absolute number of cells and their level of expression of each Ig transcript at a single-cell resolution in a given B cell population. However, a high proportion of replicated sequences suggests the presence of clonally dividing, or self-renewing B1a cells, as they are known to do. Here we define replicated sequences as those whose frequency is greater than 1% of all sequences.

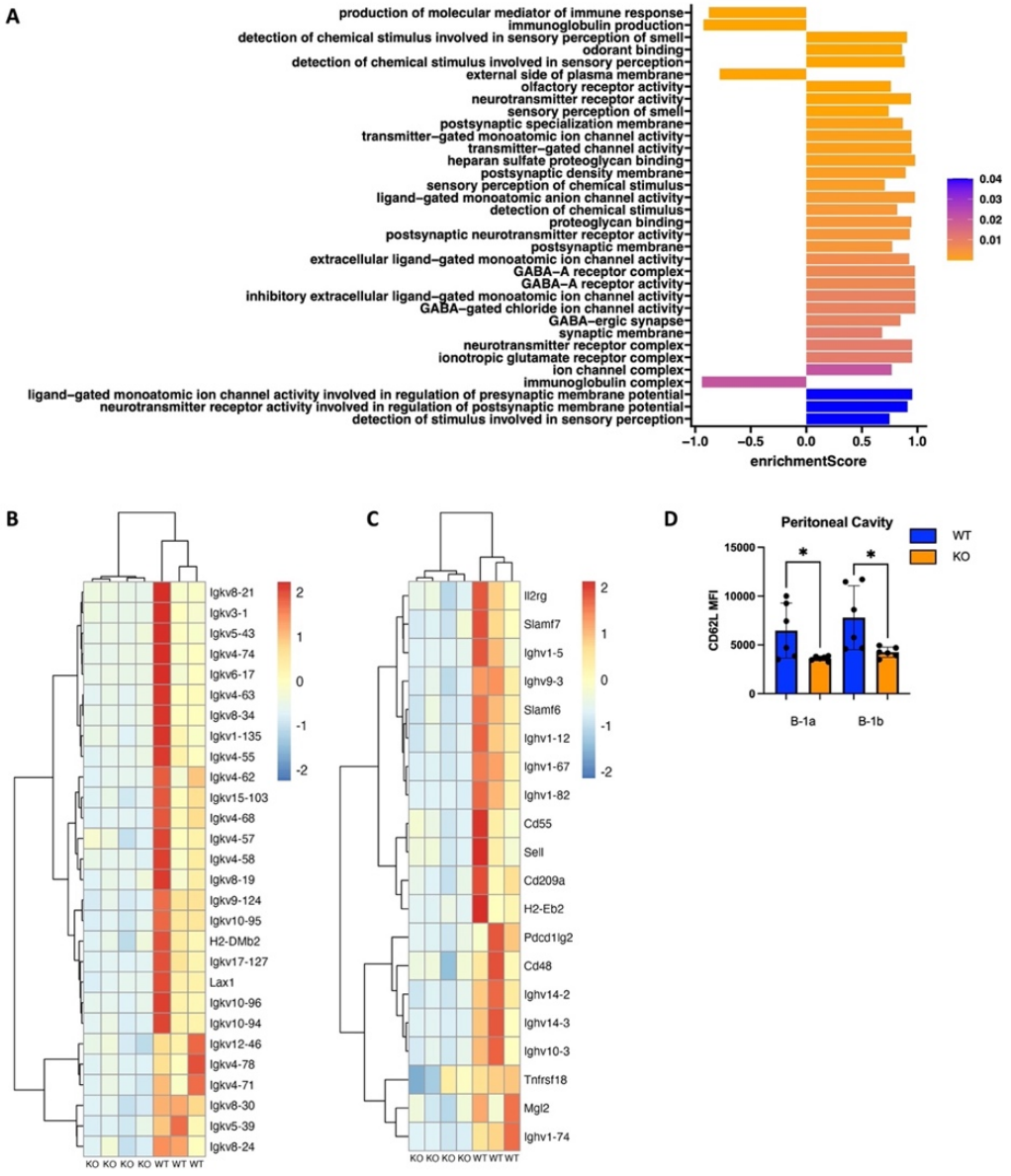

Figure 3.3 Pathway and Gene Set Enrichment Analysis (GSEA) of peritoneal B1a cells from TET2-KO mice.

(**A**) Plot of enrichment scores from GSEA on differentially expressed genes in B1a cells from TET2-KO and WT mice. The axis represents the enrichment score (ES). Higher scores indicate greater enrichment of the gene set at one end of the ranked list of genes. ES measure the degree to which a gene set is overrepresented at the extremes of the entire ranked list. ES are colored based on FDR-adjusted p-values. (**B**) Scaled expression of genes involved in the production of molecular mediators of immune response and immunoglobulin production pathways. Each row corresponds to a gene, and each column represents a WT or TET2-KO sample. The expression was scaled for each gene (from -2 to 2) and is represented by the color red for high and blue for low expression values. (**C**) Scaled expression of genes differentially expressed and found on the cell surface. Each row corresponds to a gene, and each column represents a WT or TET2-KO sample. The expression

was scaled for each gene (from -2 to 2) and is represented by the color red for high and blue for low expression values. (**D**) Bar chart displaying Median Fluorescence Intensity (MFI) of CD62L (Sell) in peritoneal B1a cells and B-1b cells from TET2-KO and WT mice. Blue and orange represent WT (n = 6) and TET2-KO mice (n = 6), respectively. Significance was determined with two-tailed Mann-Whitney U-tests (* $p < 0.05$). n: B1a: WT = 4, KO = 4 for panels A-C. Panel D made by ED.

In B1a cells from TET2-KO mice, we observed that 72% of the CDR3 sequences were replicated, compared to B1a cells from WT mice which only had 15% of the total CDR3 sequences replicated (Figure 3.5B, Figure 3.6A). Thirteen unique CDR3 sequences covered 72% of all CDR3s in B1a cells from TET2-KO mice, while 4972 CDR3 sequences made up the other 28% of the total number of identified CDR3s (Figure 3.5B, Figure 3.6A). In B-1b cells from TET2-KO mice, 25% of all CDR3 sequences are made up of 12 unique CDR3 sequences, while 11107 CDR3 sequences made up the rest of the 75% (Figure 3.5B, Figure 3.6B). Differences in the number of replicated unique CDR3 sequences were significant based on Chi-squared tests for B1a (p-value = 3.2×10^{-13}) and B-1b cells (p-value = 3.1×10^{-6}) from TET2-KO mice compared to WT (Figure 3.5B). An analysis of the commonality of replicated CDR3 sequences revealed that there was minimal overlap in the CDR3 sequence between B1a cells from TET2-KO and WT mice or in B-1b cells from TET2-KO and WT mice, respectively (Figure 3.5C). Interestingly, there was a greater degree of commonality in the CDR3 sequence comparing B1a and B-1b cells from TET2-KO mice. We visualized the proportion of replicated CDR3 sequences across B-1 cell subsets in TET2-KO and WT mice using pie charts (Figure 3.6A-B).

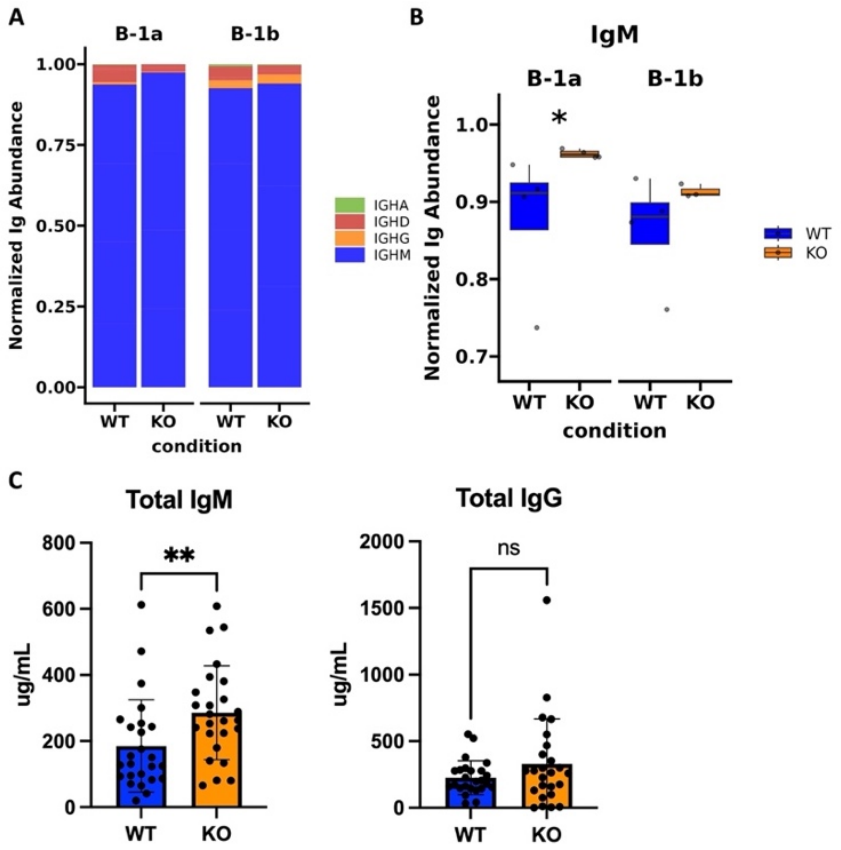

Figure 3.4 Immunoglobulin isotype analysis in peritoneal B1a and B-1b cells from TET2-KO and WT mice.

(**A**) Bar chart showing the distribution of Ig isotypes identified by TRUST4 in B1a and B-1b cells from TET2-KO and WT mice. (**B**) Proportion of IgM expression in B1a and B-1b cells from TET2-KO and WT mice. (**C**) Enzyme-linked immunosorbent assay (ELISA) of total IgM (**left**) and IgG (**right**) from plasma of TET2-KO (n = 26) and WT (n = 26) mice. Blue and orange represent WT and TET2-KO mice, respectively. Significance was calculated using Wilcoxon Rank Sum (* $p < 0.05$, ** $p < 0.01$) for panel B. Significance was determined with two-tailed Mann-Whitney U-tests (* $p < 0.05$, $p < 0.01$) for panel C. n: B1a: WT = 4, KO = 4, B-1b: WT = 4, KO = 3 in panels A and B. Panel C made by ED.

Consistent with our findings in Figure 3.5C, the CDR3 sequences that were most abundantly represented in B1a cells from WT mice were represented in B1a cells from TET2-KO mice at different proportions, and there were more similarities in replicated CDR3 sequences between B1a and B-1b cells from TET2-KO mice.

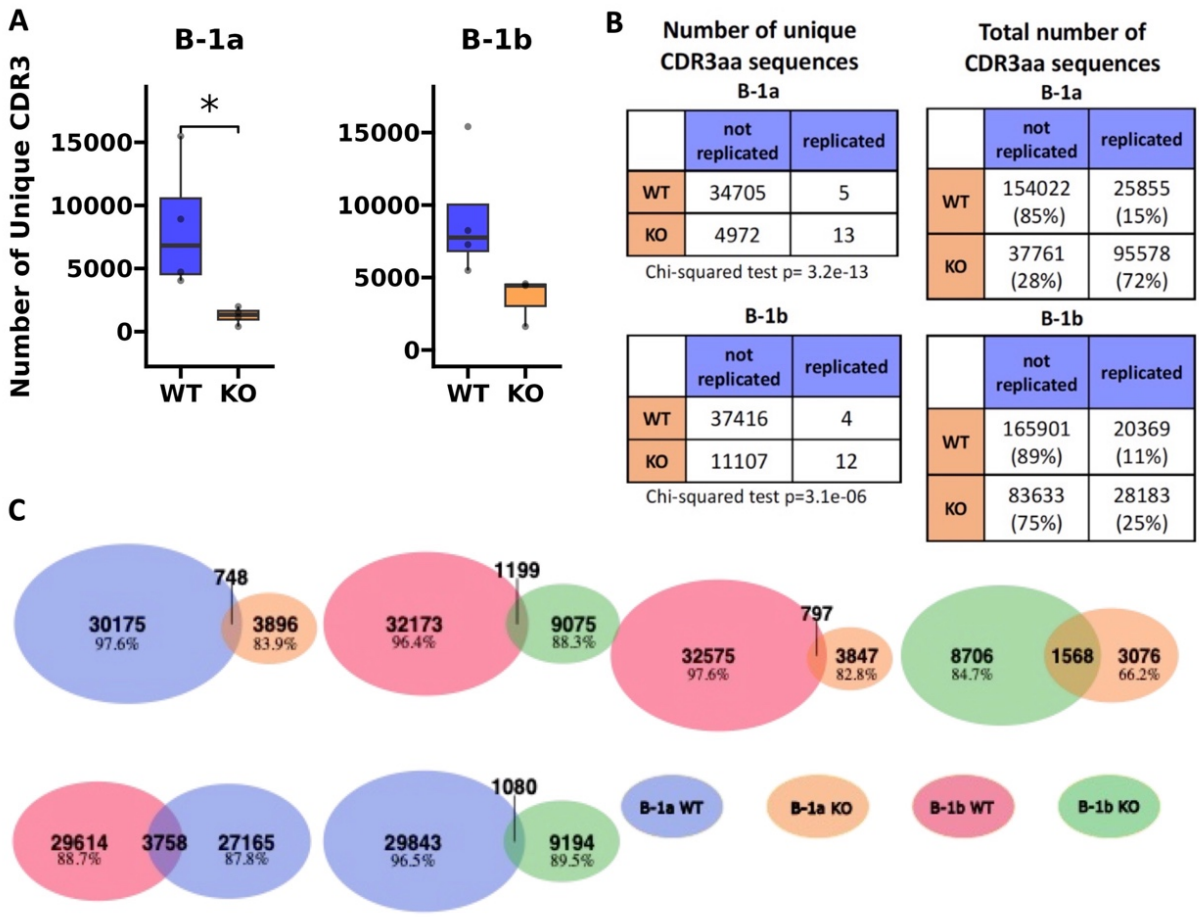

Figure 3.5 Heavy chain CDR3 sequence analysis reveals restricted BCR repertoire in peritoneal B1a and B-1b cells from TET2-KO and WT mice.

(**A**) The number of unique CDR3 sequences identified by TRUST4 in B1a and B-1b cells from TET2-KO and WT mice. (**B**) Contingency tables derived to assess the association between the number of unique CDR3 amino acid sequences (**left**) and total number of CDR3 amino acid sequences (**right**) with the mutant status of the mice (i.e., WT or TET2-KO) in B1a (**top**) and B-1b cells (**bottom**). Chi-squared test was used to assess the significance of these associations. Significance in panel A was calculated using Wilcoxon Rank Sum (* $p < 0.05$). (**C**) Venn diagrams that examine the shared repertoire of unique CDR3 sequences in the different B cell subsets. Blue represents CDR3 AA sequences from B1a cells from WT mice, orange from B1a cells from TET2-KO mice, red B-1b cells from WT mice, and green B-1b cells from TET2-KO mice, respectively. A shared sequence was defined as one expressed at least once in each of the subsets being compared. The number of shared sequences is represented by the overlapping region in each Venn diagram. Numbers and percentages of nonshared sequences of each cell subset in every comparison are indicated. For panels B-C, sequences were pooled from mice from the same cell type and condition (n: B1a: WT = 4, KO = 4, B-1b: WT = 4, KO = 3).

Since antigen binding specificity is not just determined by the heavy chain CDR3, we performed an analysis of the light chain BCR repertoire from our bulk RNASeq data with TRUST4. Results demonstrated that in both B1a and B-1b cells from TET2-KO mice, CDR3 diversity was reduced compared to WT mice (Supplemental Figure 7). The reduction in CDR3 sequence diversity in the B1a cells from TET2-KO mice compared to WT was statistically significant (p-value = 0.029) (Supplemental Figure 7A). The reduction in CDR3 sequences in B-1b cells from TET2-KO mice compared to WT was trending (p-value = 0.133) (Supplemental Figure 7A). Similar to what we observed in the heavy chain CDR3 sequences, the number of replicated light chain CDR3 sequences was over 2-fold greater in B1a cells from TET2-KO compared to WT mice (Supplemental Figure 7B-D). The number of unique CDR3 sequences from the light chain accounted for a similar percentage of total CDR3 sequences as seen in the heavy chain results in B1a cells from TET2-KO mice (Supplemental Figure 7B-D). Differences in the number of replicated unique CDR3 sequences were significant based on Chi-squared tests for B1a (p-value = 0.01) and B-1b cells (p-value = 0.02) from TET2-KO mice compared to WT.

While the role of the light chain in antigen binding and specificity remains less well-known compared to the heavy chain, it still contributes to those function (J. L. Xu & Davis, 2000). These results in the light chain CDR3 provide additional support that B1a cells are more profoundly impacted by loss of TET2 than B-1b cells, and the diversity of antigen-specific IgMs may be affected as a result.

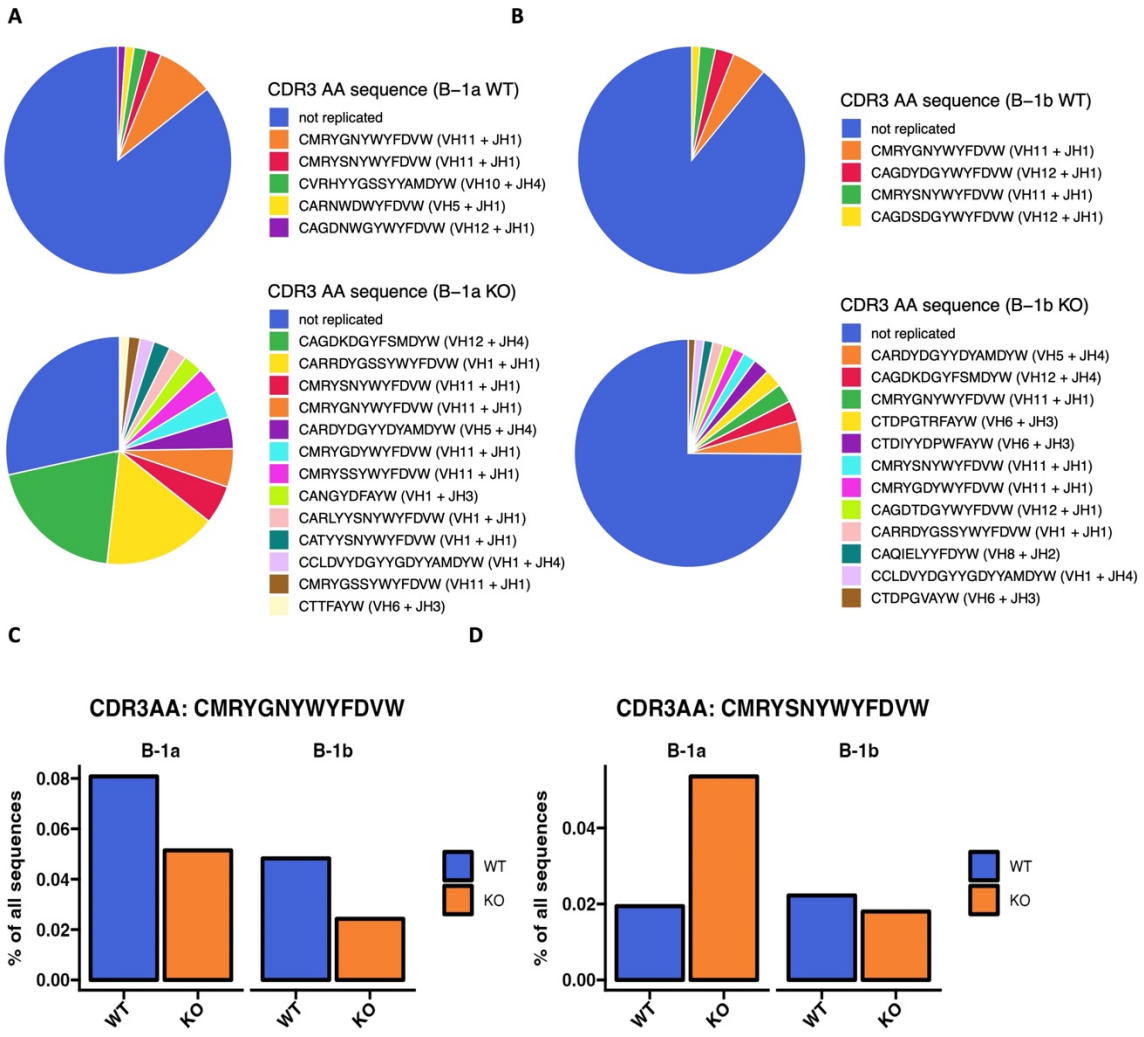

Figure 3.6. Heavy chain CDR3 sequence analysis reveals differences in most abundant CDR3 sequences in peritoneal B1a and B-1b cells from TET2-KO and WT mice.

(**A, B**) Annotated pie charts depicting the proportion of CDR3 sequences that are unique and the sequence and proportion of the replicated sequences in B1a (**A**) and B-1b (**B**) cells from WT (**top**) and TET2-KO mice (**bottom**). (**C**) Bar chart comparing the proportion of the top-most abundant CDR3 sequence in B1a cells from WT mice from of all CDR3 sequences in B1a and B-1b cells from TET2-KO and WT mice. (**D** Bar chart comparing the proportion of the second-most abundant CDR3 sequence in B1a cells from WT mice from of all CDR3 sequences in B1a and B-1b cells from TET2-KO and WT mice. Blue and orange represent WT and TET2-KO mice, respectively. Sequences were pooled from mice from the same cell type and condition (n: B1a: WT = 4, KO = 4, B-1b: WT = 4, KO = 3).

3.2.5 V_H–D_H–J_H usage shows differences between TET2-KO and WT BCR repertoires

Analysis of specific V_H–D_H–J_H gene region usage in B1a and B-1b cells from TET2-KO and WT mice revealed high usage of V_H1, V_H11, and V_H12 in B-1 cells consistent with prior findings (Supplemental Figure 8) (Holodick, Zeumer, et al., 2016; Prohaska et al., 2018; Tsuji et al., 2020). The B1a cells from the TET2-KO mouse appeared to have greater usage of these regions. There were also several reductions in V_H region usage in the B1a cells from the TET2-KO mice, but these were regions of minimal usage and of unclear significance.

We also analyzed differences in the specific $V_{K/L}$–$J_{K/L}$ gene regions of the light chain CDR3 sequence in B1a and B-1b cells from TET2-KO or WT mice (Supplemental Figure 9) and similarly found differences in V_K and J_K usage predominantly in B1a compared to B-1b cells. An analysis of kappa and lambda ratio revealed that there is more lambda light chain utilization in B-1b cells from TET2-KO mice compared to WT despite not reaching significance, while showing no difference in kappa/lambda ratio in B1a cells (Supplemental Figure 9E).

Circos plots (Figure 3.7), measuring the relative frequency of each V-J pairing revealed a greater abundance of V_H1-J $_H$1, V_H11-J $_H$1, and V_H12-J $_H$4 in B1a cells from TET2-KO mice compared to control, suggesting that TET2 has an important role in specific V-J recombination of B1a cells. These specific recombination events could be important for creating the over-representation of the specific CDR3s in B1a cells from TET2-KO mice. The increase in V_H12-J $_H$4 pairing in TET2-KO mice was also seen in the B-1b cells but only constituted 5% of all pairings compared to over 20% in the B1a cells. These data are consistent with the loss of TET2 generating a more pronounced effect on the BCR in B1a cells compared to B-1b cells.

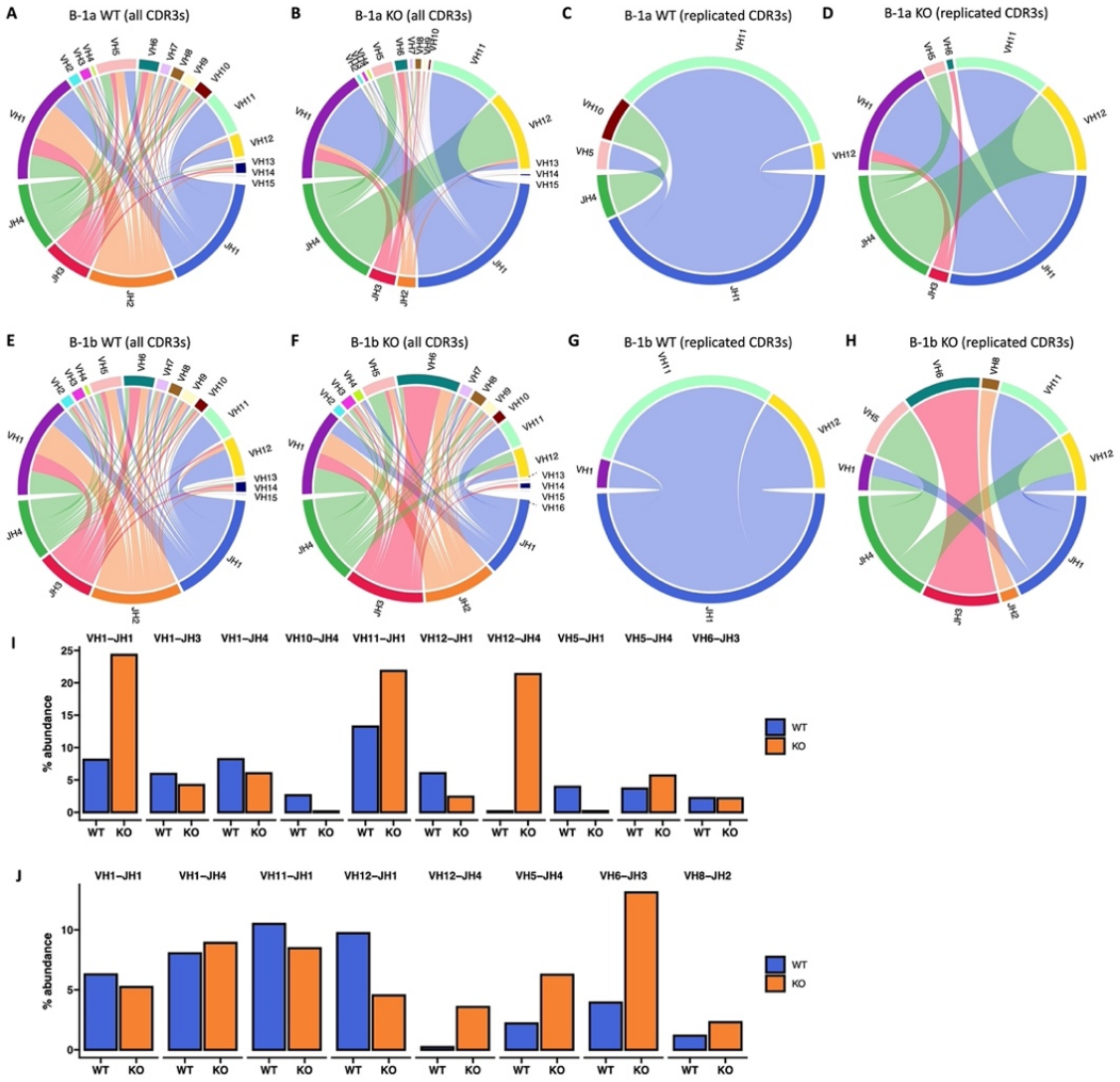

Figure 3.7 V-J Gene Association analysis of B1a and B-1b cells from TET2-KO and WT mice.

(**A-H**) Circos plot of V-J gene associations of CDR3 sequences identified by TRUST4 utilizing specific V-J gene segment pairs is displayed for B1a cells from TET2-KO (**B, D**) and WT mice (**A, C**) from all CDR3 sequences (**A, B**) and replicated CDR3 sequences (**C, D**). Circos plot of V-J gene associations of CDR3 sequences identified by TRUST4 utilizing specific V-J gene segment pairs is displayed for B-1b cells from TET2-KO (**F, H**) and WT mice (**E, G**) from all CDR3 sequences (**E, F**) and replicated CDR3 sequences (**G, H**). Cables connect V and J gene segments that are observed together within the same CDR3 region, with the thickness of each cable indicating the relative frequency of each V-J pairing. (**I, J**) The abundance of V-J gene connections identified in replicated CDR3s presented as percent abundance of all CDR3 sequences in B1a (**I**) and B-1b cells (**J**) from TET2-KO and WT mice. Each pair of bars represents the count of V-J associations combined from all samples. Blue and orange represent WT and TET2-KO mice, respectively. Sequences were pooled from mice from the same cell type and condition (n: B1a: WT = 4, KO = 4, B-1b: WT = 4, KO = 3).

3.3 Discussion

Murine B cells can broadly be divided into B-2 cells, which are derived from BM precursors and include conventional follicular and marginal zone B cells, and B-1 cells, which are largely fetal liver-derived and persist in adults through self-renewal (Deenen & Kroese, 1993; Holodick, Zeumer, et al., 2016; Kreslavsky et al., 2017; Kristiansen et al., 2016; Pattarabanjird et al., 2022). These B cell subtypes are developmentally, functionally, and phenotypically distinct (Berland & Wortis, 2002; Hardy et al., 2004; Kawahara et al., 2003; Kretschmer et al., 2003; Prohaska et al., 2018; Stall et al., 1992; Yoshimoto, 2020). Given their self-renewal capacity, we hypothesized that B-1 cells may be regulated by TET2, an epigenetic modulator that has been implicated in the clonal expansion of hematopoietic cells leading to disorders such as myelodysplastic syndromes (MDS) (Z. Li et al., 2011; Sun et al., 2018; W. Zhang, Fu, et al., 2012; W. Zhang, Shao, et al., 2012, 2015) and acute myeloid leukemia (AML) (L. Chen et al., 2020; Z. Li et al., 2011; Rasmussen et al., 2015; H. Zhao et al., 2018). Indeed, the results of the present study identified an important role for TET2 in regulating B cell numbers in specific niches. However, further studies are needed to determine if this is an effect intrinsic to the loss of TET2 specifically in B cells. Even if these findings are secondary to TET2 loss in another cell type, they still have potential relevance to diseases regulated by IgMs produced by B-1 cells such as infection (Askenase et al., 2015; Aziz et al., 2018, 2020; Choi & Baumgarth, 2008; Haas et al., 2005; L et al., 2015; Viau et al., 2005), atherosclerosis (George et al., 1998; Gruber et al., 2016; Karvonen et al., 2003; Palinski et al., 1995; Papac-Milicevic et al., 2016; Shaw et al., 2001; VJ et al., 2018), and obesity-related metabolic dysfunction (Harmon et al., 2016; Ravandi et al., 2011). Several human genetic variants of TET2 with loss of function have been identified (Bussaglia et al., 2019; Coltro et al., 2020; J et al., 2020) and these could have a broad impact similar to global TET2 deletion in

mice, resulting directly or indirectly in modulating the anti-inflammatory effects of IgM-producing B cells.

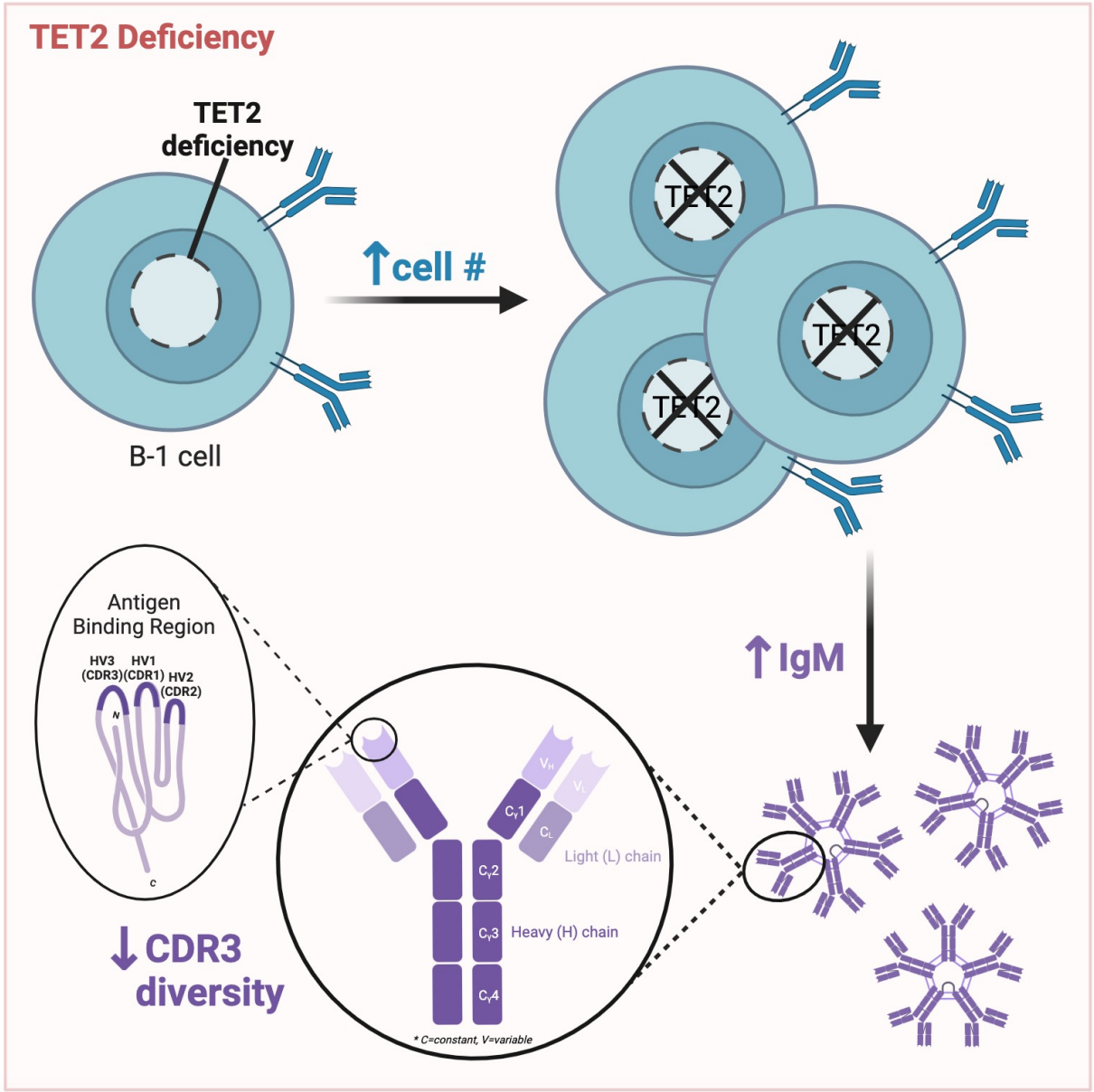

Figure 3.8 Graphical abstract of key findings.
Peritoneal B cell number is increased, circulating IgM levels are elevated, and CDR3 sequence diversity is reduced in mice null for TET2 compared to WT mice. Figure made with BioRender. Figure made by ED.

B-1 cells have been shown to have important roles in the first line of defense against pathogens (Askenase et al., 2015; Aziz et al., 2018, 2020; Choi & Baumgarth, 2008; Haas et al., 2005; L et al., 2015; Viau et al., 2005) and in mediating a reduction of inflammation (Choi et al., 2012; Gruber et al., 2016; Harmon et al., 2016; Holodick, Zeumer, et al., 2016; Kyaw et al., 2012; Upadhye et al., 2019). One of the major mechanisms mediating this effect is their production of IgM that can recognize pattern-associated molecular pattern (PAMPs) and danger-associated molecular patterns (DAMPs) such as phosphorylcholine on the cell wall of *Streptococcus pneumoniae* (Askenase et al., 2015; Grasset et al., 2015; Haas et al., 2005)and oxidation-specific epitopes (OSEs) on lipoproteins (Binder et al., 2016; Miller et al., 2011). OSEs on lipoproteins and apoptotic cells can fuel disease-associated inflammation (Binder et al., 2016; Steinberg & Witztum, 2010) and IgM to these neoepitopes can inhibit their induction of inflammatory responses (Que et al., 2018; Witztum & Lichtman, 2014). Our study presents novel findings that the global loss of TET2 increased B-1 cell number, circulating IgM level, and BCR specificity, all factors that could affect the immune response against PAMPs and DAMPs.

The first major phenotype we observed due to the global loss of TET2 was an elevation in the frequency and number of all B cell subtypes in the peritoneal cavity (Figure 3.1G, 1J). Yet, in the specialized niches that promote B cell effector function, such as antibody production, only the frequency of B1a cells in the BM (Figure 3.1H), and B-1b frequency and number in the spleen (Figure 3.1I, 1L), were higher in the TET2-KO compared to WT mice. The mechanism responsible for these subset and niche-specific increases in cell number remains unclear and requires further study to determine if proliferation, increased cell survival, or migration are responsible. As B1a cells self-renew like hematopoietic stem cells (HSCs) (Deenen & Kroese, 1993; Duber et al., 2009; Ghosn & Yang, 2015; Holodick, Vizconde, et al., 2016; Kretschmer et al., 2003; Z. Xu et al., 2004), and this self-renewal property is enhanced in HSCs with TET2-KO (Ko et al., 2011; Kunimoto et al., 2012; Z. Li et al., 2011; Pan et al., 2017; W. Zhang, Shao, et al., 2015; X. Zhang et al., 2016),

enhanced self-renewal of B1a cells from TET2-KO animals may explain the increase in B1a cells in the peritoneal cavity.

The genes and pathways that were different in B-1 cells from TET2-KO mice compared to control, particularly in the B1a cells, were immunoglobulin-related and they were expressed at a lower level (Figure 3.2C). There was a predominance of kappa light chain genes that were less expressed, in addition to several V_H genes, leading us to hypothesize that loss of TET2 may be limiting the expression of certain variable region genes, which allows for specific antigen recognition of foreign or neo-antigens (Casali & Schettino, 1996; Hardy & Hayakawa, 2012; Hayakawa et al., 1999, 2003; Holodick, Vizconde, et al., 2016). To further investigate those differences, we performed BCR analysis using our RNASeq data.

Historically, BCR identification from sequencing was facilitated by well-established algorithms like MiXCR (Bolotin et al., 2015) or BALDR (Upadhyay et al., 2018) using V-D-J enriched or single-cell RNASeq data. However, the associated costs and impracticality of research studies focusing on low-frequency cell populations were limiting factors for broader application. The introduction of the TRUST4 algorithm by Song *et al.* (Song et al., 2021) enabled the accurate detection of BCR and TCR repertoire from bulk RNASeq data. This innovation diminished the financial burden of data generation and allowed for the re-utilization of previously generated data, limiting redundancy and resources required for BCR/TCR analysis and providing opportunities for potential clinical applications. While the results are not at single-cell resolution, they offer valuable insight into the diversity of immune cell receptor repertoire and specificity. To date, a limited number of studies have performed an analogous analysis in bulk RNASeq data (K. J. Liu et al., 2023; Song et al., 2022; Y. Zhang & Lee, 2022).

The constant region of the BCR determines the effector function of the antibody. There were no differences in the transcript expression levels of antibody isotypes IgG, IgD, and IgA (Figure 3.4A). However, there was a statistically significant increase in transcript expression of

IgM, the main isotype produced by B-1 cells (Holodick et al., 2014b; Kyaw et al., 2011, 2012; Upadhye et al., 2019), in the B1a cells from TET2-KO compared to WT mice suggesting that TET2 may inhibit factors responsible for encoding the constant region downstream of the V region on chromosome 14 that determines antibody isotype or TET2 may limit isotype switching in B1a cells (Figure 3.4B). These data are consistent with no changes observed in the circulating IgG level while there was an increase in circulating IgM in the TET2-KO mice compared to the control. We could not conclude if the increase in total IgM was due to increased IgM secretion on a per-cell basis or due to the increase in overall cell number (Figure 3.4C). However, increased IgM levels could also be due to the increase in B-1 numbers in the spleen and bone marrow. Additionally, there was an increase in MZB cell number in the spleens from TET2-KO mice compared to WT, another potential source of IgM from TET2-KO and WT mice (Supplementary Figure 6).

While much more has been documented about the role of the heavy chain variable region, specifically the CDR3 of the BCR, less is known about the purpose of the light chain regarding its role in binding antigens (Andrews et al., 2013; Aoki-Ota et al., 2012; Hardy & Hayakawa, 2012; Jaffe et al., 2022; Kretschmer et al., 2002; Tornberg & B1a, 1995; J. L. Xu & Davis, 2000; Yang et al., 2015). A study by Lio *et al.* revealed that double knockout of TET2 and TET3 in the early B cell stage impaired rearrangement at the Igκ locus (C.-W. Lio et al., 2016). Our findings support previous research by detecting the lower expression of many Igκ genes, and indeed, while not reaching significance, overall kappa immunoglobulin usage is reduced in B-1b cells, but surprisingly not B1a cells from TET2-KO mice compared to WT (Supplemental Figure 9E). There was also a significant reduction in the number of unique CDR3 sequences in B1a cells and a trending reduction in B-1b cells from TET2-KO mice compared to WT (Figure 3.2, Supplemental Figure 8). Consistent with the reduced variety of CDR3 sequences, there is a higher number of replicated sequences in the light chain observed in the B1a cells from the TET2-KO mice compared to WT, and the effect was also observed in B-1b cells to a lesser extent (Supplemental Figure 8).

These data suggest that the BCR repertoire in the light chains of B1a cells is more sensitive to loss of TET2 than in B-1b cells.

B1a cells from TET2-KO mice had significantly fewer unique CDR3 sequences with 72% of the total CDR3 sequences representing replicates, suggesting that loss of TET2 impacts the diversity of antigen specificity in B-1 cells, particularly B1a cells (Figure 3.5B). The more marked lack of antigen diversity in the B1a cells from TET2-KO mice is consistent with B1a cells predominantly originating from the fetal liver and persisting through self-renewal, and a role for TET2 in promoting expansion of rapidly self-renewing cells. While our study isolated B cells from the global TET2-KO and WT mice, it must be considered that the effects of loss of TET2 in other cells, such as cytokine-secreting macrophages, could be playing a role in influencing the selection of the B cell repertoire. Additionally, the presence of IgM itself can influence the selection of the B cell repertoire (Nguyen & Baumgarth, 2016). In an analysis of V_H–D_H–J_H gene regions of the heavy chain, our data suggest that the restricted associations of V_H–D_H–J_H gene regions in the B1a cells from TET2-KO mice could be responsible for the reduction in the number of unique CDR3 sequences. A study by Wong *et al.* identified a pathway whereby B1a cells can bypass the need for a pre-BCR and generate a mature, albeit somewhat self-reactive, BCR directly (Wong et al., 2019). The V_H12/V_K4 pairing is typical for binding phosphatidylcholine, a lipid present in many bacteria membranes, and while V_H12 frequency of use is increased in B1a cells from TET2-KO mice, V_K4 frequency of use is lower in B1a cells from TET2-KO mice compared to WT (Supplemental Figure 8-9) (Wong et al., 2019). It should be noted that both V_H11 and J_H1 are associated with early fetal characteristics, which supports the potential enhancement of self-renewal that loss of TET2 regulation may foster (Kristiansen et al., 2016; Prohaska et al., 2018; Yang et al., 2015; Yoshimoto, 2020). Our CDR3 and VDJ association data from the heavy chain provide further evidence in addition to the light chain data that B1a cells are more profoundly impacted by global loss of TET2 compared to B-1b cells. The reason for this remains to be determined but may be due to the

expression of CD5 by B1a cells, given that studies have shown many of the malignant B cell samples with loss of TET2 express CD5 (Alayed et al., 2013; Ito et al., 2019; Pan et al., 2017), but this connection requires further study.

Taken together, our data reveals that loss of TET2 influences IgM level and BCR repertoire, particularly in B1a cells, which are key producers of natural IgM. Alteration to the antigen-specificity or abundance of B1a-produced IgM may have consequences in the response to PAMPs and DAMPs and in regulating antigen-driven inflammation. Our data demonstrating that loss of TET2 increased B-1 cell subset numbers in antibody-producing niches and reduced CDR3 diversity suggests that TET2 may regulate the pool of antigen-specific IgM produced by B-1 cells (Figure 3.8) and underscores the need for further study of the impact and mechanisms whereby TET2 regulates B-1 cells, especially in the context of infection and diseases involving chronic inflammation.

3.4 Methods

3.4.1 Mice

All animal protocols were approved by the Animal Care and Use Committee at the University of Virginia. TET2-KO mice (24) were provided by Dr. Kenneth Walsh (University of Virginia). The model was generated by Ko *et al.* and targeted the endogenous *TET2* locus to create a conditional allele that enabled the deletion of exons 8, 9, and 10, the catalytic region of TET2 (Ko et al., 2011). Mice were maintained on a 12-h light/dark schedule in a specific pathogen-free animal facility and given food (standard chow diet, Tekland 7012) and water *ad libitum*. The number of mice included in each study is indicated in the figures or the associated legends.

3.4.2 Sample Preparations for Flow Cytometry and Live Cell Sorting

Bone marrow, spleen, and peritoneal cavity cells were processed for flow cytometry as previously described (Rosenfeld et al., 2015). Briefly, following sacrifice by CO_2 overdose, peritoneal cells were harvested by flushing the peritoneal cavity with 10 mL FACS buffer (PBS containing 1% BSA, 0.05% NaN_3). The spleen and one femur and tibia were removed. Spleens and flushed bone marrow were filtered through a 70 μm cell strainer. Red blood cells were lysed from single-cell suspensions of bone marrow and spleen using a lysis buffer containing 155 mM NH_4Cl, 10 mM $KHCO_3$, and 0.1 mM EDTA. Cell surface Fc receptors were blocked using anti-CD16/32 (clone:93, 4 eBioscience), then cells were stained with fluorescently conjugated antibodies against cell surface markers. Cells were stained with fixable Live/Dead Zombie NIR (Life Technologies) for dead cell discrimination, then fixed in 2% PFA in PBS. For FAC sorting, cells were resuspended in modified FACS buffer (PBS with 1% BSA) and 4',6-Diamidino-2-Phenylindole (DAPI) live/dead stain then immediately taken to the University of Virginia Flow Cytometry Core for sorting. B1a and B-1b cells were sorted to better than 99% purity from their parent gate. Clone and fluorophore information for the flow cytometry antibodies used in murine experiments to immunophenotype or FAC-sort B cell subsets are given in Table 1 and Table 2 respectively. All flow cytometry was conducted at the University of Virginia Flow Cytometry Core Facility. Immunophenotyping was performed on an Aurora Borealis 5-laser (Cytek) cytometer. FAC-sorting was performed on an Influx Cell Sorter (Becton Dickinson). Data analysis and flow plots were generated using OMIQ software (Dotmatics). Representative flow plots were chosen based on the samples whose population frequencies were closest to the mean for that group. Gates on flow plots were set using fluorescence minus one (FMO) controls.

3.4.3 ELISA for quantification of total IgM in mice

Total IgM in mouse plasma was measured using colorimetric ELISA as described previously (Rosenfeld et al., 2015).-Briefly, EIA/RIA high-binding microplates were coated with goat anti-mouse IgM, capture antibody (Southern Biotech, 1020-01). Mouse IgM standards (Southern Biotech, 0101-01), or plasma samples were detected with alkaline phosphatase-conjugated goat anti-mouse IgM secondary antibody (Southern Biotech, 1020-04;) and pNPP substrate (Southern Biotech 0201-01). Absorbance measurements were analyzed with a SpectraMAX 190 microplate reader (Molecular Devices) at 405 nm. The standard curve was determined using a 4-parameter function and concentration measurements were extrapolated using Softmax Pro 3.1.2 software. Only samples with CV<15% and within the standard curve were included in the analysis.

3.4.4 Sample Preparation for Bulk RNA Sequencing

Peritoneal B1a, B-1b, and B-2 cells obtained from *TET2*-KO and *TET2*-WT C57BL/6 mice were sort-purified directly into RLT Plus Buffer (Qiagen). RNA and DNA were extracted using the Qiagen AllPrep kit. The purified RNAs were stored at −80 °C before being sent to Novogene for sequencing. Total RNA was stored in RNase-free water to directly synthesize first strand, followed by the whole-length LD-PCR amplification. The amplified ds-cDNA(double-stranded DNA) is purified with AMPure XP beads and quantified with Qubit. The cDNA samples were sheared by the Covaris system, and then the sheared fragments were end-repaired, A-tailed, and ligated to sequencing adaptors. A size selection of about 200 bp was performed before the PCR enrichment. Library concentration was first quantified using a Qubit 2.0 fluorometer (Life Technologies), and then diluted to 2 ng/μl before checking insert size on an Agilent 2100 and quantifying to greater

accuracy by qPCR. Ultra-low input bulk RNA sequencing was performed on the NovaSeq 6000 PE150 (Illumina).

3.4.5 DEG and Pathway Analysis

The quality trimming was performed using fastp (S. Chen, 2023) with default settings. Mapping to the GRCm39 genome was performed with STAR (Dobin et al., 2013), followed by featureCounts (Liao et al., 2014) to count reads mapped to genes. DESeq2 (Love et al., 2014) was used for differential analysis, followed by pathway analysis using clusterProfiler (T. Wu et al., 2021) with the Gene Ontology (GO) (Ashburner et al., 2000) database.

3.4.6 BCR Analysis

For BCR analysis, quality trimming was performed using fastp (S. Chen, 2023) and TRUST4 (K. Peng et al., 2023) was subsequently used to identify BCR repertoire in paired sequencing reads using the international ImMunoGeneTics (IMGT) information system database as a reference. Results were analyzed using R and circus plots were made using circos Bioconductor package (Gu et al., 2014). The code developed for these analyses will be available on the following Github page: https://github.com/mariamurach/TET2 and https://github.com/mariamurach/bcr_R upon publication.

3.4.7 Statistics

In Figure 3.1, Figure 3.2D, and Figure 3.4C, comparisons were conducted between the TET2-KO and WT strains using Prism 10.0 with unpaired, two-tailed Mann-Whitney U-tests. Values shown

are mean±SD. In Figure 3.3B and Figure 3.4A Wilcoxon Rank Sum and Signed Rank Tests were used to determine the significance of differences in proportions of unique CDR3 sequences, isotypes, and usages of specific V, D, and J chains between TET2-KO and WT groups. In Figure 3.5B, chi-squared test was performed to assess the significance of the association between the number of unique CDR3 amino acid sequences in B1a and B-1b cells from TET2-KO and WT mice.

Chapter 4

Mass Cytometry by Time of Flight Identifies Unique Immune Cell Signatures in Humans with Advanced Calcific Coronary Artery Disease

This chapter is a collective work of:

Jesse Cochran, † James McParland, † **Maria Murach,**† Chantel McSkimming, Hema Kothari, Christine Flora, Antony Haider, Corey Williams, Brett Ransegnola, Nisha Hosadurg, Toral Patel, Todd Villines, Angela Taylor, Stefan Bekiranov, Coleen McNamara

*authors contributed equally

List of supplementary files associated with this chapter:

- Supplement 4.1: Supplementary figures (S1-S6) and supplementary tables (S2-S3).
- Supplement 4.2: Supplementary table S1

4.1 Introduction

Atherosclerosis is characterized by the accumulation of lipid-laden plaques within the intimal layer of arteries and underlies diverse disease processes such as coronary artery disease (CAD), peripheral artery disease, and cerebrovascular disease. Rupture or erosion of unstable atherosclerotic plaques can lead to thrombus formation causing myocardial infarction (MI) and stroke, collectively the most common causes of death worldwide (Herrington et al., 2016; M. E. Kruk et al., 2018). In light of this substantial morbidity and mortality, coronary artery imaging can be a powerful tool to identify those at elevated risk for clinical events and help guide therapy. Coronary artery calcification (CAC), as a marker of total coronary plaque burden, has emerged as

a robust predictor of future coronary heart disease (CHD) events in asymptomatic individuals. Cohort studies have shown an increase in subsequent CHD event rate across strata of increasing baseline Agatston CAC scores (Detrano et al., 2008; Mohlenkamp et al., 2011). Compared against participants with a CAC score of zero, those with CAC scores >300 have approximately a 10-fold increased event rate (Tsao et al., 2023). Despite decades of advancement in the assessment and treatment of subjects with CAD, CHD remains the leading cause of death in the western world, attesting to the need for further investigation into the pathogenesis of atherosclerosis (Pahwa & Island, 2023).

PATIENT CHARACTERISTICS			
Measurement	**No CAC**	**High CAC**	**p-value**
Total	13	11	
Age (yrs)	63 (11)	66 (10)	0.535
Female	8 (0.62)	8 (0.73)	0.444
White	12 (0.92)	9 (0.82)	0.435
Diabetes	2 (0.15)	2 (0.18)	0.637
Dyslipidemia	7 (0.54)	7 (0.64)	0.473
Hypertension	6 (0.46)	8 (0.73)	0.185
History of Smoking	6 (0.46)	6 (0.55)	0.500
Renal Insufficiency	0 (0)	0 (0)	1.000
Statins	3 (0.23)	6 (0.55)	0.122
Non-statin Lipid Lowering Drugs	0 (0)	1 (0.09)	0.458
BMI (kg/m^2)	27 (3)	33 (8)	0.042
SBP (mmHg)	125 (22)	128 (20)	0.724
A1C (%)	6 (2)	6.0 (0.7)	0.073
hsCRP (mg/L)	2 (2)	2 (2)	0.507
eGFR ($mL/min/1.73m^2$)	84 (15)	92 (15)	0.221
WBC (k/uL)	7 (2)	6 (2)	1.000
Hemoglobin (k/uL)	14 (1)	13.5 (0.5)	0.356
Platelets (k/uL)	258 (44)	257 (61)	0.552
Total Cholesterol (mg/dL)	210 (53)	187 (62)	0.343
Triglycerides (mg/dL)	125 (58)	108 (47)	0.441
HDL Cholesterol (mg/dL)	51 (7)	50 (15)	0.835
LDL Cholesterol (mg/dL)	138 (50)	118 (54)	0.372
Coronary Artery Calcification Score	0 (0)	551 (284)	4×10^{-7}

Segment Involvement Score	0.2(0.6)	8 (2)	4×10^{-7}
Segment Stenosis Score	0.2(0.6)	13 (5)	4×10^{-7}

Table 4.1 Clinical characteristics for subject cohort.
Categorical variables are expressed as absolute count with frequency in parentheses while continuous variables are expressed as mean with standard deviation in parentheses. BMI: body mass index, SBP: systolic blood pressure, A1C: hemoglobin A1C, hsCRP: high sensitivity C reactive protein, eGFR: estimated glomerular filtration rate, WBC: white blood cells, HDL: high-density lipoprotein, LDL: low-density lipoprotein.

The development of atherosclerosis is a complex and multifactorial process involving vessel damage, lipid accumulation, and inflammation. While specific treatments have been developed to target many of these causes, inflammation remains a key mediator unaddressed by current targeted therapies. In atherosclerosis, cholesterol accumulation in macrophages can activate the NLRP3 inflammasome, resulting in IL-1β secretion (Curtiss & Tobias, 2009; Duewell et al., 2010). This secreted IL-1 can induce expression of IL-6, which elicits an acute phase response (Loppnow & Libby, 1990). At a cellular level, IL-1β induces phosphorylation of the transcription factor NF-κB and kinases p38 and ERK while IL-6 induces phosphorylation of the transcription factors STAT1, STAT3, and STAT5 (Kang & Kishimoto, 2021; Virtue et al., 2012). These activated transcription factors can subsequently promote inflammatory gene expression, which can drive atherosclerosis progression (Huber et al., 1999). Given the plausible causative mechanism for IL-1β, the Canakinumab Anti-Inflammatory Thrombosis Outcomes Study (CANTOS) trial was conducted, demonstrating that IL-1β inhibition with canakinumab reduced composite cardiovascular endpoints by 15% in subjects with previous MI and elevated C-reactive protein (Ridker et al., 2017). Furthermore, subjects who achieved greater reduction in IL-6 after the first dose of canakinumab had an enhanced reduction in major adverse cardiovascular event (MACE) rate compared to those who did not (Ridker et al., 2018). Additionally, in the phase 2 RESCUE trial, the IL-6 inhibitor ziltivekimab demonstrated reductions in inflammatory biomarkers linked to

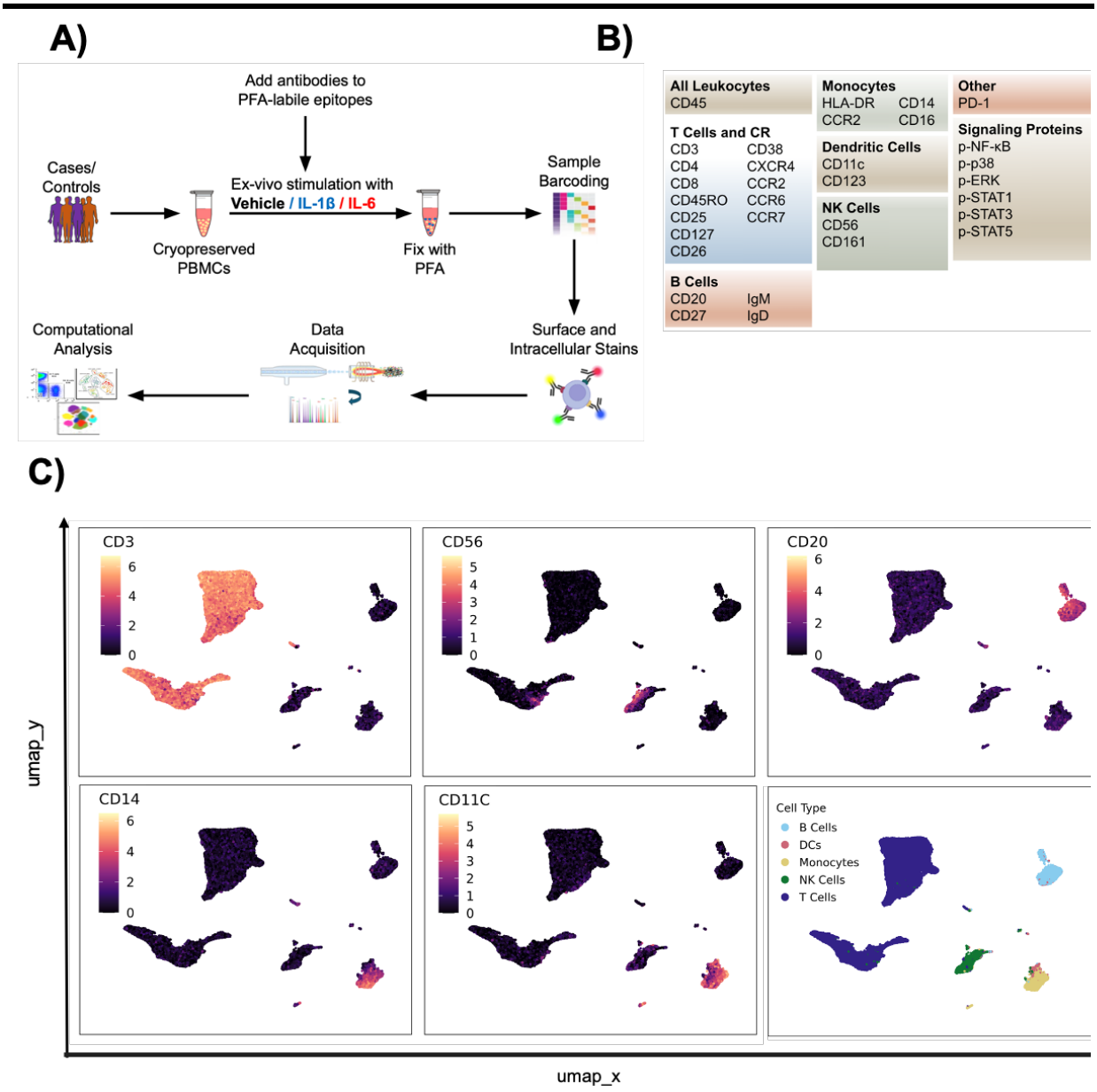

Figure 4.1 Mass cytometry identifies major immune cell populations within PBMCs from the patient cohort

A: Experimental paradigm for study. **B:** CyTOF antibody panel used for analysis. **C:** UMAP analysis of WBCs, showing expression of characteristic surface markers and annotation for cell identity. Panel A made by JMP, panel B made by JC.

MACE in subjects with advanced chronic kidney disease, a population traditionally at excessively high risk for atherosclerotic events (Ridker et al., 2021).

Collectively, a clear connection between IL-1β, IL-6, and atherosclerosis has been established; however, the specific changes in immune cell populations and immune cell signaling in subjects referred for coronary imaging remain unknown. Here we present our pilot study, where in our small 24 subject cohort, we utilized mass cytometry by time of flight (CyTOF) to identify and characterize cell populations specifically reactive to the pro-inflammatory cytokines IL-1β and IL-6 in subjects with no detectable CAC and subjects with advanced calcific atherosclerotic disease (Bandura et al., 2009; Bendall et al., 2011).

4.2 Results

4.2.1 IL-1β and IL-6 induce phosphorylation of effector molecules in distinct immune cell populations

Cytometry by time of flight (CyTOF) was performed on PBMCs from subjects undergoing clinically indicated coronary computed tomography angiography (cCTA) at the University of Virginia. A subset of this cohort composed of 13 individuals without detectable coronary artery calcification (CAC) as defined as a CAC score = 0 and 11 individuals with advanced coronary artery calcification as defined as a CAC score ≥ 300 was used for this study. Demographics and baseline characteristics among individuals with no CAC and individuals with advanced CAC were similar (**Table 4.1**) with the exception that subjects with advanced CAC had a greater BMI (33 vs 27 kg/m^2, p=0.042) compared to subjects without CAC (**Table 4.1**) Subjects with advanced CAC had higher CAC scores (551 vs 0, p= 4 x 10^{-7}), segment involvement scores (13 vs 0.2, p= 4 x 10^{-7}), and segment stenosis scores (8 vs 0.2, p= 4 x 10^{-7}) compared to subjects without CAC (Table 4.1)**.**

Carefully thawed cryopreserved PMBCs from these subjects were stimulated, fixed, barcoded, stained, and analyzed via cytometry by time of flight (CyTOF) with a 31-antibody panel

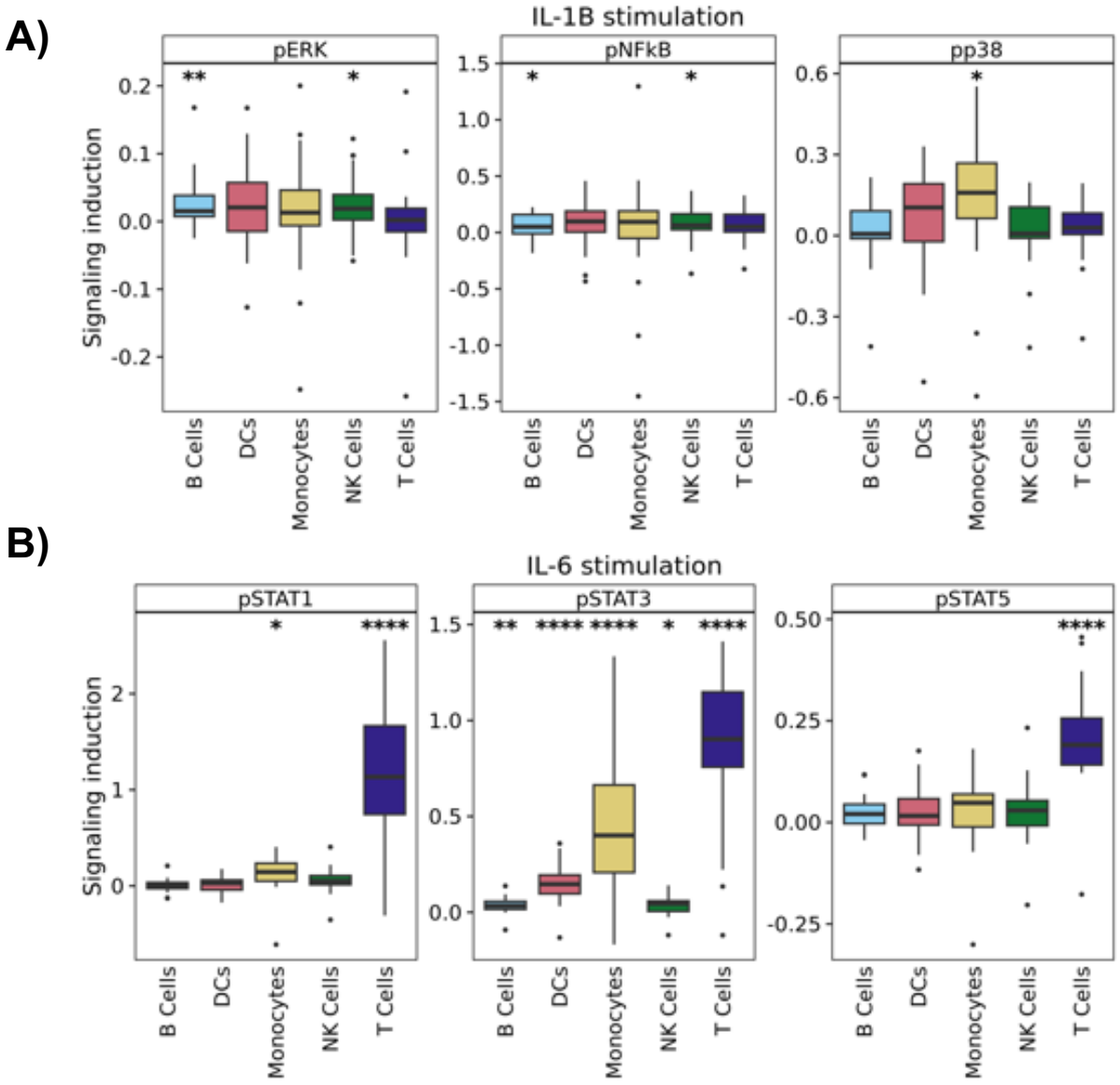

Figure 4.2 IL-1β and IL-6 induce phosphorylation of transcription factors in human T cells

A: Signal induction of the specified transcription factor or kinase within the indicated immune cell subset following IL-1β stimulation of PBMCs. Paired T test with FDR correction was used to determine if there was a statistically significant difference between the unstimulated and stimulated condition (n=24). *p<0.05, **p<0.01 **B:** Signal induction of the specified transcription factor or kinase within the indicated immune cell subset following IL-6 stimulation of PBMCs. Paired T test with FDR correction was used to determine if there was a statistically significant difference between the unstimulated and stimulated condition (n=24). *p<0.05, **p<0.01, ****p<0.0001

(**Figure 4.1A-1B**). PBMCs were stimulated with either IL-1β or IL-6 for 15 minutes as previous work by our lab has established that this incubation time confers maximal activation of several

downstream effectors of IL-1β signaling (Kothari et al., 2021). Additionally, the 15-minute stimulation with IL-6 results in maximal activation of p-STAT1 and p-STAT3 and robust activation of p-STAT5 (**Supplemental Figure 4)**. UMAP and SPADE analysis were employed on gated white blood cells (**Figure 4.1C, Supplemental Figures 5A**) and were sufficient to resolve populations of T cells, B cells, monocytes, dendritic cells (DCs), and NK cells (**Figure 4.1C-1D, Supplemental Figure 5A**). Gating on these specific cell types, we quantified the differences in median expression of downstream effector molecules between the unstimulated and stimulated condition for each immune subtype. IL-1β induced phosphorylation of ERK relative to vehicle treatment alone in B cells (**Figure 4.2A**). There were no other statistically significant differences in effector molecule activation, following IL-1β stimulation. However, monocytes and dendritic cells displayed a tendential increase in both NF-kB and p38 with IL-1β stimulation. IL-6, on the other hand, induced phosphorylation of STAT1 in myeloid cells and T cells, phosphorylation of STAT3 in all immune subtypes, and phosphorylation of STAT5 in T cells exclusively **(Figure 4.2B).** Moreover, T cells exhibited the most pronounced induction in STAT1, STAT3, and STAT5 following IL-6 stimulation relative to all other immune cell subtypes (**Figure 4.2B).**

Given CAC is a key index of CVD event risk, subjects were subsequently stratified into either no CAC or high CAC groups, and immune cell response to IL-1β and IL-6 stimulation was examined. No statistically significant changes were detected. Yet, high CAC was associated with a trending decrease in phosphorylation of NF-kB and p38 in monocytes and DCs following IL-1β stimulation (**Figure 4.3A**). Additionally, NK cells from high CAC patients tended to display a decrease in NF-kB induction with IL-1β stimulation compared to NK cells from no CAC patients**.** On the other hand, high CAC was associated with a trending increase in the activation of STAT3 in monocytes and dendritic cells following IL-6 stimulation **(Figure 4.3B).** Additionally, T cells from patients with high CAC displayed a trending decrease in the phosphorylation of STAT1, STAT3, and STAT5 with IL-6 stimulation compared to T cells from patients with no CAC**.**

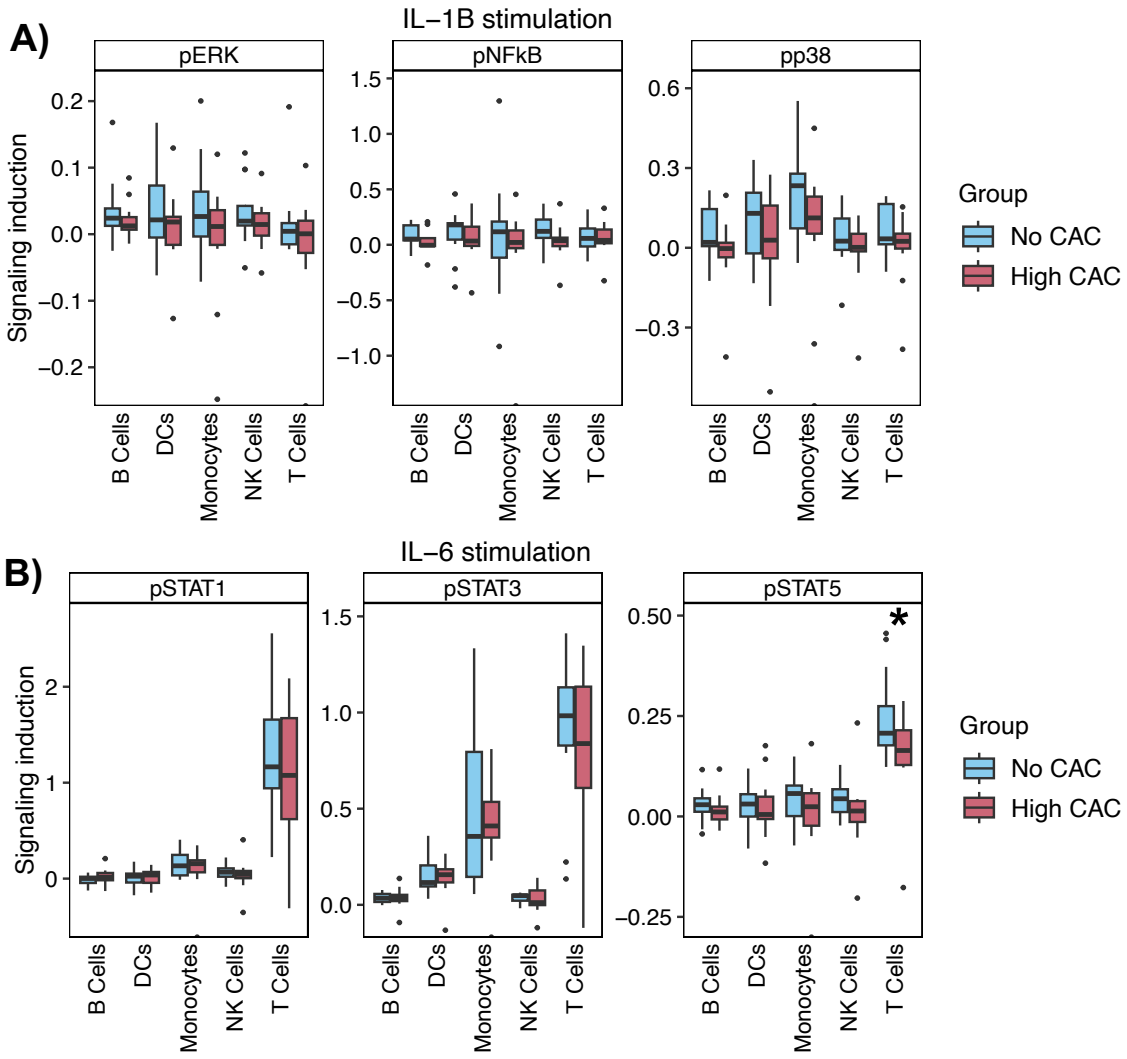

Figure 4.3 CAC burden is not associated with differences in hallmark immune response to IL-1β and IL-6 stimulation

A: CAC-stratified signal induction of the specified transcription factor or kinase within the indicated immune cell subset following IL-1β stimulation of PBMCs. Statistical significance between high CAC and no CAC was determined by one sample T test with FDR correction (n=11-13). **B:** CAC-stratified signal induction of the specified transcription factor or kinase within the indicated immune cell subset following IL-6 stimulation of PBMCs. Statistical significance between high CAC and no CAC was determined by one sample T test with FDR correction (n=11-13).

4.2.2 Circulating T cell subset frequencies are unaffected by exogenous cytokine stimulation

Given the pronounced response of T cells to inflammatory cytokines, we aimed to identify the particular T cell subsets mediating this response. As such, T cells were manually gated from the total WBC population (**Supplemental Figure 2**) and then underwent supervised Leiden clustering, yielding 12 distinct T cell subpopulations (**Figure 4.4A**). Clusters were then annotated by surface marker expression (**Figure 4.4B**). Clustering was sufficient to identify 3 subsets of $CD4^+$ naïve T cells (clusters 1, 4, and 12), 4 subsets of $CD4^+$ effector memory T cells (clusters 2, 6, 7, and 9), 2 subsets of $CD8^+$ naïve T cells (clusters 5 and 8), 1 subset of $CD8^+$ effector T cells (cluster 3), and 2 subsets of double-negative T cells (clusters 10 and 11). Follicular T (Tfh) cells (cluster 2: $CD4^+$, $CD45RO^+$, $CD127^+$, $CCR7^+$) and $CD4^+$ $CXCR4^+$ naive T cells (cluster 1: $CD4^+$, $CD45RO^-$, $CXCR4^+$) represented the two largest T cell clusters (**Figure 4.4C**). Stimulation with either IL-1β and IL-6 did not alter cell cluster frequency, confirming stability of the surface proteins used for clustering.

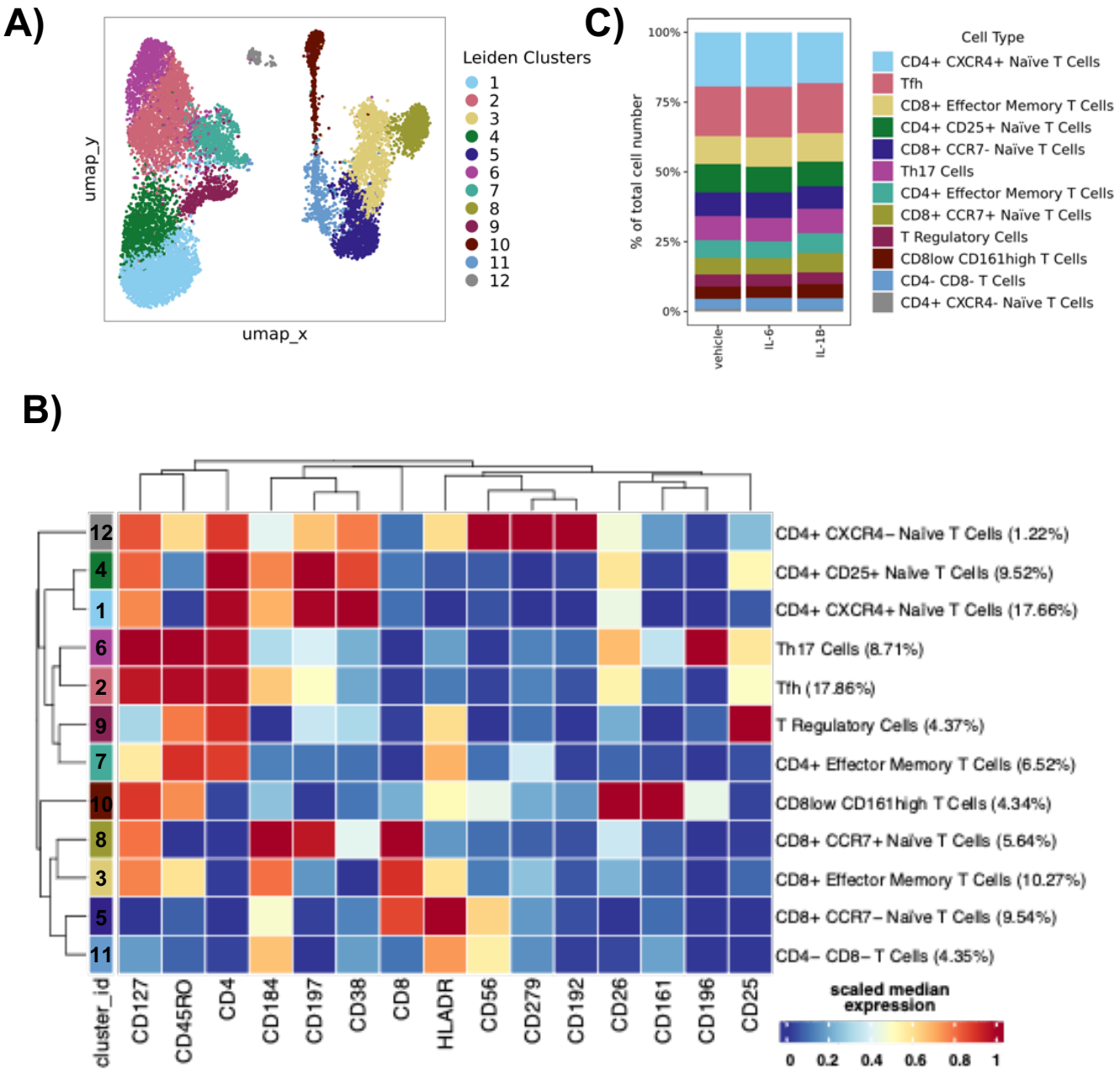

Figure 4.4 Leiden clustering of T cells reveals distinct T cell subpopulations

A: UMAP generated from Leiden clustering of T cells with annotations corresponding to cluster identity. **B:** Heatmap of surface marker expression in each of the clusters. **C:** Cluster frequency in each of the stimulation conditions. Paired T test with FDR correction was used to determine if there was a statistically significant difference between the unstimulated and stimulated condition (n=24).

4.2.3 Specific T cell subpopulations respond to IL-1β and IL-6 stimulation

In contrast, following IL-1β stimulation, there was an increase in phosphorylation of NF-κB in Th17 cells (cluster 6: $CD4^+$ $CD45RO^+CCR6^+CD161^+CD26^+$) by percent phosphorylation (**Figure 4.4A**) and mean expression (**Supplemental Table 3)**. Though not statistically significant, there was a trending increase in the phosphorylation of NF-κB in T regulatory (Treg) cells (cluster 9: $CD4^+$ $CD45RO^+CD25^+CD127^{low/-}$) and $CD8^{low}CD161^{high}$ T cells (cluster 10: $CD4^-$ $CD8^{low}CD161^{high}$) (**Figure 4.5A)**. There were no differences in the phosphorylation of ERK, p38, STAT1, STAT3, or STAT5 following IL-1β stimulation (**Figure 4.5A, Supplemental Table 3**).

IL-6 stimulation, on the other hand, caused robust phosphorylation of STATs in several T cell subsets. Unlike IL-1β, IL-6 induced phosphorylation of STAT3 in all T cell subsets with follicular T (Tfh) cells and Th17 cells, showing the most pronounced response (**Figure 4.5B, Supplemental Table 3**). Furthermore, following IL-6 stimulation, there was an increase in the phosphorylation of STAT1 in all cell types except $CD8^+$ $CCR7^-$ naïve T cells (cluster 5: $CD8^+CD45RO^-CCR7^-$) and $CD8^{low}CD161^{high}$ T cells (cluster 10: $CD4^-CD8^{low}CD161^{high}$) and an increase in the phosphorylation of STAT3 in all cell types besides $CD8^+$ effector memory T cells (cluster 3: $CD8^+CD45RO^+$), and $CD8^+$ $CCR7^-$ naïve T cells, $CD8^{low}CD161^{high}$ T cells, CD4- CD8- T cells (cluster 11: $CD4^-CD8^-$). Notably, different T cell subsets exhibited differences in IL-6-

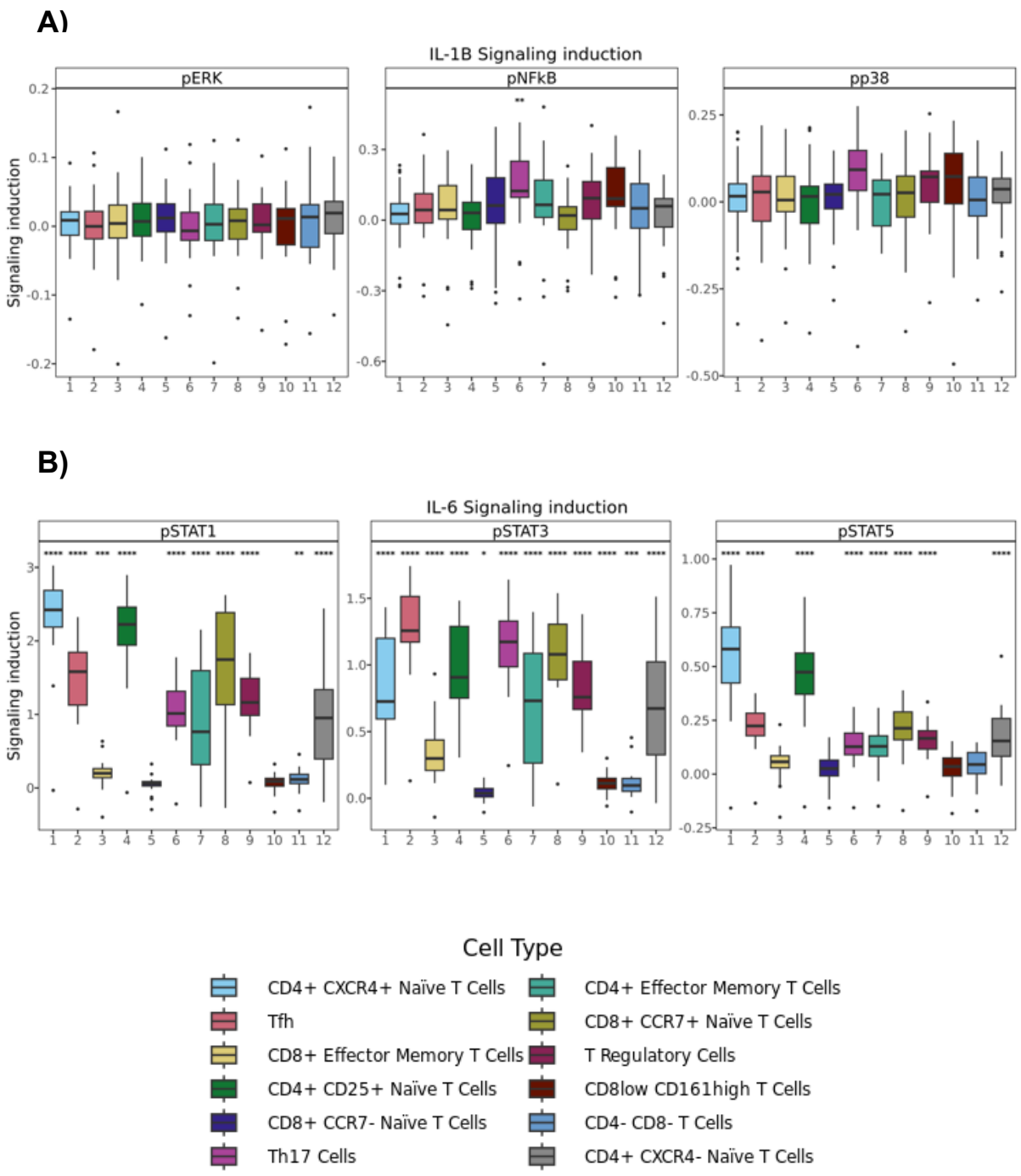

Figure 4.5 Unique T cells subsets respond to IL-1β and IL-6 stimulation

A: Signal induction of the specified transcription factor or kinase within the indicated T cell cluster following IL-1β stimulation of PBMCs. Paired T test with FDR correction was used to determine if there was a statistically significant difference between the unstimulated and stimulated condition (n=24). **p<0.01 **B:** Signal induction of the specified transcription factor or kinase within the indicated T cell cluster following IL-6 stimulation of PBMCs. Paired T test with FDR correction was used to determine if there was a statistically significant difference between the unstimulated and stimulated condition (n=24). *p<0.05, **p<0.01, ***p<0.001, ****p<0.0001

mediated phosphorylation of STAT1, STAT3, and STAT5. For both STAT3 and STAT5, $CD4^+$ $CXCR4^+$ Naïve T cells and $CD4^+$ $CD25^+$ Naïve T cells (cluster 4: $CD4^+$, $CD45RO^-$, $CD25^+$) demonstrated the most robust response (**Figure 4.5B, Supplemental Table 3**). There were no differences in the phosphorylation of ERK, NF-κB, or p38 following IL-6 stimulation (**Supplemental Table 3**).

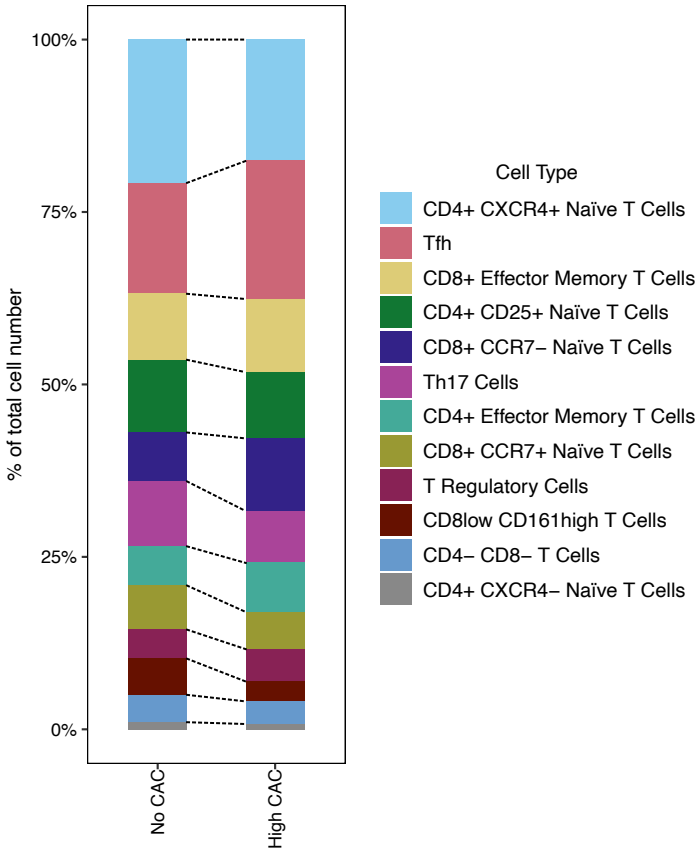

Figure 4.6 CAC burden is not associated with differences in T cell cluster frequency
T cell cluster frequency for subjects with no CAC and subjects with high CAC. Statical significance between high CAC and no CAC was determined by one sample T test with FDR correction (n=11-13).

4.2.4 Correlation of CAC burden with T cell subtype frequency and cytokine-stimulated responses

To better characterize the alterations in T cell frequency and physiology based on CAC status, subjects were subsequently stratified into either no CAC or high CAC groups, and differences in cell cluster frequency and cytokine response were determined. Though no statistically significant differences in the cluster frequency were observed between subjects with high or no CAC, there was a trend toward an increase in the frequency of effector memory T cell subsets and a trend toward a decrease in the frequency of naïve T cell subsets **(Figure 4.5)**. Specifically, there were trends toward decreases in the cluster frequencies of $CD4^+$ $CXCR4^+$ naïve T cells, $CD4^+$ $CD25^+$ naïve T cells, and $CD4^+$ $CXCR4^-$ naïve T cells and trends toward increases in the cluster frequencies of Tfh cells, $CD4^+$ effector memory T cells, and $CD8^+$ effector memory T cells **(Figure 4.5)**. Though not statistically significant, high CAC burden was trending towards an association with an attenuated response to both IL-1β and IL-6 in numerous T cell subsets **(Figure 4.6A-B, Supplemental Table 4)**. Following IL-1β stimulation, there appeared to be a decrease in the phosphorylation of NF-κB in Th17 cells and $CD8^{low}CD161^{high}$ T cells from subjects with high CAC compared to subjects without CAC **(Figure 4.6A)**. Furthermore, following IL-6 stimulation, high CAC was associated with a trend toward a decrease in the phosphorylation of STAT1 in Tfh, cells, $CD4^+$ effector memory T cells, and $CD4^+$ $CXCR4^-$ naïve T cells, a trend toward a decrease in the phosphorylation of STAT3 in $CD4^+$ $CD25^+$ naïve T cells, T regulatory cells, and $CD4^+$ $CXCR4^-$ naïve T cells, a trend toward a decrease in the phosphorylation of STAT5 in $CD4^+$ $CXCR4^+$ naïve T cells, T regulatory cells, and $CD4^+$ $CXCR4^-$ naïve T cells **(Figure 4.6B)**.

Given the attenuated response of T cells from high CAC patients, we characterized the possible role of immune checkpoint PD-1. Though PD-1 expression was not significantly

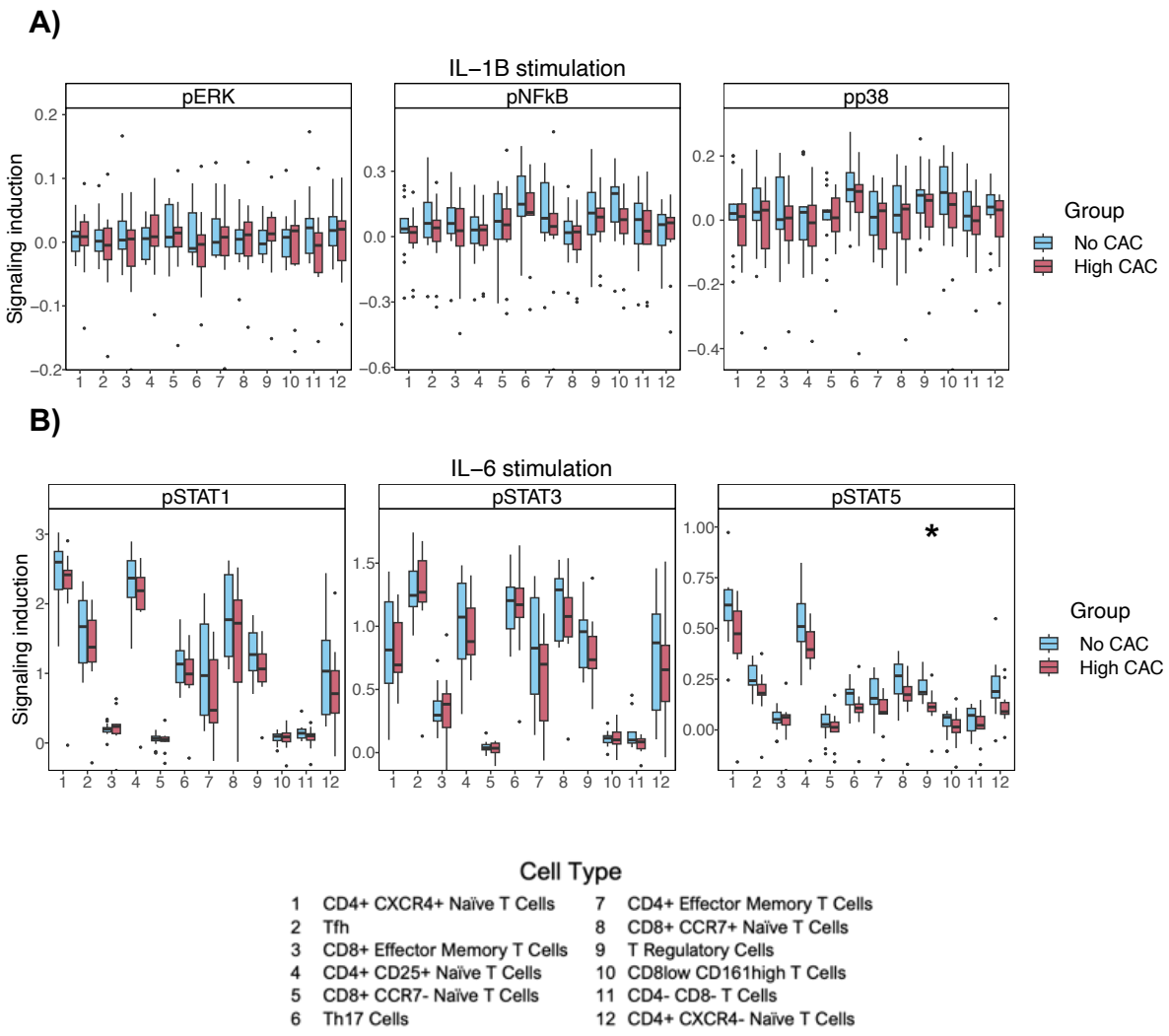

Figure 4.7 CAC burden is not associated with differences in T cell response to IL-1β and IL-6 stimulation
A: Signal induction of the specified transcription factor or kinase within the indicated T cell cluster after IL-1β stimulation of PBMCs from subjects with no CAC and subjects with high CAC. Statical significance between high CAC and no CAC was determined by one sample T test with FDR correction (n=11-13). **B:** Signal induction of the specified transcription factor or kinase within the indicated T cell cluster after IL-6 stimulation of PBMCs from subjects with no CAC and subjects with high CAC. Statical significance between high CAC and no CAC was determined by one sample T test with FDR correction (n=11-13).

differentially expressed in T cell subset based on CAC status, $CD8^+$ CCR7- naive T cells from high CAC patients tended to display increased PD-1 expression compared to $CD8^+$ CCR7- naive T cells from no CAC patients (Supplemental Figure 7). Interestingly, in high CAC patients, higher PD-1 expression on $CD8^+$ CCR7- naive T cells was tendentially associated with reduced expression of

pSTAT1 and pSTAT5 in response to IL-6 and pERK after IL-1β stimulation. Additionally, higher PD1 expression in a number of different T cells subsets was trending towards an association with reduced expression of several effectors of both IL-1β and IL-6 after stimulation (Supplemental Table 7).

Due to the high proportion of females in this cohort, a secondary analysis examining the significance of biological sex was performed. Interestingly, males had a trending increase in IL-1β -mediated NF-kB and p38 phosphorylation and a trending decrease in IL-6 mediated STAT1, STAT3, and STAT5 phosphorylation across CAC strata (Supplemental Figure 6A-6B, Supplemental Tables 8-9).

4.3 Discussion

Over the last several decades, an ever-growing body of evidence has accumulated, supporting the role of IL-1β and IL-6 in the development of atherosclerosis and its complications.(30-32) In murine models, IL-1 and specifically, the IL-1β isoform promote atherogenesis while genetic ablation of the IL-1 receptor is atheroprotective (Chi et al., 2004; Elhage et al., 1998; Kirii et al., 2003; Merhi-Soussi et al., 2005; Vromman et al., 2019). Analogously, exogenous IL-6 is atherogenic and destabilizes atherosclerotic plaques in hypercholesterolemic mice (Akita et al., 2017; Huber et al., 1999; Schuett et al., 2012; K. Zhang, Huang, et al., 2012). Clinically, disruption of IL-1β signaling has garnered considerable interest for treating cardiovascular disease (CVD). The CANTOS trial found that IL-1β blockade decreased recurrence of adverse cardiovascular events in subjects with stable atherosclerotic disease and elevated CRP. Furthermore, inhibition of the NLRP3 inflammasome, which is responsible for the production of mature IL-1β, has been associated with reduced incidence of atherothrombotic events in subjects with stable CAD and reduced incidence of ischemic events in subjects with recent acute

myocardial infarction (Nidorf et al., 2013; Tardif et al., 2019). In accordance, IL-6 has found numerous clinical uses since its emergence as a biomarker for cardiovascular risk in the mid 1990s. In genome wide association studies (GWAS), activating variants in the IL-6R have been implicated in CAD while variants connected to reduced IL-6 signaling are associated with decreased CAD risk and increased longevity (C et al., 2012; Cai et al., 2018; IRGCERF et al., 2012; Rosa et al., 2019; Theriault et al., 2019). Additionally, elevated plasma IL-6 levels predict worse outcomes in stable heart disease, acute coronary ischemia, and heart failure (Groot et al., 2019; Held et al., 2017; Markousis-Mavrogenis et al., 2019). Furthermore, in carotid atherosclerosis, IL-6 levels predict carotid plaque severity, vulnerability, and progression (Kamtchum-Tatuene et al., 2022).

In order to query response to inflammatory cytokine stimulation, our study examined differences in the phosphorylation state of effector molecules of IL-1β or IL-6 signaling (Kang & Kishimoto, 2021; Virtue et al., 2012). The transcription factor NF-κB and the kinases ERK and p38 were selected as they have been implicated as key components in interleukin 1 receptor (IL-1R)-mediated immune cell activation (Dinarello, 2009; Lee et al., 2019; Towne et al., 2004). On the other hand, the transcription factors STAT1, STAT3, and STAT5 were chosen for their role in IL-6 mediated immune cell activation (Haan et al., 2005; Tormo et al., 2012; Twohig et al., 2019; Zegeye et al., 2018). Previous work by our lab has identified human immune cell subpopulations in T cells, myeloid cells, and NK cells responsive to IL-1β stimulation and found that T cells were the most responsive population to IL-1β stimulation in a cohort of healthy controls (Kothari et al., 2021). In the present study, IL-1β also induced p-NF-κB in T cells, in addition to myeloid cells and NK cells (Fig 2A). Notably, T cells were clearly the predominant immune cell activated in response to IL-6 as evidenced by increased phosphorylation of all three STATs (Fig. 2B), although STAT3 was also activated in myeloid cells. Given the predominant role of T cells in the activation by both of these cytokines, and unique roles of various T cell subtypes in atherosclerosis (Saigusa et al., 2020), we focused our analysis on specific T cell subtypes.

Given the small number of participants and the pilot nature of the study, we were able to observe mostly trends in association of the activation stratus of immune cells with the CAC score. While our study is not powered to detect differences between subjects with no CAC and subjects with high CAC, several interesting trends emerged. Subjects with high CAC tended to have expanded effector memory T cell clusters relative to naïve T cell clusters. Consistent with these findings, in humans, effector memory T cells have been associated with increased CAC, increased common carotid artery intimal media thickness, and IL-6 levels (Ammirati et al., 2012; Olson et al., 2013). Notably, these previous studies recruited between 313 to 912 participants. Thus, the differences in sample size and therefore power may underpin the discrepancy in statistical significance between our and previous findings. In concordance with prior work (Kothari et al., 2021), $CD4^+$ effector memory T cells were robustly activated by IL-1β. Namely, Th17 cells demonstrated a pronounced induction of p-NF-κB. Interestingly, in mice, increased effector memory cells and an elevated Th17/ regulatory T cell ratio have been observed in murine genetic models of atherosclerosis (Ammirati et al., 2012; Xie et al., 2010). Moreover, in late stages of murine atherosclerosis, there was an attenuated Th17 response as evidenced by lower Th17-related transcripts within the atherosclerotic plaques and lower Th17 cytokines within the serum (Xie et al., 2010, 2010). These results are consistent with our own, which found that high CAC tended to be associated with attenuated IL-1β-induced phosphorylation of NF-κB in Th17 cells. Unlike IL-1β, IL-6 induced a widespread phosphorylation of STAT1, STAT3, and STAT5 throughout most T cell subpopulations. Additionally, in our study, subjects with high CAC tended to have an attenuated response to IL-1β and IL-6 stimulation compared to subjects with no CAC. This surprising result is intriguing and may be potentially explained by desensitization of the interleukin 1 receptor (IL-1R) and interleukin 6 receptor (IL-6R) due to chronic stimulation. In humans, serum levels of both IL-1β and IL-6 are known to be increased in subjects with coronary artery disease compared to control individuals (Parisi et al., 2020; Wainstein et al., 2017). Furthermore, *in* vitro,

IL-1β pretreatment attenuates subsequent phosphorylation of NF-κB in response to IL-1β while IL-6 pretreatment attenuates subsequent phosphorylation of STAT3 in response to IL-6 (Fischer et al., 2004; McKean et al., 1994). The feasibility of this hypothesis is further supported by findings in breast cancer. Analogously, subjects with breast cancer display attenuated IL-6 induced phosphorylation of STAT1 and STAT3 in CD4 naïve T cells compared to control subjects, which coincides with decreased expression of IL-6Rα and gp130 on the CD4 naïve T cells from subjects with breast cancer (L. Wang et al., 2017). Furthermore, in advanced atherosclerotic lesions, T cells exhibit an exhausted phenotype by surface marker expression and transcriptomics (Fernandez et al., 2019). Based on these intriguing findings, a larger sample size needs to be analyzed in the future with a CyTOF panel composed of exhaustion markers, interleukin receptors, and additional downstream effector molecules.

The identification of these novel T cell subpopulations responsible for immune cytokine response spurs myriad avenues for further investigation. Firstly, humanized mouse models adoptively transferred with these human T cell subpopulations with knockdown of the IL-1 or IL-6 receptors could be used to determine if human T cells activated by these cytokines drive vascular inflammation. These findings may be helpful in better tailoring immunotherapy against deleterious T cell subpopulations. Towards clinical applications, CyTOF of circulating immune cells may predict prognosis and/or response to immunotherapy. As IL-6 has been associated with both prognosis and response to treatment, changes in immune cell response to this cytokine may be more biologically informative and serve as a better predictor of both prognosis and treatment response than traditional inflammatory biomarkers.

Despite these advances in our understanding, there are limitations to the present study. Firstly, the sample size is modest. As such, findings will need to be corroborated in a larger cohort, allowing for multivariate analysis. Secondly, though we are capable of identifying cell types responsive to inflammatory cytokine stimulation, the biological significance of these populations

remains unknown. Therefore, further mechanistic studies are warranted to better characterize these populations.

Nevertheless, CyTOF represents a powerful tool to identify and characterize novel human immune cell populations in cohorts of subjects undergoing coronary artery imaging. Follow-on studies in a larger cohort with a more robust CyTOF panel informed by the data herein will move us closer to understanding functional differences in human immune cells in the context of CVD.

4.4 Materials and Methods

4.4.1 Subject Population

Subjects referred to the University of Virginia for clinically indicated combined coronary computed tomography angiography (CTA) and CAC scoring were consented to participate in this study (IRB #: 210006). Peripheral blood was collected for peripheral blood mononuclear cell (PBMC) isolation and carefully cryopreserved for future use. Additionally, peripheral blood samples were obtained from healthy individuals and used as internal controls for standardization of CyTOF experiments (IRB#: 16017). The study was approved by the Human Institutional Review Board, and all participants provided written informed consent before enrollment.

4.4.2 Coronary Artery Disease Measurements

CAC scores were obtained as part of clinically indicated coronary CTAs among all enrolled subjects. All scans were performed on a 3rd generation 192-detector dual source platform (SOMATOM Force, Siemens Healthcare GmbH). Subjects underwent non-contrast electrocardiogram-gated CT from the carina to below the heart using a high pitch spiral technique

(triggered at 65% of the electrocardiographic R-R interval) with a slice thickness of 3.0 mm. All scans were analyzed using semi-automated software (syngo.via VB60A_HF05, Siemens Healthcare GmbH) with calcium scores calculated using the Agatston method (Agatston et al., 1990).

The segment involvement score (SIS) and the segment stenosis score (SSS) were calculated as previously described (Ayoub et al., 2017; J. K. Min et al., 2007). Briefly, SIS was calculated as the summation of the absolute number of coronary segments exhibiting plaque with a maximum score of 16. To calculate the SSS, each coronary segment was graded based on extent of lumen occlusion (i.e., scores ranged from 0 to 3). These grades were then summed for all 16 individual segments to yield a total SSS, which ranged from 0 to 48.

4.4.3 PBMC Isolation

PBMCs were isolated as previously described (Kothari et al., 2021). Briefly, blood from participants was collected into BD K2 EDTA vacutainer tubes (CAT#: 367855, FisherScientific), incubated at room temperature for one hour, and centrifuged to remove platelet rich plasma. PBMCs were separated via Ficoll-Paque density-gradient centrifugation (CAT#: 17144003, Cytiva) and SepMate-50 (CAT#: 85460, StemCell). PBMCs were cryopreserved in freezing solution (90% FBS, 10% DMSO) using a Mr. Frosty freezing container (CAT#: 5100-0001, Thermo Scientific) and stored in liquid nitrogen until use.

4.4.4 PBMC Stimulation, Barcoding, and CyTOF Staining

Cells were thawed in complete thaw media (RPMI, 5% FBS, 1 mM sodium pyruvate and 1% Pen-Strep) supplemented with DNase and then washed once with complete thaw media. Cells

were then incubated for 5 minutes in cisplatin solution (CAT#: 201194, Fluidigm). Cisplatin solution was quenched with complete thaw media and centrifuged. Samples were aliquoted into three separate groups on a 96-well plate, allowed to rest for 1 hour, and then stained with PFA-labile metal-conjugated antibodies. Samples were then incubated with either media, IL-1β, or IL-6 solution for 15 minutes. Following stimulation, cells were immediately fixed with 1.6% PFA for 10 minutes. Samples were then resuspended in Maxpar Cell Staining Buffer (CAT#: 201068, Maxpar) and stored overnight at 4 °C. Samples were washed twice with 1x Maxpar Barcode Perm Buffer (CAT#: 201057, Maxpar) prior to barcoding with palladium-based 20-Plex Pd Barcoding Kit (CAT#: 201060, Fluidigm). Barcoded cells were pooled and blocked with Fc receptor blocking solution (CAT#: 422302, Biolegend) and stained with metal-conjugated antibody solution against cell surface markers for 30 minutes (**Supplementary Table 1**). Cells were washed with a cell staining buffer and then permeabilized with 100% methanol for 10 minutes on ice. Samples were washed twice with PBS and subsequently cell staining buffer. Samples were then incubated with metal-conjugated antibody solution against intracellular markers (**Supplementary Table 1**). Cells were washed once with cell staining buffer before being resuspended in Maxpar Fix and Perm Buffer (CAT#: 201067, Maxpar) supplemented with iridium DNA intercalator (CAT#: 201192A, Fluidigm). Cells were incubated overnight at 4 °C. The sample was then washed once with cell staining buffer and twice with Maxpar Cell Acquisition Solution (CAT#: 201237, Maxpar). Samples were filtered with 40 μm membrane strainer (CAT#: 22363547, Fisherbrand), and EQ Four Element Calibration Beads (CAT#: 201078, Fluidigm) were added before acquisition on a Helios mass cytometer (Fluidigm).

4.4.5 CyTOF data pre-processing and sub-population gating

Data obtained from Helios were exported in .fcs files. Data was normalized and debarcoded with the the Nolan lab MATLAB normalizer (http://github.com/nolanlab/bead-normalization/releases) and Zunder's lab debarcoder (https://github.com/zunderlab/single-cell-debarcoder), respectively (Finck et al., 2013; Fread et al., 2017). Data was uploaded to OMIQ for further processing. Data underwent quality control gating to obtain CD45+ WBC populations as outlined in Supplemental Figure 1. B cells, T Cells, NK cells, and myeloid cell populations were subsequently gated from the CD45+ WBC as outlined in Supplemental Figure 2. Gated populations were then exported as .fcs files for downstream analysis.

4.4.6 SPADE trees

For spanning-tree progression analysis for density-normalized events (SPADE) analysis, all .fcs files were imported to "SPADE3" program in MATLAB and clustered using following surface markers: CD3, CD4, CD8, CD11C, CD14, CD16, CD20, CD56, CD123 and HLA-DR.(22-24) Default settings were used with cluster number set to 200.

4.4.7 Statistics

All analysis was performed using R. Summary data were expressed as mean ± SEM unless otherwise specified. Box and whisker plots denote median (line), interquartile range (box), and 1.5 times interquartile range (whiskers). For continuous data with one variable, Shapiro Wilk test was performed to assess the normality of the data. Non-normally distributed data was analyzed for statistical significance by the Mann-Whitney U test while normally distributed data was analyzed by Welch's t-test. Categorical variables were analyzed for statistical significance via Fischer Exact

Test. Comparisons between groups were made using paired sample T test for comparisons of median expression between conditions (Figure 2) and one sample T test for comparisons ofmedians between no CAC and high CAC groups (Figure 3) with alpha set to 0.05. All P values were subsequently corrected for multiple testing by calculating the False Discovery Rate (FDR) using the Benjamini-Hochberg procedure (Benjamini & Hochberg, 1995). Cell types (Figure 2) were analyzed using Analysis of Variance (ANOVA) test and subsequently adjusted for multiple testing using FDR correction.

Chapter 5

Synthesis

Despite extensive global efforts to deliver novel therapies to all patients in need, designing a universal therapy remains a significant challenge. This issue led to the creation of precision medicine, defined as P4 medicine - participatory, personalized, predictive, and preventative (Hood & Friend, 2011). As described in Chapter 1.1, precision medicine targets individual patients, aiming to optimize drugs, therapies, and diagnostics to achieve the best outcomes in treating various diseases. Stratifying patients based on their medical profiles, as seen in clinical trials, helps identify populations that would benefit most from treatments, leading to more efficient healthcare. Clinical trials, such as the CANTOS trial (Libby, 2017; Ridker et al., 2018), highlight the need for understanding patient populations.

Precision medicine in the clinic is rooted in research laboratories. Scientific discoveries start with hypotheses, followed by experiments, data analysis, and integration with current knowledge to inform clinical practice, as highlighted in Chapter 1.1. Advances in genomics, bioinformatics, molecular biology, and proteomics enable personalized medical care by matching treatments to patients' genetic and molecular profiles. As our understanding of diseases deepens and research technologies evolve, the connection between research labs and clinics strengthens, offering hope for future patient-specific medical interventions.

In Chapter 1.2, I explained how multi-omics combine multiple 'omes,' such as genomics, proteomics, transcriptomics, and metabolomics, to offer a comprehensive view of biological processes. Transcriptomics and proteomics are crucial, with transcriptomics measuring mRNA levels to assess gene expression and proteomics identifying proteins to understand cellular

functions. Utilizing multi-omics data enhances precision medicine, providing deeper insights into patient-specific characteristics and enabling more personalized treatment approaches.

Cardiovascular disease is a worldwide issue taking estimated 17.9 million lives each year accounting for around 32% deaths (*Cardiovascular Diseases (CVDs)*, WHO.). It is the leading cause of death in the United States, with atherosclerosis or coronary artery disease (CAD) causing 370,000 deaths annually (Pahwa & Jialal, 2024). In Chapter 1.3, I focused on atherosclerosis, characterized by plaque accumulation in arteries, reduces oxygen supply to the heart and triggers inflammatory responses. Plaques, composed of lipids, smooth muscle cells, and immune cells, can rupture, forming thrombi that lead to myocardial infarctions (MI) or strokes (Bentzon et al., 2014). Factors influencing atherosclerosis include genetics, environment, and lifestyle. Imaging techniques like intravascular ultrasound (IVUS) and computed tomography angiography (CTA) are vital for diagnosing and assessing atherosclerosis. The coronary artery calcification (CAC) score quantifies calcified plaque burden from CTA and serves as a prognostic tool for CAD, with scores ranging from 0 (no risk) to over 300 (high risk) (Agatston et al., 1990). High CAC scores correlate with increased risks of major adverse cardiovascular events (MACE) and all-cause mortality (Biavati et al., 2024, Budoff et al., 2023). Understanding the inflammatory nature of atherosclerosis, the importance of advanced imaging, and the prognostic value of CAC scores is crucial in managing cardiovascular disease effectively.

Atherosclerosis involves various immune cells, including T cells, B cells, neutrophils, dendritic cells, and NK cells, playing complex roles in disease progression, as presented in Chapter 1.4. T cells are present in atherosclerotic plaques and can either promote or inhibit atherosclerosis depending on their type and context. Antibodies produced by B cells interact with oxidation-specific epitopes in plaques, affecting lipid uptake and foam cell formation. Their role in the disease can be protective or proatherogenic depending on the subtype and cellular context. The

involvement of B cells in atherosclerosis suggests potential markers and therapeutic targets, but further research is essential to fully understand their clinical significance.

The discovery of loss-of-function mutations in the TET2 gene has profound implications for cardiovascular disease (CVD) and hematological malignancies such as leukemia and myelodysplastic syndrome (Jaiswal, 2017). In Chapter 1.5 I explained how TET2 is essential for DNA demethylation, and its dysfunction leads to abnormal stem cell behavior and clonal expansion. By age 50, individuals accumulate approximately five coding mutations per hematopoietic stem cell (HSC), driving clonal hematopoiesis of indeterminate potential (CHIP). CHIP mutations, especially in TET2, are significantly linked to increased risks for CVD, as well as diabetes and cancer. TET2 mutations induce IL-1β production, heightening inflammation, which can worsen cardiovascular conditions. The CANTOS trial revealed that patients with TET2 CHIP mutations had a reduced incidence of major adverse cardiovascular events when treated with Canakinumab, highlighting the role of TET2 in atherosclerosis and inflammation (Svensson et al., 2022; Bing Yu et al., 2021).

In chapter 2, I presented our study where we investigated TET2's role in regulating B-1 cell numbers and functions. We hypothesized that B-1 cells might be regulated by TET2, an epigenetic modulator implicated in the clonal expansion of hematopoietic cells leading to disorders such as myelodysplastic syndromes (MDS) and acute myeloid leukemia (AML) (Z. Li et al., 2011; Sun et al., 2018; W. Zhang, Fu, et al., 2012; W. Zhang, Shao, et al., 2012, 2015). Our findings revealed a significant role for TET2 in regulating B cell numbers in specific niches. The global loss of TET2 led to increased frequency and number of all B cell subtypes in the peritoneal cavity and elevated numbers of B1a cells in the bone marrow and B1b cells in the spleen. The mechanisms for these changes require further study to determine whether they result from increased proliferation, cell survival, or migration and if the effect is intrinsic to B cells. Enhanced self-renewal observed in B1a cells from TET2-KO animals might explain the increase in B1a cells in

the peritoneal cavity (Ko et al., 2011; Kunimoto et al., 2012; Z. Li et al., 2011; Pan et al., 2017; W. Zhang, Shao, et al., 2015; X. Zhang et al., 2016).

To investigate these differences further, we performed a BCR analysis using RNASeq data. The introduction of the TRUST4 algorithm by Song et al. enabled the accurate detection of BCR and TCR repertoire from bulk RNASeq data, providing valuable insights into the diversity of immune cell receptor repertoires and specificities (Song et al., 2021;K. J. Liu et al., 2023; Song et al., 2022; Y. Zhang & Lee, 2022). B1a cells from TET2-KO mice displayed fewer unique CDR3 sequences, indicating reduced antigen diversity. This reduced diversity, combined with a higher number of replicated sequences, suggests that TET2 influences the BCR repertoire's diversity and potential specificity, particularly in B1a cells. The genes and pathways differentially expressed in B1 cells from TET2-KO mice, particularly in B1a cells, were immunoglobulin-related and expressed at lower levels.

The constant region of the BCR determines the antibody's effector function. While there were no differences in the transcript expression levels of antibody isotypes IgG, IgD, and IgA, there was a significant increase in transcript expression of IgM, the main isotype produced by B-1 cells, in B1a cells from TET2-KO compared to WT mice (Holodick et al., 2014b; Kyaw et al., 2011, 2012; Upadhye et al., 2019). This suggests that TET2 may inhibit factors responsible for encoding the constant region downstream of the V region on chromosome 14 or limit isotype switching in B1a cells. These data align with observations of increased circulating IgM in TET2-KO mice compared to controls. We could not conclude if the increase in total IgM was due to increased IgM secretion per cell or an increase in overall cell numbers. There was also an increase in marginal zone B cell numbers in the spleens from TET2-KO mice compared to WT, representing another potential IgM source.

The key finding from our study is that TET2 mutation influences IgM levels and BCR repertoire, particularly in B1a cells, which are key producers of natural IgM. Alteration to the

antigen specificity or abundance of B1a-produced IgM may impact responses to PAMPs and DAMPs and regulate antigen-driven inflammation. These findings are important for precision medicine, as understanding TET2's role in regulating B1 cells and IgM production can lead to targeted therapies for chronic inflammatory conditions, such as cardiovascular diseases (CVD) and autoimmune disorders. This aligns with precision medicine's goals to tailor healthcare to individual patients by integrating genetic and molecular data, offering a comprehensive understanding of disease mechanisms to move towards personalized healthcare interventions.

In Chapter 4, I introduced our pilot study in a small cohort of patients with No CAC and High CAC. We examined the differences between those in phosphorylation states of effector molecules involved in IL-1β and IL-6 signaling pathways, focusing on NF-κB, ERK, and p38 for IL-1β, and STAT1, STAT3, and STAT5 for IL-6. (Dinarello, 2009; Lee et al., 2019; Towne et al., 2004; Haan et al., 2005; Tormo et al., 2012; Twohig et al., 2019; Zegeye et al., 2018). Multiple studies highlighted the role of IL-1β and IL-6 in the development of atherosclerosis and its complications. In murine models, IL-1, specifically the IL-1β isoform, promotes atherogenesis, while genetic ablation of the IL-1 receptor is atheroprotective (Chi et al., 2004; Elhage et al., 1998; Kirii et al., 2003; Merhi-Soussi et al., 2005; Vromman et al., 2019). Similarly, exogenous IL-6 is atherogenic and destabilizes atherosclerotic plaques in hypercholesterolemic mice (Akita et al., 2017; Huber et al., 1999; Schuett et al., 2012; K. Zhang, Huang, et al., 2012). Clinically, disruption of IL-1β signaling has been investigated for its potential in treating cardiovascular disease (CVD). The CANTOS trial found that IL-1β blockade decreased the recurrence of adverse cardiovascular events in subjects with stable atherosclerotic disease and elevated CRP (Nidorf et al., 2013; Tardif et al., 2019). Genome-wide association studies have linked activating variants in the IL-6R with CAD, while variants connected to reduced IL-6 signaling are associated with decreased CAD risk and increased longevity (C et al., 2012; Cai et al., 2018; IRGCERF et al., 2012; Rosa et al., 2019; Theriault et al., 2019). Elevated plasma IL-6 levels predict worse outcomes in stable heart disease,

acute coronary ischemia, heart failure, plaque severity, vulnerability, and progression in carotid atherosclerosis (Groot et al., 2019; Held et al., 2017; Markousis-Mavrogenis et al., 2019; Kamtchum-Tatuene et al., 2022).

Our findings showed that T cells were the primary immune cells activated by both cytokines, with significant phosphorylation of NF-κB in T cells, myeloid cells, and NK cells upon IL-1β stimulation, and STAT phosphorylation in response to IL-6, predominantly in T cells (Kothari et al., 2021). Trends identified in our work suggest that subjects with high CAC had more effector memory T cells, consistent with studies linking these cells to increased CAC and IL-6 levels (Ammirati et al., 2012; Olson et al., 2013). IL-1β-induced NF-κB phosphorylation was attenuated in Th17 cells in subjects with high CAC, aligning with murine models showing reduced Th17 transcript levels in plaques and lower Th17 cytokines presence in serum (Xie et al., 2010).

In our study, subjects with high CAC showed a lower response to IL-1β and IL-6 stimulation compared to those with no CAC. To our knowledge, this result, which has never been reported before, may be explained by the desensitization of the interleukin 1 receptor (IL-1R) and interleukin 6 receptor (IL-6R) from chronic stimulation. Yet, follow-up studies need to be performed to support this hypothesis. Serum levels of IL-1β and IL-6 are higher in individuals with coronary artery disease than in controls (Parisi et al., 2020; Wainstein et al., 2017). In vitro, IL-1β pretreatment reduces subsequent NF-κB phosphorylation in response to IL-1β, and IL-6 pretreatment decreases STAT3 phosphorylation in response to IL-6 (Fischer et al., 2004; McKean et al., 1994). This hypothesis is supported by breast cancer studies, where subjects show reduced IL-6-induced phosphorylation of STAT1 and STAT3 in CD4 naïve T cells, along with decreased IL-6Rα and gp130 expression (L. Wang et al., 2017). Additionally, T cells in advanced atherosclerotic lesions exhibit an exhausted phenotype based on surface markers and transcriptomics (Fernandez et al., 2019).

While providing interesting findings and trends, generating novel hypotheses, and opening avenues for new experiments, the biggest caveat of this work is the lack of robust sample size. The study served as an unbiased exploration of the phosphorylation patterns in immune cells after stimulation with pro-inflammatory cytokines. The findings should be evaluated in a bigger cohort to confirm the decreasing directionality of phosphorylation of the antigens upon stimulation with IL-1β and IL-6, a result contrasting with published data.

In conclusion, the identification of specific T cell subpopulations responsive to IL-1β and IL-6 presents new research opportunities and potential therapeutic targets. Understanding immune cell dynamics in atherosclerosis could improve disease prognosis and treatment response, aligning with values represented by precision medicine. Further mechanistic studies and larger sample sizes are needed to elucidate the biological significance of these findings and their clinical applications in managing cardiovascular disease.

The research presented in this dissertation emphasizes the role of immune cell dynamics and genetic mutations in the development and progression of cardiovascular diseases, particularly atherosclerosis. By elucidating the mechanisms behind TET2 mutations and their impact on B cell subsets and exploring the activation status of immune cells in patients with different degrees of coronary artery calcification, our findings contribute to a more comprehensive understanding of how the immune system may contribute to the disease. This work highlights the importance of involving individual genetic and molecular profiles in tailoring medical interventions, following the principles of precision medicine. Integrating multi-omics data and advanced imaging techniques will be crucial in developing more effective, personalized interventions for patients with cardiovascular diseases. Future research should focus on validating these findings in larger cohorts and exploring the potential for targeted therapies that address the specific immune and genetic factors contributing to disease, ultimately improving patient outcomes and advancing the goals of precision healthcare.

Chapter 6

Future directions

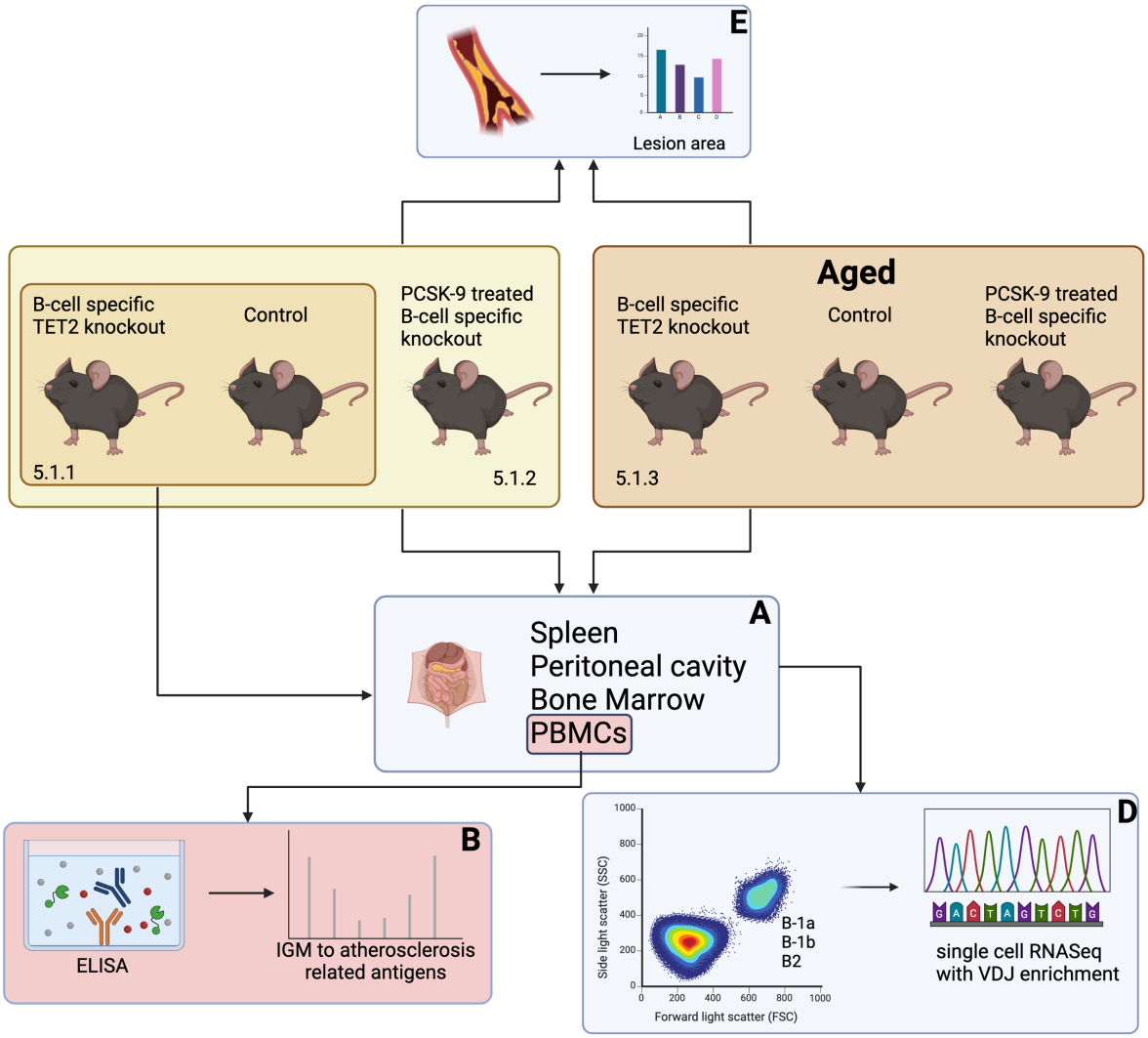

Figure 6.1 Schematic presenting ideas for future experiments to further explore the role and function of TET2 mutation in B Cells

5.1.1 Experiment involving B cell specific TET2 KO (BKO) and control mice. **5.1.2** Experiment involving TET2 BKO, PCSK9 treated TET2 BKO, control mice. **5.1.3** Experiment involving aged TET2 BKO, PCSK9 treated TET2 BKO, control mice. **A** Harvest of cells from spleen, peritoneal cavity, bone marrow and PBMCs from circulation. **B** FACS-sorting of B1a, B1b and B2 cells and scRNASeq with VDJ enrichment. **C** ELISA to assess specificity of circulating IgM to common atherosclerosis antigens

6.1 Loss of TET2 in B cells

The main finding from our study about loss of TET2 is that the TET2 mutation led to increased frequency and number of all B cell subtypes in the peritoneal cavity and elevated numbers of B1a cells in the bone marrow and B-1b cells in the spleen. The mutant mice had decreased CDR3 diversity, especially in B1a cells.

As explained in Chapter 1.4, TET2 is essential for DNA demethylation, and its dysfunction leads to abnormal stem cell behavior and clonal expansion. The results I presented in this dissertation improve our understanding of the role TET2 has in regulation of B cell subsets proliferation and diversity and generated new hypotheses and questions.

6.1.1 Is the TET2 loss related change in B cell numbers and reduced CDR3 diversity in B1a cells an effect intrinsic to B cells or is it a consequence of the interplay with other cell types?

Too answer the first question I would collaborate with experimental biologists to ensure the proper scientific rigor, to use a mouse mutant with a B-cell specific TET2 knockout (TET2 BKO) mouse ($CD19^{cre/+}$ $TET2^{fl/fl)}$ and controls ($CD19^{cre/+}$ $TET2^{+/+}$) (as depicted in Figure 6.1). I would analyze the flow cytometry results to assess the differences in the B1a, B1b, B2 cell numbers from peritoneal cavity, bone marrow and spleen and in circulation. If there is an increase in B1a, B1b or B2 cell numbers in PerC, spleen, and bone marrow, that would indicate that the change is related to the mutation in B cells and not an effect of an interaction with other cells.

We would sequence FACS-sorted B1a, B1b, B2 cells using single cell RNAseq with VDJ-enrichment using 10x Genomix platform. The reason I choose scRNASeq and not bulk RNASeq is that with single cell technologies I would be able to assign a CDR3 to cell thus I would be able to

assess if the cells are clonal. With bulk RNASeq, the analysis of diversity is based on changes in CDR3 proportions rather than analysis of actual cells and their respective CDR3.

I would analyze the sequencing results, focusing on the differentially expressed genes and enriched pathways. I would compare the DE genes and enriched pathways to the results from this dissertation to see which changes were retained. The presence of the same DE genes in this dissertation and in the result of this scRNASeq experiment would suggest that the change in the gene expression would be induced by the mutation in B cells and no other cells.

Yet, the question if the effect on the cell numbers and CDR3 diversity is direct or is it caused by e.g. changes in cytokines production that subsequently influence other immune cells will remain unanswered. To assess the changes in other cells, I would collaborate with an immunologist to do a flow cytometry experiment to analyze the frequencies of other immune cells (T Cells, Monocytes, Macrophages, NK cells) and the expression of different effector molecules to see if the TET2 mutation in B cells affected their phenotype.

6.1.2 How does the change in B cell numbers and the related diversity of CDR3 influence atherosclerosis and atherosclerotic burden?

To answer this question, I would collaborate with experimental biologists to ensure the proper scientific rigor, and use PCSK-9 -AAV (Goettsch et al., 2016) in our TET2 BKO and control mice to induce atherosclerosis. Then, atherosclerotic burden would be estimated (e.g., enface staining as described in Srikakulapu et al., 2017). I would proceed with the cell sorting, flow cytometry and sequencing as described 6.1.1.

If the changes in B cell numbers and reduced B1a cell CDR3 diversity are confirmed in the mouse model, and the atherosclerosis burden is significantly higher in TET2 BKO group, it would suggest that the mutation in B cells influences the increase in atherosclerotic burden.

As explained in Chapter 1.4.7, many IgMs were identified to be specific to common atherosclerosis

related antigens and thus presenting atheroprotective effects (Binder et al., 2016; M.-K. Chang et al., 2004; Chou et al., 2008, 2009; Miller et al., 2011; Sage et al., 2019). I would collaborate with experimental biologists to perform ELISA's to measure the differences in IgM in plasma and to assess their specificity to atherosclerosis related antigens. Then, with proper literature research, I would try to identify (if possible) and correlate the specific CDR3 sequences of known antigens from scRNASeq to the changes in secreted antibodies to investigate whether the changes in antibodies secretion are reflective of the reduced CDR3 repertoire. If the level of secreted antibodies is decreased in the BKO TET2 mutant group and correlated with a decrease in corresponding CDR3 sequences, it would suggest that the change in atherosclerotic burden could be related to decrease in CDR3 diversity and in the secretion of Igs.

6.1.3 Is the same effect of TET2 mutation in B cells seen in CHIP mutation mouse models?

To assess the changes induced by TET2 in a CHIP mutation model, I would collaborate with experimental biologists to ensure the proper scientific rigor, and induce TET2 KO in B cells in 18-24 month old mice. CHIP mutations are somatic mutations which accumulate with age, thus the induction of the mutation in aged mice would simulate the CHIP onset. Together with help from experimental biologists, I would analyze 3 groups: aged mice, aged mice with induced TET2 mutation in B cells, and aged mice with induced TET2 mutation in B cells treated with PCSK-9-AAV (as depicted in figure Figure 6.1). I would follow the experiment flow from 5.1.1 and 5.1.2. If the same changes that were seen in BKO TET2 in young mice are seen in mice with the mutation induced at an older age with the increase of B cell numbers and evidence of clonal proliferation together with the increase of atherosclerotic burden, it would suggest that the B-cell specific TET2 mutation induced at an older age has proatherogenic effects. I would assess the changes in amount of circulatory IgM specific to antigens related to atherosclerosis. If the amount of atheroprotective

IgM was decreased in the CHIP BKO TET2 mutation group compared to the control (PCSK-9 treated mice without the TET2 knockout), it would indicate that, at least partially, the increase in atherosclerotic burden is related to the changes in secreted antibodies.

6.1.4 Analysis of scRNASeq from TET2 KO and WT cells

To answer the questions mentioned in this Chapter, I will use scRNASeq data from mutant and wild type mice.

I would first use CellRanger to demultiplex, align, filter and count sequencing reads. Next, in Seurat, I would perform cell-based quality control where I would discard outliers, normalize expression for each cell and for each gene using SCTransform function. Then, cells would be clustered using Leiden algorithm (Traag et al., 2019). To annotate the cells I would use ScType (Ianevski et al., 2022). ScType allows for a fully automated and fast annotation of scRNASeq data with cell types from its database, which also contains immune cells. ScType's cell and marker database is based on two other curated databases: CellMarker (Hu et al., 2023) and PanglaoDB (Franzén et al., 2019). The process of annotation of cells by ScType requires the calculation of cell-type specificity score to quantify how uniquely a particular marker can characterize specific cell-type from a given tissue. High score corresponds to marker that is highly specific, while low score depicts low specificity. The score formula:

$$S_i^t = 1 - \frac{|M_i|_t - min(|M|_t)}{max(|M|_t) - min(|M|_t)}$$

Where *M* is a pool of all cell-type specific markers from a given tissue *t*, S is a cell-type specificity score for a given marker. $|M_i|_t$ is a number of cell types in tissue t where the *i*th marker is present,

and min($|M_i|_t$) and max($|M_i|_t$) are the minimum and maximum numbers of cell types which have the marker enlisted as cell-specific in the ScType database. Next, from all cells and markers from a specific cluster ($\underline{p}$) ScType calculates z-score across all cells. Then, expression of genes with positive and negative value is transformed using both the Z-score and cell-type specificity score (S) to create a transformed expression matrix. Subsequent cell-type specific marker-enrichment score is calculated as the normalized sum of all the individual genes supporting a cell type for each cell separately, creating a matrix where columns are specific cells and rows are unique cell-types. Then, by summing up the values for each cell-type for all cells belonging to cluster p. Cell type with the highest score is used for the describe the cluster p.

Once the clusters are assigned to specific cell types, I would perform a differential expression analysis using MAST (Finak et al., 2015). Briefly, MAST uses a hurdle model, capable of handling multiple zero values in an expression matrix. It utilizes a two-part generalized linear regression model. One component models the discrete expression rate of each gene across cells, while the second component models the conditional continues expression level. From the results of the differential gene expression analysis, I would compare the differentially expressed genes from TET2 KO cells and WT cells to the DEG list from our TET2 study in a global TET2 KO and WT mice to look for any gene differences suggesting the BCR-restriction and other identified changes could be non-B cell specific. Additionally, MAST allows for the GSEA pathway enrichment analysis. I would compare the DEG list produced by MACS for each B-1a, B-1b and B2 cell type separately and explored the enriched pathways. If any pathways enriched would relate to immunoglobulin production or regulation of immune response and would contain Ig heavy or light genes, that would suggest the CDR3 restriction is present in a B-cell specific TET2 KO model as well.

Next, I would integrate the CellChat tool in our scRNASeq analysis. CellChat is a computational framework that infers and analyzes cell-cell communication networks from single-

cell transcriptomic data (Jin et al., 2021). By applying CellChat to our scRNAseq data, we can identify and quantify the interactions between B cells and other immune cell populations in TET2-KO and wild-type (WT) cells. This analysis will enable us to uncover the signaling pathways and molecular mechanisms through which TET2 influences B cell proliferation, survival, and migration and inform us about any changes in cell-to-cell communications induced by the lack of TET2 expression in B cells, which could further elucidate whether the effect is induced by interactions with other cells. Additionally, it would help identify key ligands, receptors, and signaling molecules involved in these interactions, providing insights into how TET2 loss may alter the immune microenvironment. CellChat uses a curated database of known ligand-receptor pairs to determine their simultaneous changes in expression. It calculates the probability of each ligand-receptor interaction occurring between different cell types, and constructs a cell-cell communication network. This network shows which cell types are likely communicating with each other through specific ligand-receptor pairs. Then, through pathway analysis to determine the affected signaling pathways and the analysis of network properties like centrality and connectivity I would be able to further explore the potential mechanisms affected by the loss-of TET2 and their molecular consequences in B cells and other interacting cells. This would further elucidate whether the effect of reduced BCR repertoire being intrinsic to B cells.

Monocle is a robust computational tool designed to analyze single-cell RNA sequencing data to uncover cellular trajectories and understand cell differentiation processes (Trapnell et al., 2014). It reconstructs developmental lineages by ordering cells in pseudotime, an abstract measure of progress through a biological process. The tool identifies differentially expressed genes across the dataset and uses these genes to infer a trajectory through a technique called reverse graph embedding, which organizes cells along a continuum of cell states. Monocle constructs a minimum spanning tree (MST) that connects all cells, representing the inferred lineage. The MST's branches correspond to different cell fates, while the position of each cell on the tree indicates its pseudotime.

Monocle also facilitates the identification of genes whose expression changes dynamically along the trajectory, providing insights into key regulatory genes driving cell differentiation. In the context of the TET2 project, Monocle can be used to analyze scRNAseq data from TET2-KO and WT B cells, enabling the reconstruction of B cell developmental trajectories and the identification of gene expression changes associated with TET2 loss. This approach will help elucidate the impact of TET2 mutations on B cell maturation and function, shedding light on the molecular mechanisms underlying the observed phenotypic changes. By leveraging Monocle's capabilities we can gain a deeper understanding of how TET2 influences B cell lineage commitment and changes in the proportions of cells at each developmental stage which would help us further understand the mechanism behind the changes induced by the loss-of TET2. Furthermore, the exploration of the BCR sequence at every stage of the trajectory could explain the process of the development of potential clones.

Next, to understand the potential changes in BCR of BKO cells and to compare them to the changes induced by the total body knockout of TET2 gene, I would use TRUST4 to perform the analysis of BCR. First, I would use the same gene annotation and genomic reference as well as VDJ gene annotation I used for the study of global TET2 KO. I would then explore the changes in Ig isotype frequencies, the number of CDR3 sequences among the cells and the changes in the frequency of clonal cells and non-replicated cells. Additionally, as the activation of B cells leads to somatic hypermutation I would cluster B cells to identify the BCRs from the same lineage. Since the data has a single-cell resolution, that could also indicate the path of the introduction of different mutations into the BCR clones. By comparing SHM rates between TET2 knockout (KO) and wild-type (WT) B cells, we can elucidate how TET2 loss affects B cell maturation and antigen recognition. Additionally, clonal analysis through BCR clustering will help identify any clonal expansions, shedding light on the dysregulation associated with TET2 loss. Clustering also allows for the calculation of the clustering entropy, where lower entropy in the TET2 loss group would

indicate a less diverse BCR repertoire that could impact immune responses in the affected cells. If the magnitude of potential BCR restriction is similar to the one in total body TET2 KO, that would suggest the change is in fact intrinsic to B cells.

To further explore the differences in the BCR if the analyzed groups, I would use the IMGT/HighV-QUEST tool for analyzing B-cell receptor (BCR) sequences. IMGT/HighV-QUEST provides detailed insights into V(D)J recombination, including somatic hypermutation (SHM) rates, CDR3 hydrophobicity, and N addition profiles. By comparing these parameters between TET2 knockout (KO) and wild-type (WT) B cells, we can assess how TET2 loss impacts B cell maturation and diversity. CDR3 hydrophobicity analysis will shed light on changes in antigen-binding properties, since hydrophobicity is related to the charge of a CDR3 sequence and the stability of antigen binding. Additionally, examining N additions in the junctional regions will provide insights into the generation of BCR diversity and potential alterations in the immune repertoire. The number of N additions in the junctions between V, D and J genes informes about how far away from germline the BCR mutated. These comprehensive analyses, when integrated with scRNAseq data, will highlight critical pathways and molecular mechanisms disrupted by TET2 mutations.

All proposed analyses would enhance our understanding on transcriptomic changes induced by the loss of TET2 in B cells, its contribution to BCR formation, and the potential interactions with other cells contributing to the alterations.

6.1.5 Implications for precision medicine

The study's results underscore the potential for integrating genetic information into precision medicine. The impact of TET2 mutations on B cell subsets and CDR3 diversity suggests that patients with these mutations may benefit from personalized therapies aimed at correcting

specific immune dysregulations by novel methods like immunization to induce the production of decreased antibodies (Pattarabanjird et al., 2021). By identifying individuals with TET2 mutations and understanding their unique immune profiles, healthcare providers can design targeted interventions that address the underlying mechanisms of their disease. This approach not only enhances treatment efficacy but also opens avenues for novel therapeutic strategies in managing atherosclerosis and other related conditions, aligning with the principles of precision medicine.

6.2 CTA

The study presented in Chapter 3 shows that identifying specific T cell subpopulations responsive to IL-1β and IL-6 presents new research opportunities.

The main finding of the study is the attenuated phosphorylation of effector molecules in T cells following the stimulation with IL-6 and IL-1β in patients with High CAC compared to No CAC group. Importantly, the study was underpowered to detect significant differences between the analyzed groups. The main objective of the follow-up research should be to confirm the findings in larger cohorts.

Yet, the trends identified in our work generated new questions and hypotheses.

6.2.1 What are the phosphorylation patterns in T cells following different stimulation conditions when patients with intermediate CAC scores are included?

To answer this question, I analyzed the data from 45 patients with CAC scores varying between 0 and 1300. When analyzing all T cells, the most prominent difference was seen in the median expression of pSTAT5 (Figure 6.2). Surprisingly, the expression of pSTAT5, in accordance with previous research (Tormo et al., 2012; X. Wang et al., 2021), was increased in the

Moderate and Increased CAC groups. The High CAC group presented a lower expression of pSTAT5, as elucidated in our study in Chapter 3. However, the correlation between the CAC score and the expression of pSTAT5 in T Cells remained not statistically significant. To further explore the relationship between CAC score and phosphorylated effector molecules in T Cells, I excluded the subjects with No CAC due to high variance and spread-out distribution of the expression of pSTAT5 and other analyzed molecules. The variance could be explained by the cohort design itself, as patients presenting to the clinic had to have medically justified indications for referral for a computed tomography angiography (CTA) scan. As we cannot correct for other potential underlying issues influencing the state of the immune system, I excluded the No CAC group from further analysis to focus on exploring the disease progression and its consequences in the expression of phosphorylated effector molecules in patients with reported CAC. Additionally, it has been previously reported that in a PROMISE study, 16% of patients with a CAC score of 0 were diagnosed with CAD within 2 years after the scan, highlighting a potential weakness of the CAC score's prognostic value in patients without detectable coronary artery calcification (Budoff et al., 2017). As there were only 4 patients with CAC score of 500 or higher, I also excluded them from the future analysis.

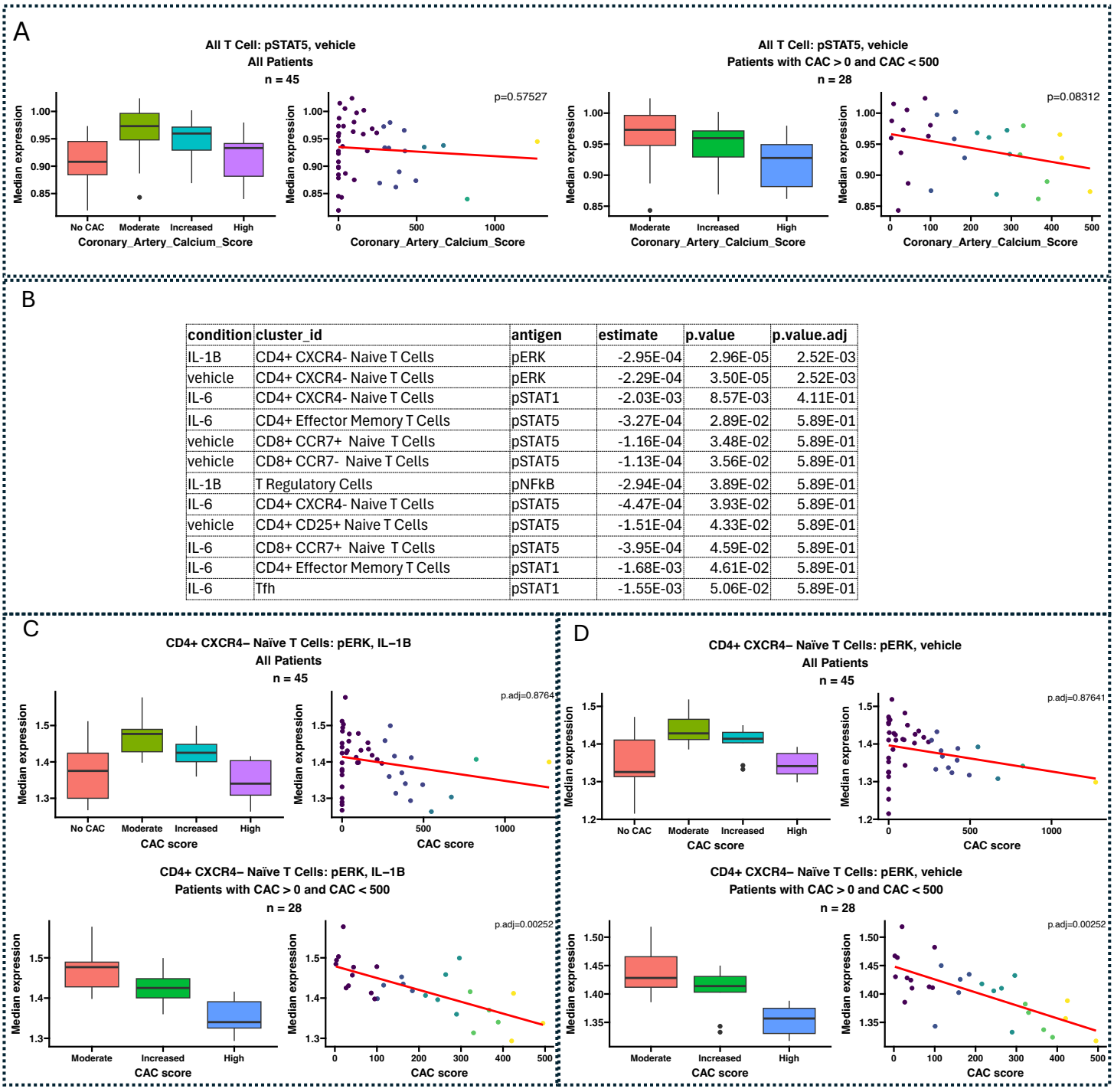

B

condition	cluster_id	antigen	estimate	p.value	p.value.adj
IL-1B	CD4+ CXCR4- Naive T Cells	pERK	-2.95E-04	2.96E-05	2.52E-03
vehicle	CD4+ CXCR4- Naive T Cells	pERK	-2.29E-04	3.50E-05	2.52E-03
IL-6	CD4+ CXCR4- Naive T Cells	pSTAT1	-2.03E-03	8.57E-03	4.11E-01
IL-6	CD4+ Effector Memory T Cells	pSTAT5	-3.27E-04	2.89E-02	5.89E-01
vehicle	CD8+ CCR7+ Naive T Cells	pSTAT5	-1.16E-04	3.48E-02	5.89E-01
vehicle	CD8+ CCR7- Naive T Cells	pSTAT5	-1.13E-04	3.56E-02	5.89E-01
IL-1B	T Regulatory Cells	pNFkB	-2.94E-04	3.89E-02	5.89E-01
IL-6	CD4+ CXCR4- Naive T Cells	pSTAT5	-4.47E-04	3.93E-02	5.89E-01
vehicle	CD4+ CD25+ Naive T Cells	pSTAT5	-1.51E-04	4.33E-02	5.89E-01
IL-6	CD8+ CCR7+ Naive T Cells	pSTAT5	-3.95E-04	4.59E-02	5.89E-01
IL-6	CD4+ Effector Memory T Cells	pSTAT1	-1.68E-03	4.61E-02	5.89E-01
IL-6	Tfh	pSTAT1	-1.55E-03	5.06E-02	5.89E-01

Figure 6.2 Exclusion of No CAC patients results in better associations between the phosphorylation levels of proteins and CAC status

A. pSTAT5 phosphorylation levels in T cells of all patients (left), and patients with CAC > 0 and CAC < 500. B. Linear regression results correlating the phosphorylation of antigens in different T cell clusters in vehicle, IL-6 stimulated, IL-1β stimulated conditions. P value was corrected for multiple testing using FDR (p.value.adj) C. Median expression of pERK in $CD4^+$ $CXCR4^-$ Naive T Cells cluster after IL-1β stimulation in all patients (top) and patients with CAC > 0 and CAC < 500. P value depicted is adjusted for multiple testing using FDR correction. Left panel presents a box plot of median expression of pERK in patients patient groups: No CAC, Moderate CAC (1-100), Increased CAC (101-300), High CAC (> 300). Right panel presents a regression plot between CAC score and Median expression of pERK with regression line presented in red. D. Median expression of pERK in $CD4^+$ $CXCR4^-$ Naive T Cells cluster in vehicle in all patients (top) and patients with CAC > 0 and CAC < 500. P value depicted is adjusted for multiple testing using FDR correction. Left panel presents a box plot of median expression of pERK in patients patient groups: No CAC, Moderate CAC (1-100), Increased CAC (101-300), High CAC (> 300). Right panel presents a regression plot between CAC score and Median expression of pERK with regression line presented in red.

After the cohort adjustments, the pSTAT5 expression in all T cells followed a negative correlation trend with the increase of CAC score, which is concordant with our previous findings.

I used a linear regression model to examine the expression of phosphorylated ERK, NF-Kβ, p38 , and STAT1, STAT2 STAT3 in different T cell subsets against CAC score. I observed a significant negative correlation of CAC score and the expression of pERK in $CD4^{+}$ $CXCR^{-}$ Naïve T cell cluster after IL-1β stimulation and in cells treated with vehicle (Figure 6.2 B-D). Additionally, the frequency of the same T cell subsets was significantly negatively correlated with CAC score (Figure 6.3).

A

cell	estimate	p.value	p.value.adj
CD4+ CXCR4- Naive T Cells	-2.53E-03	3.08E-03	3.70E-02
CD4+ Effector Memory T Cells	1.31E-03	1.53E-01	9.18E-01
Tfh	5.45E-04	2.78E-01	9.99E-01
Th17 Cells	-5.84E-04	3.85E-01	9.99E-01
CD4+ CD25+ Naive T Cells	-5.02E-04	5.99E-01	9.99E-01
CD8low CD161high T Cells	-4.46E-04	6.51E-01	9.99E-01
CD4- CD8- T Cells	-3.49E-04	7.35E-01	9.99E-01
CD8+ CCR7+ Naive T Cells	1.98E-04	8.50E-01	9.99E-01
CD8+ Effector Memory T Cells	9.48E-05	8.86E-01	9.99E-01
CD8+ CCR7- Naive T Cells	-8.97E-05	9.55E-01	9.99E-01
T Regulatory Cells	-1.56E-05	9.64E-01	9.99E-01
CD4+ CXCR4+ Naive T Cells	1.32E-06	9.99E-01	9.99E-01

B

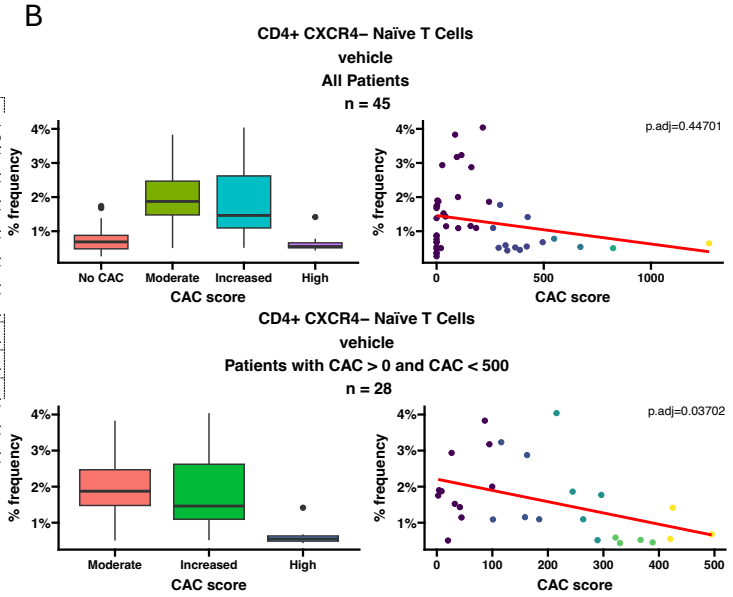

Figure 6.3 Frequency of $CD4^{+}$ $CXCR4^{-}$ Naive T Cells negatively correlates with CAC score in patients with CAC >0 and CAC < 500

A. Linear regression results correlating the logit-transformed frequency of T cell clusters with logit with CAC score. P value was adjusted for multiple testing using FDR correction. B. Frequency of $CD4^{+}$ $CXCR4^{-}$ Naive T Cells cluster in all patients (top) and patients with CAC > 0 and CAC < 500 (bottom). P value depicted is adjusted for multiple testing using FDR correction. Left panel presents a box plot of the T cell subset in patients patient groups: No CAC, Moderate CAC (1-100), Increased CAC (101-300), High CAC (> 300). Right panel presents a regression plot between CAC score and frequency of T cell cluster with regression line presented in red.

As depicted in Figure 4.4, $CD4^+$ $CXCR^-$ Naïve T cell cluster expresses both CD56 and CD161, common markers of NKT Cells (L. Peng et al., 2016). Yet, there is limited research regarding NK T cells and their impact on atherosclerosis, except for their iNKT subset. iNKT cells are defined by the expression of CD1d, a non-canonical MHC. However, our panel does not include the CD1d marker, and we cannot differentiate between potential NKT subsets. Yet, the finding, without the differentiation of NKT cell subsets, seems to follow the discoveries of recent case-control study, that presented a negative correlation between iNKT cell expression with incident CE, suggesting their atheroprotective function (Tomas et al., 2023). Yet, studies in mice indicate an atherogenic function of iNKTs in the progression of atherosclerotic disease (Major et al., 2004; Nakai, 2004; Tomas et al., 2023; Tupin et al., 2004; van Puijvelde et al., 2009). Future experiments should focus on the differentiation between different NKT subsets in our cohort, perhaps by examining PBMCs with a flow cytometry panel involving necessary NK T cell markers to assess their frequencies and their correlation with CAC.

6.2.2 Is there a correlation between the expression of phosphorylated effector molecules in immune cells with different measures of CAD progression?

Clinical research established other CAD risk scores calculated from CTA imaging. Comprehensive atherosclerotic risk score (CTA risk score) integrates maximal stenosis severity, also included in CAC, with additional parameters estimating the plaque extent, location, and composition. Previous research indicated CTA score was able to more accurately predict the incidence of coronary events compared to CAC score (van et al., 2019). CTA risk score was recently calculated for patients in our cohort based on their CTA scans. It provides an opportunity

to explore alternative endpoints and their correlation with the expression of phosphorylated effector molecules in immune cells.

Another potential measure of atherosclerosis relevant for our work is perivascular fat attenuation index (FAI). FAI quantifies spatial changes in perivascular fat composition induced by coronary inflammation rather than the extension of atherosclerotic plaques (Oikonomou et al., 2021). A recent study utilized an AI model that integrated FAI with coronary plaque metrics, and clinical risk factors (Chan et al., 2024). The model trained on the USA cohort was able to correlate and predict cardiac mortality and CE in the UK population with high accuracy. Correlating the AI-risk score, which involves information about perivascular inflammation, with our data on immune cell activation in our CTA cohort could provide additional insights into the disease dynamic going beyond the calcification of the plaques, underlying the role of inflammation and the immune system state in different stages of the disease.

Chapter 7

Abbreviations

5hmC	5-hydroxymethylcytosine
5mC	5-methylcytosine
ACVD	atherosclerotic cardiovascular disease
ACS	acute coronary syndrome
AHR	aryl hydrocarbon receptor
APC	antigen-presenting cells
apoeB	apolipoprotein B
BCL-6	B cell lymphoma 6
BCR	B cell receptors
BKO	B-cell specific knockout
BM	bone marrow
CAC	coronary artery calcification
CAD	coronary artery disease
CDR3	complementarity-determining region 3
CE	cholesterol ester
CHIP	clonal hematopoiesis of indeterminate potential
CHD	coronary heart disease
CMP	common myeloid progenitors
CpG	5'—C—phosphate—G—3'
CRP	C-reactive protein
CTA	computed tomography angiography
CTLA4	cytotoxic T-lymphocyte-associated protein 4
cyTOF	cytometry by Time-of-Flight
CVD	cardiovascular diseases
cDNA	complementary DNA
DCs	dendritic cells
DAMPs	damage-associated molecular patterns
DEGs	differentially expressed genes
DNA	deoxyribonucleic acid
DNMT	DNA methyltransferase

EC	endothelial cell
ERK	extracellular signal-regulated kinase
FC	flow cytometry
FOXP3	the transcription factor forkhead box protein P
G-CSF	granulocyte colony-stimulating factor
GATA3	GATA-binding factor 3
GO	gene ontology
GM-CSF	granulocyte–macrophage colony-stimulating factor
GSEA	gene set enrichment analysis
GWAS	genome wide association studies
hs-CRP	high-sensitivity C-reactive protein
HSC	hematopoietic stem cell
HSPC	hematopoietic stem/progenitor cell
IFNγ	interferon-γ
Ig	immunoglobulin
IgM	immunoglobulin M
IL-10	interleukin-10
IL-13	interleukin-13
IL-17	interleukin-17
IL-2	interleukin-2
IL-2RA	interleukin-2 receptor alpha
IL-22	interleukin-22
IL-33	interleukin-33
IL-3	interleukin-3
IL-4	interleukin-4
IL-5	interleukin-5
IL-9	interleukin-9
iNKT	invariant natural killer T cells
IVUS	intravascular ultrasound
LAG3	lymphocyte activation gene 3 protein
LDL	low-density lipoprotein
LSK	Lineage- Sca-1+c-Kit+
MACE	major adverse cardiac events
Macs	macrophages
MDA	malondialdehyde-modified amino groups
MHC I	major histocompatibility complex I
MI	myocardial infarction

mRNA	messenger RNA
MPP	multipotent progenitor
NK	natural killer cells
NLRP3	NOD-, LRR- and pyrin domain-containing protein 3
OSEs	oxidation-specific epitopes
ox-LDL	oxidized low-density lipoprotein
OxPL	oxidized phospholipid
PAMPs	pathogen-associated molecular patterns
PBMCs	peripheral blood mononuclear cells
PerC	peritoneal cavity
PL	phospholipid
qPCR	quantitative polymerase chain reaction
RNA	ribonucleic acid
RNASeq	RNA-sequencing
RORγt	nuclear receptor RORγt
scRNASeq	single-cell RNA sequencing
SMCs	smooth muscle cells
SPADE	spanning-tree progression of density normalized events
STAT	signal transducer and activator of transcription
T-bet	T-box transcription factor TBX21
T-box	T-box transcription factor TBX21
TCR	T-cell receptor
TET	ten-eleven translocation
TET2	ten-eleven translocation 2
TFH	T follicular helper cells
TGFβ	transforming growth factor-β
TNF	tumor necrosis factor
TNFα	tumor necrosis factor alpha
UMAP	uniform manifold approximation and projection
VCAM1	vascular cell adhesion molecule 1
VSMC	vascular smooth muscle cell
WBC	white blood cell
WT	wild-type

Bibliography

Agatston, A. S., Janowitz, W. R., Hildner, F. J., Zusmer, N. R., Viamonte, M., Jr., & Detrano, R. (1990). Quantification of coronary artery calcium using ultrafast computed tomography. *J Am Coll Cardiol*, *15*(4), 827–832.

Ahmed, S., Zhou, Z., Zhou, J., & Chen, S.-Q. (2016). Pharmacogenomics of Drug Metabolizing Enzymes and Transporters: Relevance to Precision Medicine. *Genomics, Proteomics & Bioinformatics*, *14*(5), 298–313. https://doi.org/10.1016/j.gpb.2016.03.008

Ait-Oufella, H. (2006). Natural regulatory T cells control the development of atherosclerosis in mice. *Nat. Med.*, *12*. https://doi.org/10.1038/nm1343

Akita, K., Isoda, K., Sato-Okabayashi, Y., Kadoguchi, T., Kitamura, K., & Ohtomo, F. (2017). An Interleukin-6 Receptor Antibody Suppresses Atherosclerosis in Atherogenic Mice. *Front Cardiovasc Med*, *4*(84).

Alayed, K., Patel, K. P., Konoplev, S., Singh, R. R., Routbort, M. J., & Reddy, N. (2013). TET2 mutations, myelodysplastic features, and a distinct immunoprofile characterize blastic plasmacytoid dendritic cell neoplasm in the bone marrow. *Am J Hematol*, *88*, 1055–1061. https://doi.org/10.1002/ajh.23567

Ali, A. J., Makings, J., & Ley, K. (2020). Regulatory T Cell Stability and Plasticity in Atherosclerosis. *Cells*, *9*(12), Article 12. https://doi.org/10.3390/cells9122665

Amento, E. P., Ehsani, N., Palmer, H., & Libby, P. (1991). Cytokines and growth factors positively and negatively regulate interstitial collagen gene expression in human vascular smooth muscle cells. *Arteriosclerosis and Thrombosis: A Journal of Vascular Biology*, *11*(5), 1223–1230. https://doi.org/10.1161/01.ATV.11.5.1223

Amir Ravandi, S. Matthijs Boekholdt, Amir Ravandi, Amir Ravandi, Amir Ravandi, Ziad Mallat, S. Matthijs Boekholdt, S.M. Boekholdt, Philippa J. Talmud, Ziad Mallat, P.J. Talmud, John J.P. Kastelein, Philippa J. Talmud, Nicholas J. Wareham, J.J.P. Kastelein, John J.P. Kastelein, Nicholas J. Wareham, Elizabeth R. Miller, Joëlle Bénessiano, … Sotirios Tsimikas. (2011). Relationship of IgG and IgM autoantibodies and immune complexes to oxidized LDL with markers of oxidation and inflammation and cardiovascular events: Results from the EPIC-Norfolk Study. *Journal of Lipid Research*. https://doi.org/10.1194/jlr.m015776

Ammirati, E., Cianflone, D., Vecchio, V., Banfi, M., Vermi, A. C., & Metrio, M. (2012). Effector Memory T cells Are Associated With Atherosclerosis in Humans and Animal Models. *J Am Heart Assoc*, *1*(1), 27–41.

Amoros-Perez, M., & Fuster, J. J. (2020). Clonal hematopoiesis driven by somatic mutations: A new player in atherosclerotic cardiovascular disease. *Atherosclerosis*, *297*, 120–126.

Anand Prasad, Anand Prasad, Paul Clopton, Paul Clopton, Colby Ayers, Colby R. Ayers, Amit Khera, Amit Khera, James A. de Lemos, James A. de Lemos, Joseph L. Witztum, Joseph L. Witztum, Sotirios Tsimikas, & Sotirios Tsimikas. (2017a). Relationship of Autoantibodies to MDA-LDL and ApoB-Immune Complexes to Sex, Ethnicity, Subclinical Atherosclerosis, and Cardiovascular Events. *Arteriosclerosis, Thrombosis, and Vascular Biology*. https://doi.org/10.1161/atvbaha.117.309101

Anand Prasad, Anand Prasad, Paul Clopton, Paul Clopton, Colby Ayers, Colby R. Ayers, Amit Khera, Amit Khera, James A. de Lemos, James A. de Lemos, Joseph L. Witztum, Joseph L. Witztum, Sotirios Tsimikas, & Sotirios Tsimikas. (2017b). Relationship of Autoantibodies to MDA-LDL and ApoB-Immune Complexes to Sex, Ethnicity,

Subclinical Atherosclerosis, and Cardiovascular Events. *Arteriosclerosis, Thrombosis, and Vascular Biology*. https://doi.org/10.1161/atvbaha.117.309101

Andrews, S. F., Zhang, Q., Lim, S., Li, L., Lee, J. H., & Zheng, N. Y. (2013). Global analysis of B cell selection using an immunoglobulin light chain-mediated model of autoreactivity. *J Exp Med*, *210*, 125–142. https://doi.org/10.1084/jem.20120525

Antonio Muscari, Antonio Muscari, C Bozzoli, Bozzoli C, C. Gerratana, C. Gerratana, F Zacà, Zacà F, F. Zaca, F. Zaca, C Rovinetti, Carlotta Rovinetti, Daniela Zauli, Daniela Zauli, M. La Plaça, M. La Placa, Paolo Puddu, & Paolo Emilio Puddu. (1988). Association of serum IgA and C4 with severe atherosclerosis. *Atherosclerosis*. https://doi.org/10.1016/0021-9150(88)90204-3

Aoki-Ota, M., Torkamani, A., Ota, T., Schork, N., & Nemazee, D. (2012). Skewed primary Igkappa repertoire and V-J joining in C57BL/6 mice: Implications for recombination accessibility and receptor editing. *J Immunol*, *188*, 2305–2315. https://doi.org/10.4049/jimmunol.1103484

Ashburner, M., Ball, C. A., Blake, J. A., Botstein, D., Butler, H., & Cherry, J. M. (2000). Gene ontology: Tool for the unification of biology. *The Gene Ontology Consortium. Nat Genet*, *25*, 25–29. https://doi.org/10.1038/75556

Askenase, P. W., Bryniarski, K., Paliwal, V., Redegeld, F., Groot Kormelink, T., & Kerfoot, S. (2015). A subset of AID-dependent B-1a cells initiates hypersensitivity and pneumococcal pneumonia resistance. *Ann N Y Acad Sci*, *1362*, 200–214. https://doi.org/10.1111/nyas.12975

Aslanian, A. M., Chapman, H. A., & Charo, I. F. (2005). Transient Role for CD1d-Restricted Natural Killer T Cells in the Formation of Atherosclerotic Lesions. *Arteriosclerosis,*

Thrombosis, and Vascular Biology, *25*(3), 628–632. https://doi.org/10.1161/01.ATV.0000153046.59370.13

Auffray, C., Charron, D., & Hood, L. (2010). Predictive, preventive, personalized and participatory medicine: Back to the future. *Genome Medicine*, *2*(8), 57. https://doi.org/10.1186/gm178

Ayoub, C., Erthal, F., Abdelsalam, M. A., Murad, M. H., Wang, Z., Erwin, P. J., Hillis, G. S., Kritharides, L., & Chow, B. J. W. (2017). Prognostic value of segment involvement score compared to other measures of coronary atherosclerosis by computed tomography: A systematic review and meta-analysis. *Journal of Cardiovascular Computed Tomography*, *11*(4), 258–267. https://doi.org/10.1016/j.jcct.2017.05.001

Aziz, M., Brenner, M., & Wang, P. (2020). Therapeutic potential of B-1a cells in COVID-19. *Shock*, *54*, 586–594. https://doi.org/10.1097/SHK.0000000000001610

Aziz, M., Ode, Y., Zhou, M., Ochani, M., Holodick, N. E., & Rothstein, T. L. (2018). B-1a cells protect mice from sepsis-induced acute lung injury. *Mol Med*, *24*(26). https://doi.org/10.1186/s10020-018-0029-2

Bailey-Bucktrout, S. L. (2013). Self-Antigen-Driven Activation Induces Instability of Regulatory T Cells during an Inflammatory Autoimmune Response. *Immunity*, *39*. https://doi.org/10.1016/j.immuni.2013.10.016.

Bandura, D. R., Baranov, O., VI, OI, A., A, K., R, L., & X. (2009). Mass cytometry: Technique for real time single cell multitarget immunoassay based on inductively coupled plasma time-of-flight mass spectrometry. *Anal Chem*, *81*(16), 6813–6822.

Barth, S. D. (2016). The Ratio of Regulatory (FOXP3+) to Total (CD3+) T Cells Determined by Epigenetic Cell Counting and Cardiovascular Disease Risk: A Prospective Case-Cohort Study in Non-Diabetics. *EBioMedicine*, *11*. https://doi.org/10.1016/j.ebiom.2016.07.035.

Baumgarth, N. (2011). The double life of a B-1 cell: Self-reactivity selects for protective effector functions. *Nat Rev Immunol*, *11*, 34–46. https://doi.org/10.1038/nri2901

Baumgarth, N. (2016). B-1 Cell Heterogeneity and the Regulation of Natural and Antigen-Induced IgM Production. *Frontiers in Immunology*, *7*. https://doi.org/10.3389/fimmu.2016.00324

Baumgarth, N., Herman, O. C., Jager, G. C., Brown, L., Herzenberg, L. A., & Herzenberg, L. A. (1999). Innate and acquired humoral immunities to influenza virus are mediated by distinct arms of the immune system. *Proceedings of the National Academy of Sciences*, *96*(5), 2250–2255. https://doi.org/10.1073/pnas.96.5.2250

Baylin, S. B., Baylin, S. B., Jones, P. A., & Jones, P. A. (2011). A decade of exploring the cancer epigenome—Biological and translational implications. *Nature Reviews Cancer*. https://doi.org/10.1038/nrc3130

Bendall, S. C., Simonds, E. F., Qiu, P., AD, A., Krutzik, P. O., & Finck, R. (2011). Single-cell mass cytometry of differential immune and drug responses across a human hematopoietic continuum. *Science*, *332*(6030), 687–696.

Benjamini, Y., & Hochberg, Y. (1995). Controlling the False Discovery Rate: A Practical and Powerful Approach to Multiple Testing. *Journal of the Royal Statistical Society: Series B (Methodological*, *57*(1), 289–300.

Bentzon, J. F., Otsuka, F., Virmani, R., & Falk, E. (2014). Mechanisms of Plaque Formation and Rupture. *Circulation Research*, *114*(12), 1852–1866. https://doi.org/10.1161/CIRCRESAHA.114.302721

Berland, R., & Wortis, H. H. (2002). Origins and functions of B-1 cells with notes on the role of CD5. *Annu Rev Immunol*, *20*, 253–300. https://doi.org/10.1146/annurev.immunol.20.100301.064833

Biavati, F., Saba, L., Boussoussou, M., Kofoed, K. F., Benedek, T., Donnelly, P., Rodríguez-Palomares, J., Erglis, A., Štěchovský, C., Šakalytė, G., Čemerlić Ađić, N., Gutberlet, M., Dodd, J. D., Diez, I., Davis, G., Zimmermann, E., Kępka, C., Vidakovic, R., Francone, M., … Dewey, M. (2024). Coronary Artery Calcium Score Predicts Major Adverse Cardiovascular Events in Stable Chest Pain. *Radiology*, *310*(3), e231557. https://doi.org/10.1148/radiol.231557

Binder, C. J., Papac-Milicevic, N., & Witztum, J. L. (2016). Innate sensing of oxidation-specific epitopes in health and disease. *Nature Reviews. Immunology*, *16*(8), 485–497. https://doi.org/10.1038/nri.2016.63

Bing Yu, Bing Yu, Mary B. Roberts, Mary B. Roberts, Laura M. Raffield, Laura M. Raffield, Seyedeh M. Zekavat, Seyedeh M. Zekavat, Ngoc Quynh Nguyen, Ngoc Quynh H Nguyen, Mary L. Biggs, Mary L. Biggs, Mary L Biggs, Mary L Biggs, M. R. W. Brown, Michael R. Brown, Gabriel K. Griffin, Gabriel K. Griffin, Pinkal Desai, … Charles B. Eaton. (2021). Supplemental Association of Clonal Hematopoiesis With Incident Heart Failure. *Journal of the American College of Cardiology*. https://doi.org/10.1016/j.jacc.2021.04.085

Björkbacka, H. (2016). Can Circulating Regulatory T Cells Predict Cardiovascular Disease? *EBioMedicine*, *11*, 15–16. https://doi.org/10.1016/j.ebiom.2016.08.044

Bolotin, D. A., Poslavsky, S., Mitrophanov, I., Shugay, M., Mamedov, I. Z., & Putintseva, E. V. (2015). MiXCR: software for comprehensive adaptive immunity profiling. *Nat Methods*, *12*, 380–381. https://doi.org/10.1038/nmeth.3364

Braun, N. A., Covarrubias, R., & Major, A. S. (2010). Natural Killer T Cells and Atherosclerosis: Form and Function Meet Pathogenesis. *Journal of Innate Immunity*, *2*(4), 316–324. https://doi.org/10.1159/000296915

Budoff, M. J., Achenbach, S., Blumenthal, R. S., Carr, J. J., Goldin, J. G., Greenland, P., Guerci, A. D., Lima, J. A. C., Rader, D. J., Rubin, G. D., Shaw, L. J., & Wiegers, S. E. (2006). Assessment of Coronary Artery Disease by Cardiac Computed Tomography. *Circulation*, *114*(16), 1761–1791. https://doi.org/10.1161/CIRCULATIONAHA.106.178458

Budoff, M. J., Dowe, D., Jollis, J. G., Gitter, M., Sutherland, J., Halamert, E., Scherer, M., Bellinger, R., Martin, A., Benton, R., Delago, A., & Min, J. K. (2008). Diagnostic Performance of 64-Multidetector Row Coronary Computed Tomographic Angiography for Evaluation of Coronary Artery Stenosis in Individuals Without Known Coronary Artery Disease: Results From the Prospective Multicenter ACCURACY (Assessment by Coronary Computed Tomographic Angiography of Individuals Undergoing Invasive Coronary Angiography) Trial. *Journal of the American College of Cardiology*, *52*(21), 1724–1732. https://doi.org/10.1016/j.jacc.2008.07.031

Budoff, M. J., Kinninger, A., Gransar, H., Achenbach, S., Al-Mallah, M., Bax, J. J., Berman, D. S., Cademartiri, F., Callister, T. Q., Chang, H.-J., Chow, B. J. W., Cury, R. C., Feuchtner, G., Hadamitzky, M., Hausleiter, J., Kaufmann, P. A., Leipsic, J., Lin, F. Y., Kim, Y.-J., … CONFIRM Investigators. (2023). When Does a Calcium Score Equate to Secondary Prevention?: Insights From the Multinational CONFIRM Registry. *JACC. Cardiovascular Imaging*, *16*(9), 1181–1189. https://doi.org/10.1016/j.jcmg.2023.03.008

Budoff, M. J., Lakshmanan, S., Toth, P. P., Hecht, H. S., Shaw, L. J., Maron, D. J., Michos, E. D., Williams, K. A., Nasir, K., Choi, A. D., Chinnaiyan, K., Min, J., & Blaha, M. (2022). Cardiac CT angiography in current practice: An American society for preventive cardiology clinical practice statement☆. *American Journal of Preventive Cardiology*, *9*, 100318. https://doi.org/10.1016/j.ajpc.2022.100318

Budoff, M. J., Mayrhofer, T., Ferencik, M., Bittner, D., Lee, K. L., Lu, M. T., Coles, A., Jang, J., Krishnam, M., Douglas, P. S., Hoffmann, U., & On behalf of the PROMISE Investigators. (2017). Prognostic Value of Coronary Artery Calcium in the PROMISE Study (Prospective Multicenter Imaging Study for Evaluation of Chest Pain). *Circulation*, *136*(21), 1993–2005. https://doi.org/10.1161/CIRCULATIONAHA.117.030578

Buono, C., Binder, C. J., Stavrakis, G., Witztum, J. L., Glimcher, L. H., & Lichtman, A. H. (2005). T-bet deficiency reduces atherosclerosis and alters plaque antigen-specific immune responses. *Proceedings of the National Academy of Sciences*, *102*(5), 1596–1601. https://doi.org/10.1073/pnas.0409015102

Buono, C., Come, C. E., Stavrakis, G., Maguire, G. F., Connelly, P. W., & Lichtman, A. H. (2003). Influence of Interferon-γ on the Extent and Phenotype of Diet-Induced Atherosclerosis in the LDLR-Deficient Mouse. *Arteriosclerosis, Thrombosis, and Vascular Biology*, *23*(3), 454–460. https://doi.org/10.1161/01.ATV.0000059419.11002.6E

Burke Allen P., Farb Andrew, Malcom Gray T., Liang You-hui, Smialek John, & Virmani Renu. (1997). Coronary Risk Factors and Plaque Morphology in Men with Coronary Disease Who Died Suddenly. *New England Journal of Medicine*, *336*(18), 1276–1282. https://doi.org/10.1056/NEJM199705013361802

Buscarlet, M. (2017). DNMT3A and TET2 dominate clonal hematopoiesis and demonstrate benign phenotypes and different genetic predispositions. *Blood*, *130*. https://doi.org/10.1182/blood-2017-04-777029

Bussaglia, E., Antón, R., Nomdedéu, J. F., & Fuentes-Prior, P. (2019). TET2 missense variants in human neoplasia. A proposal of structural and functional classification. *Mol Genet Genomic Med*, *7:e00772*. https://doi.org/10.1002/mgg3.772

Butcher, M. J., Filipowicz, A. R., Waseem, T. C., McGary, C. M., Crow, K. J., Magilnick, N., Boldin, M., Lundberg, P. S., & Galkina, E. V. (2016). Atherosclerosis-Driven Treg Plasticity Results in Formation of a Dysfunctional Subset of Plastic IFNγ $^{+}$ Th1/Tregs. *Circulation Research*, *119*(11), 1190–1203. https://doi.org/10.1161/CIRCRESAHA.116.309764

C, I.-6 R. M. R. A., DI, S., MV, H., KB, K., JE, E., & T, S. (2012). The interleukin-6 receptor as a target for prevention of coronary heart disease: A mendelian randomisation analysis. *Lancet*, *379*(9822), 1214–1224.

Cai, T., Zhang, Y., Ho, Y. L., Link, N., Sun, J., & Huang, J. (2018). Association of Interleukin 6 Receptor Variant With Cardiovascular Disease Effects of Interleukin 6 Receptor Blocking Therapy: A Phenome-Wide Association Study. *JAMA Cardiol*, *3*(9), 849–857.

Caligiuri, G., Rudling, M., Ollivier, V., Jacob, M.-P., Michel, J.-B., Hansson, G. K., & Nicoletti, A. (2003). Interleukin-10 Deficiency Increases Atherosclerosis, Thrombosis, and Low-density Lipoproteins in Apolipoprotein E Knockout Mice. *Molecular Medicine*, *9*(1–2), 10–17. https://doi.org/10.1007/BF03402102

Casali, P., & Schettino, E. W. (1996). Structure and function of natural antibodies. *Curr Top Microbiol Immunol*, *210*, 167–179. https://doi.org/10.1007/978-3-642-85226-8_17

Chan, K., Wahome, E., Tsiachristas, A., Antonopoulos, A. S., Patel, P., Lyasheva, M., Kingham, L., West, H., Oikonomou, E. K., Volpe, L., Mavrogiannis, M. C., Nicol, E., Mittal, T. K., Halborg, T., Kotronias, R. A., Adlam, D., Modi, B., Rodrigues, J., Screaton, N., … Fairbairn, T. A. (2024). Inflammatory risk and cardiovascular events in patients without obstructive coronary artery disease: The ORFAN multicentre, longitudinal cohort study. *The Lancet*, *403*(10444), 2606–2618. https://doi.org/10.1016/S0140-6736(24)00596-8

Chang, M. K. (1999). Monoclonal antibodies against oxidized low-density lipoprotein bind to apoptotic cells and inhibit their phagocytosis by elicited macrophages: Evidence that oxidation-specific epitopes mediate macrophage recognition. *Proc Natl Acad Sci U S A*, *96*(11), 6353–6358.

Chang, M.-K., Binder, C. J., Miller, Y. I., Subbanagounder, G., Silverman, G. J., Berliner, J. A., & Witztum, J. L. (2004). Apoptotic Cells with Oxidation-specific Epitopes Are Immunogenic and Proinflammatory. *Journal of Experimental Medicine*, *200*(11), 1359–1370. https://doi.org/10.1084/jem.20031763

Chen, L., Fan, X., Zhu, J., Chen, X., Liu, Y., & Zhou, H. (2020). LncRNA MAGI2-AS3 inhibits the self-renewal of leukaemic stem cells by promoting TET2-dependent DNA demethylation of the LRIG1 promoter in acute myeloid leukaemia. *RNA Biol*, *17*, 784–793. https://doi.org/10.1080/15476286.2020.1726637

Chen, S. (2023). *Ultrafast one-pass FASTQ data preprocessing, quality control, and deduplication using fastp. iMeta* (p. 2 107). https://doi.org/10.1002/imt2.107

Cheng, H.-Y., Wu, R., Gebre, A. K., Hanna, R. N., Smith, D. J., Parks, J. S., Ley, K., & Hedrick, C. C. (2013). Increased Cholesterol Content in Gammadelta (γδ) T Lymphocytes Differentially Regulates Their Activation. *PLoS ONE*, *8*(5), e63746. https://doi.org/10.1371/journal.pone.0063746

Cheng, X., Yu, X., Ding, Y., Fu, Q., Xie, J., Tang, T., Yao, R., Chen, Y., & Liao, Y. (2008). The Th17/Treg imbalance in patients with acute coronary syndrome. *Clinical Immunology*, *127*(1), 89–97. https://doi.org/10.1016/j.clim.2008.01.009

Chi, H., Messas, E., Levine, R. A., Graves, D. T., & Amar, S. (2004). Interleukin-1 receptor signaling mediates atherosclerosis associated with bacterial exposure and/or a high-fat diet

in a murine apolipoprotein E heterozygote model: Pharmacotherapeutic implications. *Circulation*, *110*(12), 1678–1685.

Choi, Y. S., & Baumgarth, N. (2008). Dual role for B-1a cells in immunity to influenza virus infection. *J Exp Med*, *205*, 3053–3064. https://doi.org/10.1084/jem.20080979

Choi, Y. S., Dieter, J. A., Rothaeusler, K., Luo, Z., & Baumgarth, N. (2012). B-1 cells in the bone marrow are a significant source of natural IgM. *European Journal of Immunology*, *42*(1), 120–129. https://doi.org/10.1002/eji.201141890

Chou, M.-Y., Fogelstrand, L., Hartvigsen, K., Hansen, L. F., Woelkers, D., Shaw, P. X., Choi, J., Perkmann, T., Bäckhed, F., Miller, Y. I., Hörkkö, S., Corr, M., Witztum, J. L., & Binder, C. J. (2009). Oxidation-specific epitopes are dominant targets of innate natural antibodies in mice and humans. *The Journal of Clinical Investigation*, *119*(5), 1335–1349. https://doi.org/10.1172/JCI36800

Chou, M.-Y., Hartvigsen, K., Hansen, L. F., Fogelstrand, L., Shaw, P. X., Boullier, A., Binder, C. J., & Witztum, J. L. (2008). Oxidation-specific epitopes are important targets of innate immunity. *Journal of Internal Medicine*, *263*(5), 479–488. https://doi.org/10.1111/j.1365-2796.2008.01968.x

Chu, E. (2014). Personalized medicine and anti-EGFR antibody therapy in the treatment of metastatic colorectal cancer: KRAS and beyond. *Oncology*. https://www.semanticscholar.org/paper/Personalized-medicine-and-anti-EGFR-antibody-in-the-Chu/627becce3f88cf682c15e1da1cceec769a202e35

Chyu, K.-. Y. (2012). CD8+ T Cells Mediate the Athero-Protective Effect of Immunization with an ApoB-100 Peptide. *PLoS One*, *7*. https://doi.org/10.1371/journal.pone.0030780.

Clarke, M. C. H., & Bennett, M. R. (2009). Cause or Consequence. *Arteriosclerosis, Thrombosis, and Vascular Biology*, *29*(2), 153–155. https://doi.org/10.1161/ATVBAHA.108.179903

Clement, M., Guedj, K., Andreata, F., Morvan, M., Bey, L., Khallou-Laschet, J., Gaston, A.-T., Delbosc, S., Alsac, J.-M., Bruneval, P., Deschildre, C., Le Borgne, M., Castier, Y., Kim, H.-J., Cantor, H., Michel, J.-B., Caligiuri, G., & Nicoletti, A. (2015). Control of the T Follicular Helper–Germinal Center B-Cell Axis by CD8 $^{+}$ Regulatory T Cells Limits Atherosclerosis and Tertiary Lymphoid Organ Development. *Circulation*, *131*(6), 560–570. https://doi.org/10.1161/CIRCULATIONAHA.114.010988

Cochain, C. (2015). CD8+ T Cells Regulate Monopoiesis and Circulating Ly6Chigh Monocyte Levels in Atherosclerosis in Mice. *Circ. Res*, *117*. https://doi.org/10.1161/CIRCRESAHA.117.304611.

Colantonio, L. D., Bittner, V., Reynolds, K., Levitan, E. B., Rosenson, R. S., Banach, M., Kent, S. T., Derose, S. F., Zhou, H., Safford, M. M., & Muntner, P. (2016). Association of Serum Lipids and Coronary Heart Disease in Contemporary Observational Studies. *Circulation*, *133*(3), 256–264. https://doi.org/10.1161/CIRCULATIONAHA.115.011646

Coltro, G., Mangaonkar, A. A., Lasho, T. L., Finke, C. M., Pophali, P., & Carr, R. (2020). Clinical, molecular, and prognostic correlates of number, type, and functional localization of TET2 mutations in chronic myelomonocytic leukemia (CMML)-a study of 1084 patients. *Leukemia*, *34*, 1407–1421. https://doi.org/10.1038/s41375-019-0690-7

Crotty, S. (2019). T Follicular Helper Cell Biology: A Decade of Discovery and Diseases. *Immunity*, *50*(5), 1132–1148. https://doi.org/10.1016/j.immuni.2019.04.011

Cull, A. H., Snetsinger, B., Buckstein, R., Wells, R. A., & Rauh, M. J. (2017). Tet2 restrains inflammatory gene expression in macrophages. *Exp Hematol*, *55*, 56–70. https://doi.org/10.1016/j.exphem.2017.08.001

Curtiss, L. K., & Tobias, P. S. (2009). Emerging role of Toll-like receptors in atherosclerosis. *J Lipid Res*, *50 Suppl(Suppl):S340-5*.

Daniel O. Griffin, Daniel O. Griffin, Nichol E. Holodick, Thomas L. Rothstein, Nichol E. Holodick, & Thomas L. Rothstein. (2011). Human B1 cells in umbilical cord and adult peripheral blood express the novel phenotype CD20+CD27+CD43+CD70−. *Journal of Experimental Medicine*. https://doi.org/10.1084/jem.20101499

Das, P., Das, P., Singal, R., & Singal, R. (2004). DNA Methylation and Cancer. *Journal of Clinical Oncology*. https://doi.org/10.1200/jco.2004.07.151

Davenport, P., & Tipping, P. G. (2003). The Role of Interleukin-4 and Interleukin-12 in the Progression of Atherosclerosis in Apolipoprotein E-Deficient Mice. *The American Journal of Pathology*, *163*(3), 1117–1125. https://doi.org/10.1016/S0002-9440(10)63471-2

David G. Schatz, David G. Schatz, Yanhong Ji, & Yanhong Ji. (2011). Recombination centres and the orchestration of V(D)J recombination. *Nature Reviews Immunology*. https://doi.org/10.1038/nri2941

Deenen, G. J., & Kroese, F. G. (1993). Kinetics of peritoneal B-1a cells (CD5 B cells) in young adult mice. *Eur J Immunol*, *23*, 12–16. https://doi.org/10.1002/eji.1830230104

Detrano, R., Guerci, A. D., Carr, J. J., Bild, D. E., Burke, G., & Folsom, A. R. (2008). Coronary calcium as a predictor of coronary events in four racial or ethnic groups. *N Engl J Med*, *358*(13), 1336–1345.

Dimayuga, P. C. (2017). Identification of apoB-100 peptide-specific CD8+ T cells in. *Atherosclerosis. J. Am. Heart Assoc.*, *6*.

Dinah V. Parums, D.V. Parums, M. J. Mitchinson, & Malcolm J. Mitchinson. (1981). Demonstration of immunoglobulin in the neighbourhood of advanced atherosclerotic plaques. *Atherosclerosis*. https://doi.org/10.1016/0021-9150(81)90118-0

Dinarello, C. A. (2009). Immunological and inflammatory functions of the interleukin-1 family. *Annu Rev Immunol*, *27*, 519–550.

Dobin, A., Davis, C. A., Schlesinger, F., Drenkow, J., Zaleski, C., & Jha, S. (2013). STAR: ultrafast universal RNA-seq aligner. *Bioinformatics*, *29*, 15–21. https://doi.org/10.1093/bioinformatics/bts635

Dominguez, P. M., Ghamlouch, H., Rosikiewicz, W., Kumar, P., Beguelin, W., & Fontan, L. (2018). TET2 deficiency causes germinal center hyperplasia, impairs plasma cell differentiation, and promotes B-cell lymphomagenesis. *Cancer Discovery*, *8*, 1632–1653. https://doi.org/10.1158/2159-8290.CD-18-0657

Duber, S., Hafner, M., Krey, M., Lienenklaus, S., Roy, B., & Hobeika, E. (2009). Induction of B-cell development in adult mice reveals the ability of bone marrow to produce B-1a cells. *Blood*, *114*, 4960–4967. https://doi.org/10.1182/blood-2009-04-218156

Duewell, P., Kono, H., Rayner, K. J., Sirois, C. M., Vladimer, G., & Bauernfeind, F. G. (2010). NLRP3 inflammasomes are required for atherogenesis and activated by cholesterol crystals. *Nature*, *464*(7293), 1357–1361.

Dumitriu, I. E. (2012). High Levels of Costimulatory Receptors OX40 and 4-1BB Characterize CD4+CD28null T Cells in Patients with Acute Coronary Syndrome. *Circ. Res*, *110*. https://doi.org/10.1161/CIRCRESAHA.111.261933.

Eid, R. E., Rao, D. A., Zhou, J., Lo, S. L., Ranjbaran, H., Gallo, A., Sokol, S. I., Pfau, S., Pober, J. S., & Tellides, G. (2009). Interleukin-17 and Interferon-γ Are Produced Concomitantly by

Human Coronary Artery–Infiltrating T Cells and Act Synergistically on Vascular Smooth Muscle Cells. *Circulation*, *119*(10), 1424–1432. https://doi.org/10.1161/CIRCULATIONAHA.108.827618

Elhage, R., Maret, A., Pieraggi, M. T., Thiers, J. C., Arnal, J. F., & Bayard, F. (1998). Differential effects of interleukin-1 receptor antagonist and tumor necrosis factor binding protein on fatty-streak formation in apolipoprotein E-deficient mice. *Circulation*, *97*(3), 242–244.

Engelbertsen, D., Andersson, L., Ljungcrantz, I., Wigren, M., Hedblad, B., Nilsson, J., & Björkbacka, H. (2013). T-Helper 2 Immunity Is Associated With Reduced Risk of Myocardial Infarction and Stroke. *Arteriosclerosis, Thrombosis, and Vascular Biology*, *33*(3), 637–644. https://doi.org/10.1161/ATVBAHA.112.300871

Engelbertsen, D., Rattik, S., Knutsson, A., Björkbacka, H., Bengtsson, E., & Nilsson, J. (2014). Induction of T helper 2 responses against human apolipoprotein B100 does not affect atherosclerosis in ApoE−/− mice. *Cardiovascular Research*, *103*(2), 304–312. https://doi.org/10.1093/cvr/cvu131

Evans, M. A., Sano, S., & Walsh, K. (2020). Cardiovascular Disease, Aging, and Clonal Hematopoiesis. *Annu Rev Pathol*, *15*, 419–438.

Falk Nimmerjahn, Jeffrey V. Ravetch, Falk Nimmerjahn, & Jeffrey V. Ravetch. (2005). Divergent Immunoglobulin G Subclass Activity Through Selective Fc Receptor Binding. *Science*. https://doi.org/10.1126/science.1118948

Fatkhullina, A. R., Peshkova, I. O., Dzutsev, A., Aghayev, T., McCulloch, J. A., Thovarai, V., Badger, J. H., Vats, R., Sundd, P., Tang, H.-Y., Kossenkov, A. V., Hazen, S. L., Trinchieri, G., Grivennikov, S. I., & Koltsova, E. K. (2018). An Interleukin-23-Interleukin-22 Axis Regulates Intestinal Microbial Homeostasis to Protect from Diet-Induced Atherosclerosis. *Immunity*, *49*(5), 943-957.e9. https://doi.org/10.1016/j.immuni.2018.09.011

Fernandez, D. M., Rahman, A. H., Fernandez, N. F., Chudnovskiy, A., Amir, E. D., & Amadori, L. (2019). Single-cell immune landscape of human atherosclerotic plaques. *Nat Med*, *25*(10), 1576–1588.

Finak, G., McDavid, A., Yajima, M., Deng, J., Gersuk, V., Shalek, A. K., Slichter, C. K., Miller, H. W., McElrath, M. J., Prlic, M., Linsley, P. S., & Gottardo, R. (2015). MAST: A flexible statistical framework for assessing transcriptional changes and characterizing heterogeneity in single-cell RNA sequencing data. *Genome Biology*, *16*(1), 278. https://doi.org/10.1186/s13059-015-0844-5

Finck, R., Simonds, E. F., Jager, A., Krishnaswamy, S., Sachs, K., & Fantl, W. (2013). Normalization of mass cytometry data with bead standards. *Cytometry A*, *83*(5), 483–494.

Fischer, P., Lehmann, U., Sobota, R. M., Schmitz, J., Niemand, C., & Linnemann, S. (2004). The role of the inhibitors of interleukin-6 signal transduction SHP2 and SOCS3 for desensitization of interleukin-6 signalling. *Biochem J*, *378*(Pt 2), 449–460.

Forloni, G. (2020). Alzheimer's disease: From basic science to precision medicine approach. *BMJ Neurology Open*, *2*(2), e000079. https://doi.org/10.1136/bmjno-2020-000079

Franks, A., Airoldi, E., & Slavov, N. (2017). Post-transcriptional regulation across human tissues. *PLOS Computational Biology*, *13*(5), e1005535. https://doi.org/10.1371/journal.pcbi.1005535

Franzén, O., Gan, L.-M., & Björkegren, J. L. M. (2019). PanglaoDB: A web server for exploration of mouse and human single-cell RNA sequencing data. *Database*, *2019*, baz046. https://doi.org/10.1093/database/baz046

Fread, K. I., Strickland, W. D., Nolan, G. P., & Zunder, E. R. (2017). An Updated Debarcoding Tool for Mass Cytometry with Cell Type-Specific and Cell Sample-Specific Stringency Adjustment. *Pac Symp Biocomput*, *22*, 588–598.

Frostegård, J., Ulfgren, A.-K., Nyberg, P., Hedin, U., Swedenborg, J., Andersson, U., & Hansson, G. K. (1999). Cytokine expression in advanced human atherosclerotic plaques: Dominance of pro-inflammatory (Th1) and macrophage-stimulating cytokines. *Atherosclerosis*, *145*(1), 33–43. https://doi.org/10.1016/S0021-9150(99)00011-8

Fuster, J. J. (2017). Clonal hematopoiesis associated with TET2 deficiency accelerates atherosclerosis development in mice. *Science*, *355*(6327), 842–847.

Fuster, J. J., MacLauchlan, S., Zuriaga, M. A., Polackal, M. N., Ostriker, A. C., & Chakraborty, R. (2017). Clonal hematopoiesis associated with TET2 deficiency accelerates atherosclerosis development in mice. *Science*, *355*, 842–847. https://doi.org/10.1126/science.aag1381

Fuster, J. J., Zuriaga, M. A., Zorita, V., MacLauchlan, S., Polackal, M. N., Viana-Huete, V., Ferrer-Pérez, A., Matesanz, N., Herrero-Cervera, A., Sano, S., Cooper, M. A., González-Navarro, H., & Walsh, K. (2020). TET2-Loss-of-Function-Driven Clonal Hematopoiesis Exacerbates Experimental Insulin Resistance in Aging and Obesity. *Cell Reports*, *33*(4), 108326. https://doi.org/10.1016/j.celrep.2020.108326

Gaddis, D. E., Padgett, L. E., Wu, R., McSkimming, C., Romines, V., Taylor, A. M., McNamara, C. A., Kronenberg, M., Crotty, S., Thomas, M. J., Sorci-Thomas, M. G., & Hedrick, C. C. (2018). Apolipoprotein AI prevents regulatory to follicular helper T cell switching during atherosclerosis. *Nature Communications*, *9*(1). https://doi.org/10.1038/s41467-018-03493-5

Gagliani, N. (2013). Coexpression of CD49b and LAG-3 Identifies Human and Mouse T Regulatory Type 1 Cells. *Nat. Med*, *19*. https://doi.org/10.1038/nm.3179.

Garcia-Gomez, A., Li, T., Kerick, M., Catala-Moll, F., Comet, N. R., & Rodriguez-Ubreva, J. (2017). TET2- and TDG-mediated changes are required for the acquisition of distinct histone modifications in divergent terminal differentiation of myeloid cells. *Nucleic Acids Res*, *45*, 10002–10017. https://doi.org/10.1093/nar/gkx666

Gardiner, L.-J., Carrieri, A. P., Bingham, K., Macluskie, G., Bunton, D., McNeil, M., & Pyzer-Knapp, E. O. (2022). Combining explainable machine learning, demographic and multi-omic data to inform precision medicine strategies for inflammatory bowel disease. *PLOS ONE*, *17*(2), e0263248. https://doi.org/10.1371/journal.pone.0263248

Genovese, G. (2014). Clonal hematopoiesis and blood-cancer risk inferred from blood DNA sequence. *N. Engl. J. Med*, *371*. https://doi.org/10.1056/NEJMoa1409405

George, J. (2012). Regulatory T Cells and IL-10 Levels Are Reduced in Patients with Vulnerable Coronary Plaques. *Atherosclerosis*, *222*. https://doi.org/10.1016/j.atherosclerosis.2012.03.016.

George, J., Afek, A., Gilburd, B., Levkovitz, H., Shaish, A., & Goldberg, I. (1998). Hyperimmunization of apo-E-deficient mice with homologous malondialdehyde low-density lipoprotein suppresses early atherogenesis. *Atherosclerosis*, *138*, 147–152. https://doi.org/10.1016/S0021-9150(98)00015-X

Gewaltig, J., Kummer, M., Koella, C., Cathomas, G., & Biedermann, B. C. (2008). Requirements for CD8 T-cell migration into the human arterial wall. *Human Pathology*, *39*(12), 1756–1762. https://doi.org/10.1016/j.humpath.2008.04.018

Ghosn, E. E., & Yang, Y. (2015). Hematopoietic stem cell-independent B-1a lineage. *Ann N Y Acad Sci*, *1362*, 23–38. https://doi.org/10.1111/nyas.12881

Gisterå, A., Robertson, A.-K. L., Andersson, J., Ketelhuth, D. F. J., Ovchinnikova, O., Nilsson, S. K., Lundberg, A. M., Li, M. O., Flavell, R. A., & Hansson, G. K. (2013). Transforming Growth Factor–β Signaling in T Cells Promotes Stabilization of Atherosclerotic Plaques Through an Interleukin-17–Dependent Pathway. *Science Translational Medicine*, *5*(196). https://doi.org/10.1126/scitranslmed.3006133

Giudicelli, V., Chaume, D., & Lefranc, M. P. (2005). IMGT/GENE-DB: a comprehensive database for human and mouse immunoglobulin and T cell receptor genes. *Nucleic Acids Res*, *33:D256–61*. https://doi.org/10.1093/nar/gki010

Goettsch, C., Hutcheson, J. D., Hagita, S., Rogers, M. A., Creager, M. D., Pham, T., Choi, J., Mlynarchik, A. K., Pieper, B., Kjolby, M., Aikawa, M., & Aikawa, E. (2016). A single injection of gain-of-function mutant PCSK9 adeno-associated virus vector induces cardiovascular calcification in mice with no genetic modification. *Atherosclerosis*, *251*, 109–118. https://doi.org/10.1016/j.atherosclerosis.2016.06.011

Göran K. Hansson, Göran K. Hansson, Göran Bondjers, Göran Bondjers, Anders Bylock, A. Bylock, Anders Bylock, Anders Bylock, Lena Hjalmarsson, & Lena Hjalmarsson. (1980). Ultrastructural studies on the localization of IgG in the aortic endothelium and subendothelial intima of atherosclerotic and nonatherosclerotic rabbits. *Experimental and Molecular Pathology*. https://doi.org/10.1016/0014-4800(80)90028-3

Grasset, E. K., Duhlin, A., Agardh, H. E., Ovchinnikova, O., Hagglof, T., & Forsell, M. N. (2015). Sterile inflammation in the spleen during atherosclerosis provides oxidation-specific epitopes that induce a protective B-cell response. *Proc Natl Acad Sci U.S.A*, *112:E2030–8*. https://doi.org/10.1073/pnas.1421227112

Gregersen, I., Skjelland, M., Holm, S., Holven, K. B., Krogh-Sørensen, K., Russell, D., Askevold, E. T., Dahl, C. P., Ørn, S., Gullestad, L., Mollnes, T. E., Ueland, T., Aukrust, P., &

Halvorsen, B. (2013). Increased Systemic and Local Interleukin 9 Levels in Patients with Carotid and Coronary Atherosclerosis. *PLoS ONE*, *8*(8), e72769. https://doi.org/10.1371/journal.pone.0072769

Groot, H. E., Al Ali, L., Horst, I. C. C., Schurer, R. A. J., Werf, H. W., & Lipsic, E. (2019). Plasma interleukin 6 levels are associated with cardiac function after ST-elevation myocardial infarction. *Clin Res Cardiol*, *108*(6), 612–621.

Gruber, S., Hendrikx, T., Tsiantoulas, D., Ozsvar-Kozma, M., Goderle, L., & Mallat, Z. (2016). Sialic acid-binding immunoglobulin-like lectin G promotes atherosclerosis and liver inflammation by suppressing the protective functions of B-1 cells. *Cell Rep*, *14*, 2348–2361. https://doi.org/10.1016/j.celrep.2016.02.027

Gu, Z., Gu, L., Eils, R., Schlesner, M., & Brors, B. (2014). Circlize Implements and enhances circular visualization in R. *Bioinformatics*, *30*, 2811–2812. https://doi.org/10.1093/bioinformatics/btu393

Guasti, L. (2016). Relationship between Regulatory T Cells Subsets and Lipid Profile in Dyslipidemic Patients: A Longitudinal Study during Atorvastatin Treatment. *BMC Cardiovasc. Disord*, *16*. https://doi.org/10.1186/s12872-016-0201-y.

Guimarães, J., de Almeida, J., Mendes, P. L., Ferreira, M. J., & Gonçalves, L. (2024). Advancements in non-invasive imaging of atherosclerosis: Future perspectives. *Journal of Clinical Lipidology*, *18*(2), e142–e152. https://doi.org/10.1016/j.jacl.2023.11.008

Guo, J. U., Su, Y., Guo, J. U., Zhong, C., Su, Y., Zhong, C., Guo, M., Ming, G. L., Song, H., & Song, H. (2011). Emerging roles of TET proteins and 5-hydroxymethylcytosines in active DNA demethylation and beyond. *Cell Cycle*. https://doi.org/10.4161/cc.10.16.17093

Gupta, S., Pablo, A. M., Jiang, X. c, Wang, N., Tall, A. R., & Schindler, C. (1997). IFN-gamma potentiates atherosclerosis in ApoE knock-out mice. *Journal of Clinical Investigation*, *99*(11), 2752–2761. https://doi.org/10.1172/JCI119465

Haan, S., Keller, J. F., Behrmann, I., Heinrich, P. C., & Haan, C. (2005). Multiple reasons for an inefficient STAT1 response upon IL-6-type cytokine stimulation. *Cell Signal*, *17*(12), 1542–1550.

Haas, K. M., Poe, J. C., Steeber, D. A., & Tedder, T. F. (2005). B-1a and B-1b cells exhibit distinct developmental requirements and have unique functional roles in innate and adaptive immunity to S. pneumoniae. *Immunity*, *23*, 7–18. https://doi.org/10.1016/j.immuni.2005.04.011

Hardy, R. R., & Hayakawa, K. (2012). Positive and negative selection of natural autoreactive B cells. *Adv Exp Med Biol*, *750*, 227–238. https://doi.org/10.1084/jem.20021459

Hardy, R. R., Wei, C. J., & Hayakawa, K. (2004). Selection during development of VH11+ B cells: A model for natural autoantibody-producing CD5+ B cells. *Immunol Rev*, *197*, 60–74. https://doi.org/10.1111/j.0105-2896.2004.0100.x

Harmon, D. B., Srikakulapu, P., Kaplan, J. L., Oldham, S. N., McSkimming, C., & Garmey, J. C. (2016). Protective role for B-1b B cells and igM in obesity-associated inflammation, glucose intolerance, and insulin resistance. *Arterioscler Thromb Vasc Biol*, *36*, 682–691. https://doi.org/10.1161/ATVBAHA.116.307166

Hashmi, S., & Zeng, Q. T. (2006). Role of interleukin-17 and interleukin-17-induced cytokines interleukin-6 and interleukin-8 in unstable coronary artery disease. *Coronary Artery Disease*, *17*(8), 699–706. https://doi.org/10.1097/01.mca.0000236288.94553.b4

Hausleiter, J., Meyer, T., Hermann, F., Hadamitzky, M., Krebs, M., Gerber, T. C., McCollough, C., Martinoff, S., Kastrati, A., Schömig, A., & Achenbach, S. (2009). Estimated Radiation Dose Associated With Cardiac CT Angiography. *JAMA*, *301*(5), 500–507. https://doi.org/10.1001/jama.2009.54

Hausmann, D., Erbel, R., Alibelli-Chemarin, M. J., Boksch, W., Caracciolo, E., Cohn, J. M., Culp, S. C., Daniel, W. G., De Scheerder, I., & DiMario, C. (1995). The safety of intracoronary ultrasound. A multicenter survey of 2207 examinations. *Circulation*, *91*(3), 623–630. https://doi.org/10.1161/01.cir.91.3.623

Hayakawa, K., Asano, M., Shinton, S. A., Gui, M., Allman, D., & Stewart, C. L. (1999). Positive selection of natural autoreactive B cells. *Science*, *285*, 113–116. https://doi.org/10.1126/science.285.5424.113

Hayakawa, K., Asano, M., Shinton, S. A., Gui, M., Wen, L. J., & Dashoff, J. (2003). Positive selection of anti-thy-1 autoreactive B-1 cells and natural serum autoantibody production independent from bone marrow B cell development. *J Exp Med*, *197*, 87–99. https://doi.org/10.1084/jem.20021459

Held, C., White, H. D., Stewart, R. A. H., Budaj, A., Cannon, C. P., & Hochman, J. S. (2017). Inflammatory Biomarkers Interleukin-6 and C-Reactive Protein and Outcomes in Stable Coronary Heart Disease: Experiences From the STABILITY (Stabilization of Atherosclerotic Plaque by Initiation of Darapladib Therapy. *Trial. J Am Heart Assoc*, *6*(10).

Herrington, W., Lacey, B., Sherliker, P., Armitage, J., & Lewington, S. (2016). Epidemiology of Atherosclerosis and the Potential to Reduce the Global Burden of Atherothrombotic Disease. *Circ Res*, *118*(4), 535–546.

Holger Winkels, Erik Ehinger, Holger Winkels, Melanie Vassallo, Erik Ehinger, Konrad Buscher, Melanie Vassallo, Huy Q. Dinh, Konrad Buscher, Huy Q. Dinh, Kouji Kobiyama, Kouji Kobiyama, Anouk A.J. Hamers, Kouji Kobiyama, Anouk A.J. Hamers, Clément Cochain, Clément Cochain, Ehsan Vafadarnejad, Ehsan Vafadarnejad, … Dennis Wolf. (2018). Atlas of the Immune Cell Repertoire in Mouse Atherosclerosis Defined by Single-Cell RNA-Sequencing and Mass Cytometry. *Circulation Research*. https://doi.org/10.1161/circresaha.117.312513

Holodick, N. E., Tumang, J. R., & Rothstein, T. L. (2010). Immunoglobulin secretion by B1 cells: Differential intensity and IRF4-dependence of spontaneous IgM secretion by peritoneal and splenic B1 cells. *European Journal of Immunology*, *40*(11), 3007–3016. https://doi.org/10.1002/eji.201040545

Holodick, N. E., Vizconde, T., Hopkins, T. J., & Rothstein, T. L. (2016). Age-Related Decline in Natural IgM Function: Diversification and Selection of the B-1a Cell Pool with Age. *The Journal of Immunology*, *196*(10), 4348–4357. https://doi.org/10.4049/jimmunol.1600073

Holodick, N. E., Vizconde, T., & Rothstein, T. L. (2014a). B-1a Cell Diversity: Nontemplated Addition in B-1a Cell Ig Is Determined by Progenitor Population and Developmental Location. *The Journal of Immunology*, *192*(5), 2432–2441. https://doi.org/10.4049/jimmunol.1300247

Holodick, N. E., Vizconde, T., & Rothstein, T. L. (2014b). Splenic B-1a Cells Expressing CD138 Spontaneously Secrete Large Amounts of Immunoglobulin in Naïve Mice. *Frontiers in Immunology*, *5*. https://doi.org/10.3389/fimmu.2014.00129

Holodick, N. E., Zeumer, L., Rothstein, T. L., & Morel, L. (2016). Expansion of B-1a cells with germline heavy chain sequence in lupus mice. *Front Immunol*, *7*(108). https://doi.org/10.3389/fimmu.2016.00108

Hood, L., & Friend, S. H. (2011). Predictive, personalized, preventive, participatory (P4) cancer medicine. *Nature Reviews Clinical Oncology*, *8*(3), 184–187. https://doi.org/10.1038/nrclinonc.2010.227

Hooijkaas, H., Benner, R., Pleasants, J. R., & Wostmann, B. S. (1984). Isotypes and specificities of immunoglobulins produced by germ-free mice fed chemically defined ultrafiltered "antigen-free" diet. *European Journal of Immunology*, *14*(12), 1127–1130. https://doi.org/10.1002/eji.1830141212

Horkko, S. (1999). Monoclonal autoantibodies specific for oxidized phospholipids or oxidized phospholipid-protein adducts inhibit macrophage uptake of oxidized low-density lipoproteins. *J Clin Invest*, *103*(1), 117–128.

Horstmann, H., Lindau, A., Hansen, S., Stachon, P., Hilgendorf, I., Bode, C., Zirlik, A., & Wolf, D. (2020). Atlas of the immune cell repertoire in human atherosclerotic plaques characterized by single cell RNA-sequencing and multi-color flow cytometry. *European Heart Journal*, *41*(Supplement_2), ehaa946.2353. https://doi.org/10.1093/ehjci/ehaa946.2353

Hu, C., Li, T., Xu, Y., Zhang, X., Li, F., Bai, J., Chen, J., Jiang, W., Yang, K., Ou, Q., Li, X., Wang, P., & Zhang, Y. (2023). CellMarker 2.0: An updated database of manually curated cell markers in human/mouse and web tools based on scRNA-seq data. *Nucleic Acids Research*, *51*(D1), D870–D876. https://doi.org/10.1093/nar/gkac947

Huan, T., Zhang, B., Huan, T., Zhang, B., Wang, Z., Joehanes, R., Wang, Z., Zhu, J., Joehanes, R., Zhu, J., Johnson, A. D., Zhu, J., Zhu, J., Zhu, J., Johnson, A. D., Johnson, A. D., Ying, S., Ying, S., Munson, P. J., … Levy, D. (2013). A Systems Biology Framework Identifies Molecular Underpinnings of Coronary Heart Disease. *Arteriosclerosis, Thrombosis, and Vascular Biology*. https://doi.org/10.1161/atvbaha.112.300112

Huber, S. A., Sakkinen, P., Conze, D., Hardin, N., & Tracy, R. (1999). Interleukin-6 exacerbates early atherosclerosis in mice. *Arterioscler Thromb Vasc Biol*, *19*(10), 2364–2367.

Hulsen, T., Jamuar, S. S., Moody, A. R., Karnes, J. H., Varga, O., Hedensted, S., Spreafico, R., Hafler, D. A., & McKinney, E. F. (2019). From Big Data to Precision Medicine. *Frontiers in Medicine*, *6*, 34. https://doi.org/10.3389/fmed.2019.00034

Ianevski, A., Giri, A. K., & Aittokallio, T. (2022). Fully-automated and ultra-fast cell-type identification using specific marker combinations from single-cell transcriptomic data. *Nature Communications*, *13*(1), 1246. https://doi.org/10.1038/s41467-022-28803-w

IRGCERF, C., N, S., AS, B., DF, F., J, G., & P, W. (2012). Interleukin-6 receptor pathways in coronary heart disease: A collaborative meta-analysis of 82 studies. *Lancet*, *379*(9822), 1205–1213.

Ito, K., Lee, J., Chrysanthou, S., Zhao, Y., Josephs, K., & Sato, H. (2019). Non-catalytic roles of tet2 are essential to regulate hematopoietic stem and progenitor cell homeostasis. *Cell Rep*, *28*(2480–90), 4. https://doi.org/10.1016/j.celrep.2019.07.094

J. McClatchy, R. Strogantsev, E. Wolfe, H. Y. Lin, M. Mohammadhosseini, B. Davis, C. Eden, D. Goldman, W. Fleming, P. Conley, G. Wu, L. Cimmino, H. Mohammed, & A. Agarwal. (2023). Clonal hematopoiesis related TET2 loss-of-function impedes IL1β-mediated epigenetic reprogramming in hematopoietic stem and progenitor cells. *Nature Communications*. https://doi.org/10.1038/s41467-023-43697-y

J, S. S., D, L., SMB, M., KR, E., G, D., & J, S. (2020). Germline TET2 loss of function causes childhood immunodeficiency and lymphoma. *Blood*, *136*, 1055–1066. https://doi.org/10.1182/blood.2020005844

Jaffe, D. B., Shahi, P., Adams, B. A., Chrisman, A. M., Finnegan, P. M., & Raman, N. (2022). Functional antibodies exhibit light chain coherence. *Nature*, *611*, 352–357. https://doi.org/10.1038/s41586-022-05371-z

Jaiswal, S. (2014). Age-related clonal hematopoiesis associated with adverse outcomes. *N Engl J Med*, *371*(26), 2488–2498.

Jaiswal, S. (2017a). Clonal Hematopoiesis and Risk of Atherosclerotic Cardiovascular Disease. *N Engl J Med*, *377*(2), 111–121.

Jaiswal, S. (2017b). Clonal hematopoiesis and risk of atherosclerotic cardiovascular disease. *N. Engl. J. Med*, *377*. https://doi.org/10.1056/NEJMoa1701719

Jaiswal, S., & Libby, P. (2020). Clonal haematopoiesis: Connecting ageing and inflammation in cardiovascular disease. *Nat Rev Cardiol*, *17*(3), 137–144.

Jeroen M. J. Tas, Jeroen M. J. Tas, Luka Mesin, Luka Mesin, Giulia Pasqual, Giulia Pasqual, Sasha Targ, Sasha Targ, Johanne T. Jacobsen, Sasha Targ, Johanne T. Jacobsen, Johanne T. Jacobsen, Yasuko M. Mano, Casie S. Chen, Yasuko M. Mano, Jean–Claude Weill, Casie S. Chen, Claude-Agnès Reynaud, Jean-Claude Weill, … Gabriel D. Victora. (2016). Visualizing antibody affinity maturation in germinal centers. *Science*. https://doi.org/10.1126/science.aad3439

Jiao, J., Jin, Y., Zheng, M., Zhang, H., Yuan, M., & Lv, Z. (2019). AID and TET2 co-operation modulates FANCA expression by active demethylation in diffuse large B cell lymphoma. *Clin Exp Immunol*, *195*, 190–201. https://doi.org/10.1111/cei.13227

Jin, S., Guerrero-Juarez, C. F., Zhang, L., Chang, I., Ramos, R., Kuan, C.-H., Myung, P., Plikus, M. V., & Nie, Q. (2021). Inference and analysis of cell-cell communication using CellChat. *Nature Communications*, *12*(1), 1088. https://doi.org/10.1038/s41467-021-21246-9

Jung, C., Evans, M. A., & Walsh, K. (2020). *Genetics of age-related clonal hematopoiesis and atherosclerotic cardiovascular disease*. Curr Opin Cardiol.

Kale Satish & Shinde Sandeep. (2023). Data-Driven Diagnostics: Leveraging Machine Learning for Precision Medicine. *International Journal of Advanced Research in Science, Communication and Technology*, 548–551. https://doi.org/10.48175/IJARSCT-11138

Kamtchum-Tatuene, J., Saba, L., Heldner, M. R., Poorthuis, M. H. F., Borst, G. J., & Rundek, T. (2022). Interleukin-6 Predicts Carotid Plaque Severity, Vulnerability, and Progression. *Circ Res*, *131*(2).

Kang, S., & Kishimoto, T. (2021). Interplay between interleukin-6 signaling and the vascular endothelium in cytokine storms. *Exp Mol Med*, *53*(7), 1116–1123.

Kaplan, M. H. (2013). Th9 cells: Differentiation and disease. *Immunological Reviews*, *252*(1), 104–115. https://doi.org/10.1111/imr.12028

Karvonen, J., Paivansalo, M., Kesaniemi, Y. A., & Horkko, S. (2003). Immunoglobulin M type of autoantibodies to oxidized low-density lipoprotein has an inverse relation to carotid artery atherosclerosis. *Circulation*, *108*, 2107–2112. https://doi.org/10.1161/01.CIR.0000092891.55157.A7

Kawahara, T., Ohdan, H., Zhao, G., Yang, Y.-G., & Sykes, M. (2003). Peritoneal Cavity B Cells Are Precursors of Splenic IgM Natural Antibody-Producing Cells 1. *The Journal of Immunology*, *171*(10), 5406–5414. https://doi.org/10.4049/jimmunol.171.10.5406

Kelly, N. J., & Chan, S. Y. (2022). Pulmonary Arterial Hypertension: Emerging Principles of Precision Medicine across Basic Science to Clinical Practice. *Reviews in Cardiovascular Medicine*, *23*(11), 378. https://doi.org/10.31083/j.rcm2311378

Khamis, R. Y. (2016). High Serum Immunoglobulin G and M Levels Predict Freedom From Adverse Cardiovascular Events in Hypertension: A Nested Case-Control Substudy of the Anglo-Scandinavian Cardiac Outcomes Trial. *EBioMedicine*, *9*, 372–380.

Khan, S. R., Dalm, V. A. S. H., Ikram, M. K., Peeters, R. P., van Hagen, P. M., Kavousi, M., & Chaker, L. (2023). The Association of Serum Immunoglobulins with Risk of Cardiovascular Disease and Mortality: The Rotterdam Study. *Journal of Clinical Immunology*, *43*(4), 769–779. https://doi.org/10.1007/s10875-023-01433-7

Kidd, B. A., Peters, L. A., Schadt, E. E., & Dudley, J. T. (2014). Unifying immunology with informatics and multiscale biology. *Nature Immunology*, *15*(2), 118–127. https://doi.org/10.1038/ni.2787

King, V. L., Cassis, L. A., & Daugherty, A. (2007). Interleukin-4 Does Not Influence Development of Hypercholesterolemia or Angiotensin II-Induced Atherosclerotic Lesions in Mice. *The American Journal of Pathology*, *171*(6), 2040–2047. https://doi.org/10.2353/ajpath.2007.060857

Kirii, H., Niwa, T., Yamada, Y., Wada, H., Saito, K., & Iwakura, Y. (2003). Lack of interleukin-1beta decreases the severity of atherosclerosis in ApoE-deficient mice. *Arterioscler Thromb Vasc Biol*, *23*(4), 656–660.

Kita, T., Yamashita, T., Sasaki, N., Kasahara, K., Sasaki, Y., Yodoi, K., Takeda, M., Nakajima, K., & Hirata, K. (2014). Regression of atherosclerosis with anti-CD3 antibody via augmenting a regulatory T-cell response in mice. *Cardiovascular Research*, *102*(1), 107–117. https://doi.org/10.1093/cvr/cvu002

Kleindienst, R. (1993). Immunology of atherosclerosis. Demonstration of heat shock protein 60 expression and T lymphocytes bearing alpha/beta or gamma/delta receptor in human atherosclerotic lesions. *Am. J. Pathol.*, *142*.

Ko, M., Bandukwala, H. S., An, J., Lamperti, E. D., Thompson, E. C., & Hastie, R. (2011). Ten-Eleven-Translocation 2 (TET2) negatively regulates homeostasis and differentiation of hematopoietic stem cells in mice. *Proc Natl Acad Sci U.S.A*, *108*, 14566–14571. https://doi.org/10.1073/pnas.1112317108

Kobiyama, K., & Ley, K. (2018). Atherosclerosis. *Circulation Research*, *123*(10), 1118–1120. https://doi.org/10.1161/CIRCRESAHA.118.313816

Kolbus, D., Ramos, O. H., Berg, K. E., Persson, J., Wigren, M., Björkbacka, H., Fredrikson, G. N., & Nilsson, J. (2010). CD8+ T cell activation predominate early immune responses to hypercholesterolemia in Apoe-/- mice. *BMC Immunology*, *11*(1). https://doi.org/10.1186/1471-2172-11-58

Kolodgie Frank D., Gold Herman K., Burke Allen P., Fowler David R., Kruth Howard S., Weber Deena K., Farb Andrew, Guerrero L.J., Hayase Motoya, Kutys Robert, Narula Jagat, Finn Aloke V., & Virmani Renu. (2003). Intraplaque Hemorrhage and Progression of Coronary Atheroma. *New England Journal of Medicine*, *349*(24), 2316–2325. https://doi.org/10.1056/NEJMoa035655

Komatsu, N. (2014). Pathogenic Conversion of Foxp3+ T Cells into TH17 Cells in Autoimmune Arthritis. *Nat. Med*, *20*. https://doi.org/10.1038/nm.3432.

Korn, T. (2007). Myelin-Specific Regulatory T Cells Accumulate in the CNS but Fail to Control Autoimmune Inflammation. *Nat. Med*, *13*. https://doi.org/10.1038/nm1564.

Kothari, H., Williams, C. M., McSkimming, C., Drago, F., Marshall, M. A., & Garmey, J. (2021). Identification of human immune cell subtypes most responsive to IL-1beta-induced inflammatory signaling using mass cytometry. *Sci Signal*, *14*(673).

Kovalcsik, E., Antunes, R. F., Baruah, P., Kaski, J. C., & Dumitriu, I. E. (2015). Proteasome-Mediated Reduction in Proapoptotic Molecule Bim Renders CD4 $^{+}$ CD28 ^{null} T Cells Resistant to Apoptosis in Acute Coronary Syndrome. *Circulation*, *131*(8), 709–720. https://doi.org/10.1161/CIRCULATIONAHA.114.013710

Kragel, A. H., Reddy, S. G., Wittes, J. T., & Roberts, W. C. (1989). Morphometric analysis of the composition of atherosclerotic plaques in the four major epicardial coronary arteries in acute myocardial infarction and in sudden coronary death. *Circulation*, *80*(6), 1747–1756. https://doi.org/10.1161/01.CIR.80.6.1747

Kreslavsky, T., Vilagos, B., Tagoh, H., Poliakova, D. K., Schwickert, T. A., & Wohner, M. (2017). Essential role for the transcription factor Bhlhe41 in regulating the development, self-renewal and BCR repertoire of B-1a cells. *Nat Immunol*, *18*, 442–455. https://doi.org/10.1038/ni.3694

Kretschmer, K., Engel, H., & Weiss, S. (2002). Strong antigenic selection shaping the immunoglobulin heavy chain repertoire of B-1a lymphocytes in lambda 2(315) transgenic mice. *Eur J Immunol*, *32*, 2317–2327. https://doi.org/10.1002/1521-4141(200208)32:8

Kretschmer, K., Jungebloud, A., Stopkowicz, J., Kleinke, T., Hoffmann, R., & Weiss, S. (2003). The selection of marginal zone B cells differs from that of B-1a cells. *J Immunol*, *171*, 6495–6501. https://doi.org/10.4049/jimmunol.171.12.6495

Kristiansen, T. A., Jaensson Gyllenback, E., Zriwil, A., Bjorklund, T., Daniel, J. A., & Sitnicka, E. (2016). Cellular barcoding links B-1a B cell potential to a fetal hematopoietic stem cell state at the single-cell level. *Immunity*, *45*, 346–357. https://doi.org/10.1016/j.immuni.2016.07.014

Kruk, M. E., Gage, A. D., Joseph, N. T., Danaei, G., Garcia-Saiso, S., & Salomon, J. A. (2018). Mortality due to low-quality health systems in the universal health coverage era: A systematic analysis of amenable deaths in 137 countries. *Lancet*, *392*(10160), 2203–2212.

Kruk, M., Wardziak, Ł., Mintz, G. S., Achenbach, S., Pręgowski, J., Rużyłło, W., Dzielińska, Z., Demkow, M., Witkowski, A., & Kępka, C. (2014). Accuracy of coronary computed tomography angiography vs intravascular ultrasound for evaluation of vessel area. *Journal of Cardiovascular Computed Tomography*, *8*(2), 141–148. https://doi.org/10.1016/j.jcct.2013.12.014

Kubuki, Y., Yamaji, T., Hidaka, T., Kameda, T., Shide, K., & Sekine, M. (2017). TET2 mutation in diffuse large B-cell lymphoma. *J Clin Exp Hematop*, *56*, 145–149. https://doi.org/10.3960/jslrt.56.145

Kumamoto, M., Nakashima, Y., & Sueishi, K. (1995). Intimal neovascularization in human coronary atherosclerosis: Its origin and pathophysiological significance. *Human Pathology*, *26*(4), 450–456. https://doi.org/10.1016/0046-8177(95)90148-5

Kumar, P. (2020). Clonal Hematopoiesis of Indeterminate Potential and Cardiovascular Disease. *Curr Oncol Rep*, *22*(9), 87.

Kunimoto, H., Fukuchi, Y., Sakurai, M., Sadahira, K., Ikeda, Y., & Okamoto, S. (2012). Tet2 disruption leads to enhanced self-renewal and altered differentiation of fetal liver hematopoietic stem cells. *Sci Rep*, *2*(273). https://doi.org/10.1038/srep00273

Kyaw, T. (2013). Cytotoxic and Proinflammatory CD8+ T Lymphocytes Promote Development of Vulnerable Atherosclerotic Plaques in ApoE-Deficient Mice. *Circulation*, *127*. https://doi.org/10.1161/CIRCULATIONAHA.112.001347.

Kyaw, T., Tay, C., Krishnamurthi, S., Kanellakis, P., Agrotis, A., & Tipping, P. (2011). B1a B lymphocytes are atheroprotective by secreting natural IgM that increases IgM deposits and reduces necrotic cores in atherosclerotic lesions. *Circ Res*, *109*, 830–840. https://doi.org/10.1161/CIRCRESAHA.111.248542

Kyaw, T., Tipping, P., Bobik, A., & Toh, B. H. (2012). Protective role of natural IgM-producing B1a cells in atherosclerosis. *Trends Cardiovasc Med*, *22*, 48–53. https://doi.org/10.1016/j.tcm.2012.06.011

L, B., M, S., L, L., JM, R., I, C.-O., & F, R. (2015). Production of anti-LPS IgM by B1a B cells depends on IL-1β and is protective against lung infection with Francisella tularensis LVS. *PloS Pathog*, *11:e1004706*. https://doi.org/10.1371/journal.ppat.1004706

Langmead, B., Trapnell, C., Pop, M., & Salzberg, S. L. (2009). Ultrafast and memory-efficient alignment of short DNA sequences to the human genome. *Genome Biology*, *10*(3), R25. https://doi.org/10.1186/gb-2009-10-3-r25

Lee, H. G., Lee, J. U., Kim, D. H., Lim, S., Kang, I., & Choi, J. M. (2019). Pathogenic function of bystander-activated memory-like CD4(+) T cells in autoimmune encephalomyelitis. *Nat Commun*, *10*(1).

Leone, G., Teofili, L., Leone, G., Voso, M. T., Teofili, L., Lübbert, M., Voso, M. T., & Lübbert, M. (2002). DNA methylation and demethylating drugs in myelodysplastic syndromes and secondary leukemias. *Haematologica*. https://doi.org/null

Lewis, M. J. (2009). Immunoglobulin M is required for protection against atherosclerosis in low-density lipoprotein receptor-deficient mice. *Circulation*, *120*(5), 417–426.

Li, H., & Durbin, R. (2009). Fast and accurate short read alignment with Burrows–Wheeler transform. *Bioinformatics*, *25*(14), 1754–1760. https://doi.org/10.1093/bioinformatics/btp324

Li, J. (2016). CCR5+T-bet+FoxP3+ effector CD4 T cells drive atherosclerosis. *Circ. Res.*, *118*. https://doi.org/10.1161/CIRCRESAHA.116.308648

Li, J., McArdle, S., Gholami, A., Kimura, T., Wolf, D., Gerhardt, T., Miller, J., Weber, C., & Ley, K. (2016). CCR5 $^{+}$ T-bet $^{+}$ FoxP3 $^{+}$ Effector CD4 T Cells Drive Atherosclerosis. *Circulation Research*, *118*(10), 1540–1552. https://doi.org/10.1161/CIRCRESAHA.116.308648

Li, R., Zhou, Y., Cao, Z., Liu, L., Wang, J., & Chen, Z. (2018). TET2 loss dysregulates the behavior of bone marrow mesenchymal stromal cells and accelerates tet2(-/-)-driven myeloid Malignancy progression. *Stem Cell Rep*, *10*, 166–179. https://doi.org/10.1016/j.stemcr.2017.11.019

Li, Z. (2011). Deletion of Tet2 in mice leads to dysregulated hematopoietic stem cells and subsequent development of myeloid malignancies. *Blood*, *118*(17), 4509–4518.

Li, Z., Cai, X., Cai, C. L., Wang, J., Zhang, W., & Petersen, B. E. (2011). Deletion of Tet2 in mice leads to dysregulated hematopoietic stem cells and subsequent development of myeloid Malignancies. *Blood*, *118*, 4509–4518. https://doi.org/10.1182/blood-2010-12-325241

Liao, Y., Smyth, G. K., & Shi, W. (2014). featureCounts: An efficient general purpose program for assigning sequence reads to genomic features. *Bioinformatics*, *30*, 923–930. https://doi.org/10.1093/bioinformatics/btt656

Libby, P. (2017). Interleukin-1 Beta as a Target for Atherosclerosis Therapy: Biological Basis of CANTOS and Beyond. *J Am Coll Cardiol*, *70*(18), 2278–2289.

Libby, P., & Ebert, B. L. (2018). CHIP (Clonal Hematopoiesis of Indeterminate Potential): Potent and Newly Recognized Contributor to Cardiovascular Risk. *Circulation*, *138*(7), 666–668.

Lin, Y. (2013). Circulating Th22 and Th9 levels in patients with acute coronary syndrome. *Mediators Inflamm.*, *2013*.

Lio, C. J., Shukla, V., Samaniego-Castruita, D., Gonzalez-Avalos, E., Chakraborty, A., & Yue, X. (2019). TET enzymes augment activation-induced deaminase (AID) expression via 5-hydroxymethylcytosine modifications at the Aicda superenhancer. *Sci Immunol*, 4. https://doi.org/10.1126/sciimmunol.aau7523

Lio, C.-W., Zhang, J., González-Avalos, E., Hogan, P. G., Chang, X., & Rao, A. (2016). Tet2 and Tet3 cooperate with B-lineage transcription factors to regulate DNA modification and chromatin accessibility. *eLife*, *5*, e18290. https://doi.org/10.7554/eLife.18290

Liu, K. J., Zelazowska, M. A., & McBride, K. M. (2023). The longitudinal analysis of convergent antibody VDJ regions in SARS-coV-2-positive patients using RNA-seq. *Viruses*, *15*(1253). https://doi.org/10.3390/v15061253

Liu, Y., Beyer, A., & Aebersold, R. (2016). On the Dependency of Cellular Protein Levels on mRNA Abundance. *Cell*, *165*(3), 535–550. https://doi.org/10.1016/j.cell.2016.03.014

Liuzzo, G. (2000). Monoclonal T-Cell Proliferation and Plaque Instability in Acute Coronary Syndromes. *Circulation*, *101*. https://doi.org/10.1161/01.CIR.101.25.2883.

Loppnow, H., & Libby, P. (1990). Proliferating or interleukin 1-activated human vascular smooth muscle cells secrete copious interleukin 6. *J Clin Invest*, *85*(3), 731–738.

Love, M. I., Huber, W., & Anders, S. (2014). Moderated estimation of fold change and dispersion for RNA-seq data with DESeq2. *Genome Biol*, *15*(550). https://doi.org/10.1186/s13059-014-0550-8

Maganto-García, E., Tarrio, M. L., Grabie, N., Bu, D., & Lichtman, A. H. (2011). Dynamic Changes in Regulatory T Cells Are Linked to Levels of Diet-Induced Hypercholesterolemia. *Circulation*, *124*(2), 185–195. https://doi.org/10.1161/CIRCULATIONAHA.110.006411

Mailer, R. K. W. (2017). Hypercholesterolemia Induces Differentiation of Regulatory T Cells in the Liver. *Circ. Res*, *120*. https://doi.org/10.1161/CIRCRESAHA.116.310054.

Major, A. S., Wilson, M. T., McCaleb, J. L., Ru Su, Y., Stanic, A. K., Joyce, S., Van Kaer, L., Fazio, S., & Linton, M. F. (2004). Quantitative and Qualitative Differences in Proatherogenic NKT Cells in Apolipoprotein E–Deficient Mice. *Arteriosclerosis, Thrombosis, and Vascular Biology*, *24*(12), 2351–2357. https://doi.org/10.1161/01.ATV.0000147112.84168.87

Mallat, Z. (2003). Induction of a Regulatory T Cell Type 1 Response Reduces the Development of Atherosclerosis in Apolipoprotein E-Knockout Mice. *Circulation*, *108*. https://doi.org/10.1161/01.CIR.0000089083.61317.A1.

Markousis-Mavrogenis, G., Tromp, J., Ouwerkerk, W., Devalaraja, M., Anker, S. D., & Cleland, J. G. (2019). The clinical significance of interleukin-6 in heart failure: Results from the BIOSTAT-CHF study. *Eur J Heart Fail*, *21*(8), 965–973.

McHeyzer-Williams, L. J., & McHeyzer-Williams, M. G. (2005). ANTIGEN-SPECIFIC MEMORY B CELL DEVELOPMENT. *Annual Review of Immunology*, *23*(Volume 23, 2005), 487–513. https://doi.org/10.1146/annurev.immunol.23.021704.115732

McKean, D. J., Huntoon, C., & Bell, M. (1994). Ligand-induced desensitization of interleukin 1 receptor-initiated intracellular signaling events in T helper lymphocytes. *J Exp Med*, *180*(4), 1321–1328.

Meeuwsen, J. A. L., van Duijvenvoorde, A., Gohar, A., Kozma, M. O., van de Weg, S. M., Gijsberts, C. M., Haitjema, S., Björkbacka, H., Fredrikson, G. N., de Borst, G. J., den Ruijter, H. M., Pasterkamp, G., Binder, C. J., Hoefer, I. E., & de Jager, S. C. A. (2017). High Levels of (Un)Switched Memory B Cells Are Associated With Better Outcome in Patients With Advanced Atherosclerotic Disease. *Journal of the American Heart Association*, *6*(9). https://doi.org/10.1161/jaha.117.005747

Merhi-Soussi, F., Kwak, B. R., Magne, D., Chadjichristos, C., Berti, M., & Pelli, G. (2005). Interleukin-1 plays a major role in vascular inflammation and atherosclerosis in male apolipoprotein E-knockout mice. *Cardiovasc Res*, *66*(3), 583–593.

Miller, Y. I., Choi, S.-H., Wiesner, P., Fang, L., Harkewicz, R., & Hartvigsen, K. (2011). Oxidation-specific epitopes are danger-associated molecular patterns recognized by pattern recognition receptors of innate immunity. *Circ Res*, *108*, 235–248. https://doi.org/10.1161/CIRCRESAHA.110.223875

Min, J. K., Shaw, L. J., Devereux, R. B., Okin, P. M., Weinsaft, J. W., Russo, D. J., Lippolis, N. J., Berman, D. S., & Callister, T. Q. (2007). Prognostic Value of Multidetector Coronary Computed Tomographic Angiography for Prediction of All-Cause Mortality. *Journal of the American College of Cardiology*, *50*(12), 1161–1170. https://doi.org/10.1016/j.jacc.2007.03.067

Min, K.-B., & Min, J.-Y. (2019). Risk of Cardiovascular Mortality in Relation to Increased Total Serum IgE Levels in Older Adults: A Population-Based Cohort Study. *International Journal of Environmental Research and Public Health*, *16*(22), Article 22. https://doi.org/10.3390/ijerph16224350

Mohlenkamp, S., Lehmann, N., Moebus, S., Schmermund, A., Dragano, N., & Stang, A. (2011). Quantification of coronary atherosclerosis and inflammation to predict coronary events and all-cause mortality. *J Am Coll Cardiol*, *57*(13), 1455–1464.

Montecino-Rodriguez, E., & Dorshkind, K. (2012). B-1 B cell development in the fetus and adult. *Immunity*, *36*(1), 13–21. https://doi.org/10.1016/j.immuni.2011.11.017

Montecino-Rodriguez, E., Leathers, H., & Dorshkind, K. (2006). Identification of a B-1 B cell-specified progenitor. *Nature Immunology*, *7*(3), 293–301. https://doi.org/10.1038/ni1301

Moore, K. J., & Tabas, I. (2011). Macrophages in the Pathogenesis of Atherosclerosis. *Cell*, *145*(3), 341–355. https://doi.org/10.1016/j.cell.2011.04.005

Mor, A., Luboshits, G., Planer, D., Keren, G., & George, J. (2006). Altered status of CD4+CD25+ regulatory T cells in patients with acute coronary syndromes. *European Heart Journal*, *27*(21), 2530–2537. https://doi.org/10.1093/eurheartj/ehl222

Moran-Crusio, K., Reavie, L., Shih, A., Abdel-Wahab, O., Ndiaye-Lobry, D., & Lobry, C. (2011). Tet2 loss leads to increased hematopoietic stem cell self-renewal and myeloid transformation. *Cancer Cell*, *20*, 11–24. https://doi.org/10.1016/j.ccr.2011.06.001

Mouly, E., Ghamlouch, H., Della-Valle, V., Scourzic, L., Quivoron, C., & Roos-Weil, D. (2018). B-cell tumor development in Tet2-deficient mice. *Blood Adv*, *2*, 703–714. https://doi.org/10.1182/bloodadvances.2017014118

Nabbout, R., & Kuchenbuch, M. (2020). Impact of predictive, preventive and precision medicine strategies in epilepsy. *Nature Reviews Neurology*, *16*(12), 674–688. https://doi.org/10.1038/s41582-020-0409-4

Nakai, Y. (2004). Natural killer T cells accelerate atherogenesis in mice. *Blood*, *104*(7), 2051–2059. https://doi.org/10.1182/blood-2003-10-3485

Nakajima, H., & Kunimoto, H. (2014). TET2 as an epigenetic master regulator for normal and malignant hematopoiesis. *Cancer Science*, *105*(9), 1093–1099. https://doi.org/10.1111/cas.12484

Nguyen, T. T., & Baumgarth, N. (2016). Natural igM and the development of B cell-mediated autoimmune diseases. *Crit Rev Immunol*, *36*, 163–177. https://doi.org/10.1615/CritRevImmunol.v36.i2

Nidorf, S. M., Eikelboom, J. W., Budgeon, C. A., & Thompson, P. L. (2013). Low-dose colchicine for secondary prevention of cardiovascular disease. *J Am Coll Cardiol*, *61*(4), 404–410.

Nielsen, M. M., Witherden, D. A., & Havran, W. L. (2017). Γδ T cells in homeostasis and host defence of epithelial barrier tissues. *Nature Reviews Immunology*, *17*(12), 733–745. https://doi.org/10.1038/nri.2017.101

Niwa, T., Wada, H., Ohashi, H., Iwamoto, N., Ohta, H., Kirii, H., Fujii, H., Saito, K., & Seishima, M. (2004). Interferon-γ Produced by Bone Marrow-derived Cells Attenuates Atherosclerotic Lesion Formation in LDLR-deficient Mice. *Journal of Atherosclerosis and Thrombosis*, *11*(2), 79–87. https://doi.org/10.5551/jat.11.79

Nowicka, M., Krieg, C., Crowell, H. L., Weber, L. M., Hartmann, F. J., Guglietta, S., Becher, B., Levesque, M. P., & Robinson, M. D. (2019). *CyTOF workflow: Differential discovery in high-throughput high-dimensional cytometry datasets* (6:748). F1000Research. https://doi.org/10.12688/f1000research.11622.3

Nus, M., Sage, A. P., Lu, Y., Masters, L., Lam, B. Y. H., Newland, S., Weller, S., Tsiantoulas, D., Raffort, J., Marcus, D., Finigan, A., Kitt, L., Figg, N., Schirmbeck, R., Kneilling, M., Yeo, G. S. H., Binder, C. J., de la Pompa, J. L., & Mallat, Z. (2017). Marginal zone B cells control the response of follicular helper T cells to a high-cholesterol diet. *Nature Medicine*, *23*(5), 601–610. https://doi.org/10.1038/nm.4315

Oikonomou, E., Schottlander, D., Antonopoulos, A., Marwan, M., Kotanidis, C., Kluner, L., Shirodaria, C., Channon, K., Neubauer, S., Desai, M., Deanfield, J., Achenbach, S., & Antoniades, C. (2021). Standardised quantification of coronary inflammation using cardiac computed tomography: The Fat Attenuation Index Score (FAI-Score). *European Journal of Preventive Cardiology*, *28*(Supplement_1), zwab061.451. https://doi.org/10.1093/eurjpc/zwab061.451

Olson, N. C., Doyle, M. F., Jenny, N. S., Huber, S. A., Psaty, B. M., & Kronmal, R. A. (2013). Decreased naive and increased memory CD4(+) T cells are associated with subclinical atherosclerosis: The multi-ethnic study of atherosclerosis. *PLoS One*, *8*(8).

Orecchioni, M., Ghosheh, Y., Pramod, A. B., & Ley, K. (2019). Macrophage Polarization: Different Gene Signatures in M1(LPS+) vs. Classically and M2(LPS–) vs. Alternatively Activated Macrophages. *Frontiers in Immunology*, *10*. https://doi.org/10.3389/fimmu.2019.01084

Owen, D. R. J., Lindsay, A. C., Choudhury, R. P., & Fayad, Z. A. (2011). Imaging of Atherosclerosis. *Annual Review of Medicine*, *62*, 25–40. https://doi.org/10.1146/annurev-med-041709-133809

Pahwa, R., & Island, J. I. A. S. T. (2023).

Pahwa, R., & Jialal, I. (2024). Atherosclerosis. In *StatPearls*. StatPearls Publishing. http://www.ncbi.nlm.nih.gov/books/NBK507799/

Palinski, W., Miller, E., & Witztum, J. L. (1995). Immunization of low density lipoprotein (LDL) receptor-deficient rabbits with homologous malondialdehyde-modified LDL reduces atherogenesis. *Proc Natl Acad Sci U.S.A*, *92*, 821–825. https://doi.org/10.1073/pnas.92.3.821

Pan, F., Weeks, O., Yang, F.-C., & Xu, M. (2015). The TET2 interactors and their links to hematological malignancies. *IUBMB Life*, *67*(6), 438–445. https://doi.org/10.1002/iub.1389

Pan, F., Wingo, T. S., Zhao, Z., Gao, R., Makishima, H., & Qu, G. (2017). Tet2 loss leads to hypermutagenicity in haematopoietic stem/progenitor cells. *Nat Commun*, *8*(15102). https://doi.org/10.1038/ncomms15102

Papac-Milicevic, N., Busch, C. J., & Binder, C. J. (2016). Malondialdehyde epitopes as targets of immunity and the implications for atherosclerosis. *Adv Immunol*, *131*, 1–59. https://doi.org/10.1016/bs.ai.2016.02.001

Paramo Fernandez, J. A. (2018). Atherosclerosis and clonal hematopoyesis: A new risk factor. *Clin Investig Arterioscler*, *30*(3), 133–136.

Parisi, V., Petraglia, L., Cabaro, S., D'Esposito, V., Bruzzese, D., & Ferraro, G. (2020). Imbalance Between Interleukin-1beta and Interleukin-1 Receptor Antagonist in Epicardial Adipose Tissue Is Associated With Non ST-Segment Elevation Acute Coronary Syndrome. *Front Physiol*, *11*(42).

Pattarabanjird, T., Li, C., & McNamara, C. (2021). B Cells in Atherosclerosis: Mechanisms and Potential Clinical Applications. *JACC: Basic to Translational Science*, *6*(6), 546–563. https://doi.org/10.1016/j.jacbts.2021.01.006

Pattarabanjird, T., Marshall, M., Upadhye, A., Srikakulapu, P., Garmey, J. C., & Haider, A. (2022). B-1b cells possess unique bHLH-driven P62-dependent self-renewal and atheroprotection. *Circ Res*, *130*, 981–993. https://doi.org/10.1161/CIRCRESAHA.121.320436

Paul, V. S. V. (2016). Quantification of various inflammatory cells in advanced atherosclerotic plaques. *J. Clin. Diagn. Res.*, *10*.

Pedersen, C. B., Dam, S. H., Barnkob, M. B., Leipold, M. D., Purroy, N., & Rassenti, L. Z. (2022). cyCombine allows for robust integration of single-cell cytometry datasets within and across technologies. *Nat Commun*, *13*(1).

Peng, K., Nowicki, T. S., Campbell, K., Vahed, M., Peng, D., & Meng, Y. (2023). Rigorous benchmarking of T-cell receptor repertoire profiling methods for cancer RNA sequencing. *Briefings Bioinf*, 24. https://doi.org/10.1093/bib/bbad220

Peng, L., Mao, F., Zhao, Y., Wang, T., Chen, N., Zhang, J., Cheng, P., Li, W., Lv, Y., Teng, Y., Guo, G., Luo, P., Chen, W., Zou, Q., & Zhuang, Y. (2016). Altered phenotypic and functional characteristics of CD3+CD56+ NKT-like cells in human gastric cancer. *Oncotarget*, *7*(34), 55222–55230. https://doi.org/10.18632/oncotarget.10484

Peterson, V. M., Zhang, K. X., Kumar, N., Wong, J., Li, L., Wilson, D. C., Moore, R., McClanahan, T. K., Sadekova, S., & Klappenbach, J. A. (2017). Multiplexed quantification of proteins and transcripts in single cells. *Nature Biotechnology*, *35*(10), 936–939. https://doi.org/10.1038/nbt.3973

Prabahar, A., Zamora, R., Barclay, D., Yin, J., Ramamoorthy, M., Bagheri, A., Johnson, S. A., Badylak, S., Vodovotz, Y., & Jiang, P. (2024). Unraveling the complex relationship between mRNA and protein abundances: A machine learning-based approach for imputing protein levels from RNA-seq data. *NAR Genomics and Bioinformatics*, *6*(1), lqae019. https://doi.org/10.1093/nargab/lqae019

Prohaska, T. A., Que, X., Diehl, C. J., Hendrikx, S., Chang, M. W., Jepsen, K., Glass, C. K., Benner, C., & Witztum, J. L. (2018). Massively parallel sequencing of peritoneal and splenic B cell repertoires highlights unique properties of B-1 cell antibodies. *Journal of Immunology (Baltimore, Md. : 1950)*, *200*(5), 1702–1717. https://doi.org/10.4049/jimmunol.1700568

Qu, Y., Dang, S., Qu, Y., Dang, S., Hou, P., & Hou, P. (2013). Gene methylation in gastric cancer. *Clinica Chimica Acta*. https://doi.org/10.1016/j.cca.2013.05.002

Que, X., Hung, M.-Y., Yeang, C., Gonen, A., Prohaska, T. A., & Sun, X. (2018). Oxidized phospholipids are proinflammatory and proatherogenic in hypercholesterolaemic mice. *Nature*, *558*, 301–306. https://doi.org/10.1038/s41586-018-0198-8

Quek, R. G. W., & Mardekian, J. (2019). Clinical Outcomes, Treatment Patterns, and Health Resource Utilization Among Metastatic Breast Cancer Patients with Germline BRCA1/2 Mutation: A Real-World Retrospective Study. *Advances in Therapy*, *36*(3), 708–720. https://doi.org/10.1007/s12325-018-0867-x

Quivoron, C. (2011). TET2 inactivation results in pleiotropic hematopoietic abnormalities in mouse and is a recurrent event during human lymphomagenesis. *Cancer Cell*, *20*(1), 25–38.

Raj, A., & Oudenaarden, A. van. (2008). Nature, Nurture, or Chance: Stochastic Gene Expression and Its Consequences. *Cell*, *135*(2), 216–226. https://doi.org/10.1016/j.cell.2008.09.050

Rasmussen, K. D., & Helin, K. (2016). Role of TET enzymes in DNA methylation, development, and cancer. *Genes & Development*, *30*(7), 733–750. https://doi.org/10.1101/gad.276568.115

Rasmussen, K. D., Jia, G., Johansen, J. V., Pedersen, M. T., Rapin, N., & Bagger, F. O. (2015). Loss of TET2 in hematopoietic cells leads to DNA hypermethylation of active enhancers and induction of leukemogenesis. *Genes Dev*, *29*, 910–922. https://doi.org/10.1101/gad.260174.115

Rattik, S., Hultman, K., Rauch, U., Söderberg, I., Sundius, L., Ljungcrantz, I., Hultgårdh-Nilsson, A., Wigren, M., Björkbacka, H., Fredrikson, G. N., & Nilsson, J. (2015). IL-22 affects

smooth muscle cell phenotype and plaque formation in apolipoprotein E knockout mice. *Atherosclerosis*, *242*(2), 506–514. https://doi.org/10.1016/j.atherosclerosis.2015.08.006

Ravandi, A., Boekholdt, S. M., Mallat, Z., Talmud, P. J., Kastelein, J. J., & Wareham, N. J. (2011). Relationship of IgG and IgM autoantibodies and immune complexes to oxidized LDL with markers of oxidation and inflammation and cardiovascular events: Results from the EPIC-Norfolk Study. *J Lipid Res*, *52*, 1829–1836. https://doi.org/10.1194/jlr.M015776

Reimegård, J., Tarbier, M., Danielsson, M., Schuster, J., Baskaran, S., Panagiotou, S., Dahl, N., Friedländer, M. R., & Gallant, C. J. (2021). A combined approach for single-cell mRNA and intracellular protein expression analysis. *Communications Biology*, *4*(1), 1–11. https://doi.org/10.1038/s42003-021-02142-w

Ridker, P. M., Devalaraja, M., Baeres, F. M. M., Engelmann, M. D. M., Hovingh, G. K., & Ivkovic, M. (2021). IL-6 inhibition with ziltivekimab in patients at high atherosclerotic risk (RESCUE): A double-blind, randomised, placebo-controlled, phase 2 trial. *Lancet*, *397*(10289), 2060–2069.

Ridker, P. M., Everett, B. M., Thuren, T., MacFadyen, J. G., Chang, W. H., & Ballantyne, C. (2017). Antiinflammatory Therapy with Canakinumab for Atherosclerotic Disease. *N Engl J Med*, *377*(12), 1119–1131.

Ridker, P. M., Libby, P., MacFadyen, J. G., Thuren, T., Ballantyne, C., & Fonseca, F. (2018). Modulation of the interleukin-6 signalling pathway and incidence rates of atherosclerotic events and all-cause mortality: Analyses from the Canakinumab Anti-Inflammatory Thrombosis Outcomes Study (CANTOS. *Eur Heart J*, *39*(38), 3499–3507.

Robinson, M. D., McCarthy, D. J., & Smyth, G. K. (2010). edgeR: A Bioconductor package for differential expression analysis of digital gene expression data. *Bioinformatics*, *26*(1), 139–140. https://doi.org/10.1093/bioinformatics/btp616

Rocha, V. Z., Folco, E. J., Sukhova, G., Shimizu, K., Gotsman, I., Vernon, A. H., & Libby, P. (2008). Interferon-γ, a Th1 Cytokine, Regulates Fat Inflammation. *Circulation Research*, *103*(5), 467–476. https://doi.org/10.1161/CIRCRESAHA.108.177105

Roche-Lestienne, C., Marceau, A., Roche-Lestienne, C., Marceau, A., Labis, E., Labis, E., Nibourel, O., Nibourel, O., Coiteux, V., Coiteux, Coiteux, V., Guilhot, J., Guilhot, J., Legros, L., Legros, L., Nicolini, F.-E., Legros, L., Nicolini, F.-E., Rousselot, P., … Preudhomme, C. (2011). Mutation analysis of TET2, IDH1, IDH2 and ASXL1 in chronic myeloid leukemia. *Leukemia*. https://doi.org/10.1038/leu.2011.139

Roncarolo, M., & Gregori, S. (2008). Is FOXP3 a bona fide marker for human regulatory T cells? *European Journal of Immunology*, *38*(4), 925–927. https://doi.org/10.1002/eji.200838168

Rosa, M., Chignon, A., Li, Z., Boulanger, M. C., Arsenault, B. J., & Bosse, Y. (2019). A Mendelian randomization study of IL6 signaling in cardiovascular diseases, immune-related disorders and longevity. *NPJ Genom Med*, *4*(23).

Rosenfeld, S. M. (2015). B-1b Cells Secrete Atheroprotective IgM and Attenuate Atherosclerosis. *Circ Res*, *117*(3), 28–39.

Rosenfeld, S. M., Perry, H. M., Gonen, A., Prohaska, T. A., Srikakulapu, P., & Grewal, S. (2015). B-1b cells secrete atheroprotective igM and attenuate atherosclerosis. *Circ Res*, *117:e28–39*. https://doi.org/10.1161/CIRCRESAHA.117.306044

Rosikiewicz, W., Chen, X., Dominguez, P. M., Ghamlouch, H., Aoufouchi, S., & Bernard, O. A. (2020). TET2 deficiency reprograms the germinal center B cell epigenome and silences genes linked to lymphomagenesis. *Sci Adv*, 6 5872. https://doi.org/10.1126/sciadv.aay5872

Ryu, H., Lim, H., Choi, G., Park, Y.-J., Cho, M., Na, H., Ahn, C. W., Kim, Y. C., Kim, W.-U., Lee, S.-H., & Chung, Y. (2018). Atherogenic dyslipidemia promotes autoimmune follicular

helper T cell responses via IL-27. *Nature Immunology*, *19*(6), 583–593. https://doi.org/10.1038/s41590-018-0102-6

Sage, A. P., Tsiantoulas, D., Binder, C. J., & Mallat, Z. (2019). The role of B cells in atherosclerosis. *Nature Reviews Cardiology*, *16*(3), 180–196. https://doi.org/10.1038/s41569-018-0106-9

Saigusa, R., Winkels, H., & Ley, K. (2020). T cell subsets and functions in atherosclerosis. *Nat Rev Cardiol*, *17*(7), 387–401.

San Segundo-Val, I., & Sanz-Lozano, C. S. (2016). Introduction to the Gene Expression Analysis. In M. Isidoro García (Ed.), *Molecular Genetics of Asthma* (pp. 29–43). Springer. https://doi.org/10.1007/978-1-4939-3652-6_3

Sano, S., Oshima, K., Wang, Y., MacLauchlan, S., Katanasaka, Y., & Sano, M. (2018). Tet2-mediated clonal hematopoiesis accelerates heart failure through a mechanism involving the IL-1beta/NLRP3 inflammasome. *J Am Coll Cardiol*, *71*, 875–886. https://doi.org/10.1016/j.jacc.2017.12.037

Schoeler, K., Aufschnaiter, A., Messner, S., Derudder, E., Herzog, S., & Villunger, A. (2019). TET enzymes control antibody production and shape the mutational landscape in germinal centre B cells. *FEBS J*, *286*, 3566–3581. https://doi.org/10.1111/febs.14934

Schrijvers, D. M., De Meyer, G. R. Y., Kockx, M. M., Herman, A. G., & Martinet, W. (2005). Phagocytosis of Apoptotic Cells by Macrophages Is Impaired in Atherosclerosis. *Arteriosclerosis, Thrombosis, and Vascular Biology*, *25*(6), 1256–1261. https://doi.org/10.1161/01.ATV.0000166517.18801.a7

Schuett, H., Oestreich, R., Waetzig, G. H., Annema, W., Luchtefeld, M., & Hillmer, A. (2012). Transsignaling of interleukin-6 crucially contributes to atherosclerosis in mice. *Arterioscler Thromb Vasc Biol*, *32*(2), 281–290.

Seijkens, T. T. P. (2019). Deficiency of the T Cell Regulator Casitas B-Cell Lymphoma-B Aggravates Atherosclerosis by Inducing CD8+ T Cell-Mediated Macrophage Death. *Eur. Heart J*, *40*. https://doi.org/10.1093/eurheartj/ehy714.

Seppo Ylä-Herttuala, Seppo Ylä-Herttuala, Wulf Palinski, Wulf Palinski, Susan Butler, Susan Butler, Sylvie Picard, Sylvie Picard, Daniel Steinberg, Daniel Steinberg, Joseph L. Witztum, & Joseph L. Witztum. (1994). Rabbit and human atherosclerotic lesions contain IgG that recognizes epitopes of oxidized LDL. *Arteriosclerosis, Thrombosis, and Vascular Biology*. https://doi.org/10.1161/01.atv.14.1.32

Sethi, Y., Patel, N., Kaka, N., Kaiwan, O., Kar, J., Moinuddin, A., Goel, A., Chopra, H., & Cavalu, S. (2023). Precision Medicine and the future of Cardiovascular Diseases: A Clinically Oriented Comprehensive Review. *Journal of Clinical Medicine*, *12*(5), Article 5. https://doi.org/10.3390/jcm12051799

Shaw, P. X., Horkko, S., Tsimikas, S., Chang, M. K., Palinski, W., & Silverman, G. J. (2001). Human-derived anti-oxidized LDL autoantibody blocks uptake of oxidized LDL by macrophages and localizes to atherosclerotic lesions in vivo. *Arterioscler Thromb Vasc Biol*, *21*, 1333–1339. https://doi.org/10.1161/hq0801.093587

Sohag, M. M. H., Raqib, S. M., & Akhmad, S. A. (2021). OMICS approaches in cardiovascular diseases: A mini review. *Genomics & Informatics*, *19*(2). https://doi.org/10.5808/gi.21002

Song, L., Cohen, D., Ouyang, Z., Cao, Y., Hu, X., & Liu, X. S. (2021). TRUST4: Immune repertoire reconstruction from bulk and single-cell RNA-seq data. *Nature Methods*, *18*(6), 627–630. https://doi.org/10.1038/s41592-021-01142-2

Song, L., Ouyang, Z., Cohen, D., Cao, Y., Altreuter, J., & Bai, G. (2022). Comprehensive characterizations of immune receptor repertoire in tumors and cancer immunotherapy studies. *Cancer Immunol Res*, *10*, 788–799. https://doi.org/10.1158/2326-6066.CIR-21-0965

Specht, H., Emmott, E., Petelski, A. A., Huffman, R. G., Perlman, D. H., Serra, M., Kharchenko, P., Koller, A., & Slavov, N. (2021). Single-cell proteomic and transcriptomic analysis of macrophage heterogeneity using SCoPE2. *Genome Biology*, *22*(1), 50. https://doi.org/10.1186/s13059-021-02267-5

Spitzer, M. H., & Nolan, G. P. (2016). Mass Cytometry: Single Cells, Many Features. *Cell*, *165*(4), 780–791. https://doi.org/10.1016/j.cell.2016.04.019

Srikakulapu, P., Pattarabanjird, T., Upadhye, A., Bontha, S. V., Osinski, V., Marshall, M. A., Garmey, J., Deroissart, J., Prohaska, T. A., Witztum, J. L., Binder, C. J., Holodick, N. E., Rothstein, T. L., & McNamara, C. A. (2022). B-1b Cells Have Unique Functional Traits Compared to B-1a Cells at Homeostasis and in Aged Hyperlipidemic Mice With Atherosclerosis. *Frontiers in Immunology*, *13*. https://www.frontiersin.org/articles/10.3389/fimmu.2022.909475

Srikakulapu, P., Upadhye, A., Rosenfeld, S. M., Marshall, M. A., McSkimming, C., Hickman, A. W., Mauldin, I. S., Ailawadi, G., Lopes, M. B. S., Taylor, A. M., & McNamara, C. A. (2017). Perivascular Adipose Tissue Harbors Atheroprotective IgM-Producing B Cells. *Frontiers in Physiology*, *8*. https://doi.org/10.3389/fphys.2017.00719

Stall, A. M., Adams, S., Herzenberg, L. A., & Kantor, A. B. (1992). Characteristics and development of the murine B-1b (Ly-1 B sister) cell population. *Ann N Y Acad Sci*, *651*, 33–43. https://doi.org/10.1111/j.1749-6632.1992.tb24591.x

Stark, R., Grzelak, M., & Hadfield, J. (2019). RNA sequencing: The teenage years. *Nature Reviews. Genetics*, *20*(11), 631–656. https://doi.org/10.1038/s41576-019-0150-2

Steinberg, D., & Witztum, J. L. (2010). Oxidized low-density lipoprotein and atherosclerosis. *Arterioscler Thromb Vasc Biol*, *30*, 2311–2316. https://doi.org/10.1161/ATVBAHA.108.179697

Stemme, S., Faber, B., Holm, J., Wiklund, O., Witztum, J. L., & Hansson, G. K. (1995). T lymphocytes from human atherosclerotic plaques recognize oxidized low density lipoprotein. *Proceedings of the National Academy of Sciences*, *92*(9), 3893–3897. https://doi.org/10.1073/pnas.92.9.3893

Stoeckius, M., Hafemeister, C., Stephenson, W., Houck-Loomis, B., Chattopadhyay, P. K., Swerdlow, H., Satija, R., & Smibert, P. (2017). Simultaneous epitope and transcriptome measurement in single cells. *Nature Methods*, *14*(9), 865–868. https://doi.org/10.1038/nmeth.4380

Subramanian, A., Tamayo, P., Mootha, V. K., Mukherjee, S., Ebert, B. L., Gillette, M. A., Paulovich, A., Pomeroy, S. L., Golub, T. R., Lander, E. S., & Mesirov, J. P. (2005). Gene set enrichment analysis: A knowledge-based approach for interpreting genome-wide expression profiles. *Proceedings of the National Academy of Sciences*, *102*(43), 15545–15550. https://doi.org/10.1073/pnas.0506580102

Sun, J., He, X., Zhu, Y., Ding, Z., Dong, H., & Feng, Y. (2018). SIRT1 activation disrupts maintenance of myelodysplastic syndrome stem and progenitor cells by restoring TET2 function. *Cell Stem Cell*, *23*, 355–369. https://doi.org/10.1016/j.stem.2018.07.018

Svensson, E. C., Madar, A., Campbell, C. D., He, Y., Sultan, M., Healey, M. L., Xu, H., D'Aco, K., Fernandez, A., Wache-Mainier, C., Libby, P., Ridker, P. M., Beste, M. T., & Basson, C. T. (2022). TET2-Driven Clonal Hematopoiesis and Response to Canakinumab: An

Exploratory Analysis of the CANTOS Randomized Clinical Trial. *JAMA Cardiology*, *7*(5), 521–528. https://doi.org/10.1001/jamacardio.2022.0386

Tabas, I. (2010). Macrophage death and defective inflammation resolution in atherosclerosis. *Nature Reviews Immunology*, *10*(1), 36–46. https://doi.org/10.1038/nri2675

Tabas, I., & Lichtman, A. H. (2017). Monocyte-Macrophages and T Cells in Atherosclerosis. *Immunity*, *47*(4), 621–634. https://doi.org/10.1016/j.immuni.2017.09.008

Tahiliani, M., Koh, K. P., Tahiliani, M., Shen, Y., Koh, K. P., Pastor, W. A., Shen, Y., Shen, Y., Pastor, W. A., Bandukwala, H. S., Bandukwala, H. S., Brudno, Y., Agarwal, S., Brudno, Y., Agarwal, S., Iyer, L. M., Liu, D. R., Iyer, L. M., Iyer, L. M., … Rao, A. (2009). Conversion of 5-Methylcytosine to 5-Hydroxymethylcytosine in Mammalian DNA by MLL Partner TET1. *Science*. https://doi.org/10.1126/science.1170116

Tajani, A., Sadeghi, M., Omidkhoda, N., Mohammadpour, A. H., Samadi, S., & Jomehzadeh, V. (2024). The association between C-reactive protein and coronary artery calcification: A systematic review and meta-analysis. *BMC Cardiovascular Disorders*, *24*(1), 204. https://doi.org/10.1186/s12872-024-03856-5

Taleb, S., Romain, M., Ramkhelawon, B., Uyttenhove, C., Pasterkamp, G., Herbin, O., Esposito, B., Perez, N., Yasukawa, H., Van Snick, J., Yoshimura, A., Tedgui, A., & Mallat, Z. (2009). Loss of SOCS3 expression in T cells reveals a regulatory role for interleukin-17 in atherosclerosis. *Journal of Experimental Medicine*, *206*(10), 2067–2077. https://doi.org/10.1084/jem.20090545

Tardif, J. C., Kouz, S., Waters, D. D., Bertrand, O. F., Diaz, R., & Maggioni, A. P. (2019). Efficacy and Safety of Low-Dose Colchicine after Myocardial Infarction. *N Engl J Med*, *381*(26), 2497–2505.

Tellides, G., Tereb, D. A., Kirkiles-Smith, N. C., Kim, R. W., Wilson, J. H., Schechner, J. S., Lorber, M. I., & Pober, J. S. (2000). Interferon-γ elicits arteriosclerosis in the absence of leukocytes. *Nature*, *403*(6766), 207–211. https://doi.org/10.1038/35003221

Téo, F. H. (2013). Characterization of CD4+CD28null T Cells in Patients with Coronary Artery Disease and Individuals with Risk Factors for Atherosclerosis. *Cell. Immunol*, *281*. https://doi.org/10.1016/j.cellimm.2013.01.007.

Theriault, S., Dina, C., Messika-Zeitoun, D., Le Scouarnec, S., Capoulade, R., & Gaudreault, N. (2019). Genetic Association Analyses Highlight IL6, ALPL, and NAV1 As 3 New Susceptibility Genes Underlying Calcific Aortic Valve Stenosis. *Circ Genom Precis Med*, *12*(10).

Thomas, P. D., Ebert, D., Muruganujan, A., Mushayahama, T., Albou, L.-P., & Mi, H. (2022). PANTHER: Making genome-scale phylogenetics accessible to all. *Protein Science*, *31*(1), 8–22. https://doi.org/10.1002/pro.4218

Timmis, A., & Roobottom, C. A. (2017). National Institute for Health and Care Excellence updates the stable chest pain guideline with radical changes to the diagnostic paradigm. *Heart*, *103*(13), 982–986. https://doi.org/10.1136/heartjnl-2015-308341

Tomas, L., Katra, P., Badn, W., Andersson, L., Nilsson, J., Schiopu, A., Engelbertsen, D., Gonçalves, I., Bengtsson, E., & Björkbacka, H. (2023). Invariant natural killer T cells and incidence of first-time coronary events: A nested case-control study. *European Heart Journal Open*, *3*(6), oead094. https://doi.org/10.1093/ehjopen/oead094

Tormo, A. J., Letellier, M. C., Sharma, M., Elson, G., Crabe, S., & Gauchat, J. F. (2012). IL-6 activates STAT5 in T cells. *Cytokine*, *60*(2), 575–582.

Tornberg, U. C., & B-1a, H. D. (1995). B-1b and B-2 B cells display unique VHDJH repertoires formed at different stages of ontogeny and under different selection pressures. *EMBO J*, *14*, 1680–1689. https://doi.org/10.1002/embj.1995.14.issue-8

Towne, J. E., Garka, K. E., Renshaw, B. R., Virca, G. D., & Sims, J. E. (2004). Interleukin (IL)-1F6, IL-1F8, and IL-1F9 signal through IL-1Rrp2 and IL-1RAcP to activate the pathway leading to NF-kappaB and MAPKs. *J Biol Chem*, *279*(14), 13677–13688.

Traag, V. A., Waltman, L., & Eck, N. J. (2019). From Louvain to Leiden: Guaranteeing well-connected communities. *Sci Rep*, *9*(1).

Tracy, R. P., Doyle, M. F., Olson, N. C., Huber, S. A., Jenny, N. S., Sallam, R., Psaty, B. M., & Kronmal, R. A. (2013). T-Helper Type 1 Bias in Healthy People Is Associated With Cytomegalovirus Serology and Atherosclerosis: The Multi-Ethnic Study of Atherosclerosis. *Journal of the American Heart Association*, *2*(3). https://doi.org/10.1161/JAHA.113.000117

Trapnell, C., Cacchiarelli, D., Grimsby, J., Pokharel, P., Li, S., Morse, M., Lennon, N. J., Livak, K. J., Mikkelsen, T. S., & Rinn, J. L. (2014). The dynamics and regulators of cell fate decisions are revealed by pseudotemporal ordering of single cells. *Nature Biotechnology*, *32*(4), 381–386. https://doi.org/10.1038/nbt.2859

Trattner, S., Halliburton, S., Thompson, C. M., Xu, Y., Chelliah, A., Jambawalikar, S. R., Peng, B., Peters, M. R., Jacobs, J. E., Ghesani, M., Jang, J. J., Al-Khalidi, H., & Einstein, A. J. (2018). Cardiac-Specific Conversion Factors to Estimate Radiation Effective Dose From Dose-Length Product in Computed Tomography. *JACC: Cardiovascular Imaging*, *11*(1), 64–74. https://doi.org/10.1016/j.jcmg.2017.06.006

Tsao, C. W., Aday, A. W., Almarzooq, Z. I., Anderson, C. A. M., Arora, P., & Avery, C. L. (2023). Heart Disease and Stroke Statistics-2023 Update: A Report From the American Heart Association. *Circulation*, *147*(8).

Tsuji, N., Rothstein, T. L., & Holodick, N. E. (2020). Antigen receptor specificity and cell location influence the diversification and selection of the B-1a cell pool with age. *J Immunol*, *205*, 741–759. https://doi.org/10.4049/jimmunol.1901302

Tupin, E., Nicoletti, A., Elhage, R., Rudling, M., Ljunggren, H.-G., Hansson, G. K., & Berne, G. P. (2004). CD1d-dependent Activation of NKT Cells Aggravates Atherosclerosis. *The Journal of Experimental Medicine*, *199*(3), 417–422. https://doi.org/10.1084/jem.20030997

Twohig, J. P., Cardus Figueras, A., Andrews, R., Wiede, F., Cossins, B. C., & Derrac Soria, A. (2019). Activation of naive CD4(+) T cells re-tunes STAT1 signaling to deliver unique cytokine responses in memory CD4(+) T cells. *Nat Immunol*, *20*(4), 458–470.

Upadhyay, A. A., Kauffman, R. C., Wolabaugh, A. N., Cho, A., Patel, N. B., & Reiss, S. M. (2018). BALDR: a computational pipeline for paired heavy and light chain immunoglobulin reconstruction in single-cell RNA-seq data. *Genome Med*, *10*(20). https://doi.org/10.1186/s13073-018-0528-3

Upadhye, A., Srikakulapu, P., Gonen, A., Hendrikx, S., Perry, H. M., Nguyen, A., McSkimming, C., Marshall, M. A., Garmey, J. C., Taylor, A. M., Bender, T. P., Tsimikas, S., Holodick, N. E., Rothstein, T. L., Witztum, J. L., & McNamara, C. A. (2019). Diversification and CXCR4-Dependent Establishment of the Bone Marrow B-1a Cell Pool Governs Atheroprotective IgM Production Linked to Human Coronary Atherosclerosis. *Circulation Research*, *125*(10), e55–e70. https://doi.org/10.1161/CIRCRESAHA.119.315786

Vallejo, J., Cochain, C., Zernecke, A., & Ley, K. (2021). Heterogeneity of immune cells in human atherosclerosis revealed by scRNA-Seq. *Cardiovascular Research*, cvab260. https://doi.org/10.1093/cvr/cvab260

van Duijn, J., Kritikou, E., Benne, N., van der Heijden, T., van Puijvelde, G. H., Kröner, M. J., Schaftenaar, F. H., Foks, A. C., Wezel, A., Smeets, H., Yagita, H., Bot, I., Jiskoot, W., Kuiper, J., & Slütter, B. (2018). CD8+ T-cells contribute to lesion stabilization in advanced atherosclerosis by limiting macrophage content and CD4+ T-cell responses. *Cardiovascular Research*, *115*(4), 729–738. https://doi.org/10.1093/cvr/cvy261

Van Gassen, S., Callebaut, B., Van Helden, M. J., Lambrecht, B. N., Demeester, P., Dhaene, T., & Saeys, Y. (2015). FlowSOM: Using self-organizing maps for visualization and interpretation of cytometry data. *Cytometry Part A*, *87*(7), 636–645. https://doi.org/10.1002/cyto.a.22625

van Kuijk, K., Kuppe, C., Betsholtz, C., Vanlandewijck, M., Kramann, R., & Sluimer, J. C. (2019). Heterogeneity and plasticity in healthy and atherosclerotic vasculature explored by single-cell sequencing. *Cardiovascular Research*, *115*(12), 1705–1715. https://doi.org/10.1093/cvr/cvz185

van Puijvelde, G., van Wanrooij, E., Hauer, A., de Vos, P., van Berkel, T., & Kuiper, J. (2009). Effect of natural killer T cell activation on initiation of atherosclerosis. *Thrombosis and Haemostasis*, *102*(08), 223–230. https://doi.org/10.1160/TH09-01-0020

van, R. A. R., Shaw, L. J., Xie, J. X., Dimitriu, -Leen Aukelien C., Smit, J. M., Scholte, A. J., van, W. J. M., Callister, T. Q., DeLago, A., Berman, D. S., Hadamitzky, M., Hausleiter, J., Al, -Mallah Mouaz H., Budoff, M. J., Kaufmann, P. A., Raff, G., Chinnaiyan, K., Cademartiri, F., Maffei, E., … Bax, J. J. (2019). Superior Risk Stratification With Coronary Computed

Tomography Angiography Using a Comprehensive Atherosclerotic Risk Score. *JACC: Cardiovascular Imaging*, *12*(10), 1987–1997. https://doi.org/10.1016/j.jcmg.2018.10.024

Vergnes, L., Phan, J., Strauss, M., Tafuri, S., & Reue, K. (2003). Cholesterol and Cholate Components of an Atherogenic Diet Induce Distinct Stages of Hepatic Inflammatory Gene Expression. *Journal of Biological Chemistry*, *278*(44), 42774–42784. https://doi.org/10.1074/jbc.M306022200

Viau, M., Longo, N. S., Lipsky, P. E., & Zouali, M. (2005). Staphylococcal protein a deletes B-1a and marginal zone B lymphocytes expressing human immunoglobulins: An immune evasion mechanism. *J Immunol*, *175*, 7719–7727. https://doi.org/10.4049/jimmunol.175.11.7719

Virtue, A., Wang, H., & Yang, X. F. (2012). MicroRNAs and toll-like receptor/interleukin-1 receptor signaling. *J Hematol Oncol*, *5*(66).

VJ, B., DO, H., A, F., A, H., I, K., & M, C.-A. (2018). IgM anti-malondialdehyde low density lipoprotein antibody levels indicate coronary heart disease and necrotic core characteristics in the Nordic Diltiazem (NORDIL. *Study and the Integrated Imaging and Biomarker Study*, *3*(IBIS-3), 63–72. https://doi.org/10.1016/j.ebiom.2018.08.023

Vromman, A., Ruvkun, V., Shvartz, E., Wojtkiewicz, G., Santos Masson, G., & Tesmenitsky, Y. (2019). Stage-dependent differential effects of interleukin-1 isoforms on experimental atherosclerosis. *Eur Heart J*, *40*(30), 2482–2491.

Vu, D. M. (2014). γδT cells are prevalent in the proximal aorta and drive nascent atherosclerotic lesion progression and neutrophilia in hypercholesterolemic mice. *PLoS One*, *9*.

Wainstein, M. V., Mossmann, M., Araujo, G. N., Goncalves, S. C., Gravina, G. L., & Sangalli, M. (2017). Elevated serum interleukin-6 is predictive of coronary artery disease in

intermediate risk overweight patients referred for coronary angiography. *Diabetol Metab Syndr*, *9*(67).

Wal, A. C., Das, P. K., Bentz van de Berg, D., Loos, C. M., & Becker, A. E. (1989). Atherosclerotic lesions in humans. In situ immunophenotypic analysis suggesting an immune mediated response. *Lab. Invest.*, *61*.

Walsh, C. P., Walsh, C. P., Gl, X., & Xu, G. (2006). Cytosine methylation and DNA repair. *Current Topics in Microbiology and Immunology*. https://doi.org/10.1007/3-540-31390-7_11

Wang, L., Miyahira, A. K., Simons, D. L., Lu, X., Chang, A. Y., & Wang, C. (2017). IL6 Signaling in Peripheral Blood T Cells Predicts Clinical Outcome in Breast Cancer. *Cancer Res*, *77*(5), 1119–1126.

Wang, X., Ding, X., Yan, J., Lu, Z., Cao, H., Ni, X., & Ying, Y. (2021). STAT5 inhibitor attenuates atherosclerosis via inhibition of inflammation: The role of STAT5 in atherosclerosis. *American Journal of Translational Research*, *13*(3), 1422–1431.

Wang, Y. (2007). Interferon-γ induces human vascular smooth muscle cell proliferation and intimal expansion by phosphatidylinositol 3-kinase–dependent mammalian target of rapamycin raptor complex 1 activation. *Circ. Res.*, *101*. https://doi.org/10.1161/CIRCRESAHA.107.151068

Wang, Y., Liu, J., Burrows, P. D., & Wang, J.-Y. (2020). B Cell Development and Maturation. *Advances in Experimental Medicine and Biology*, *1254*, 1–22. https://doi.org/10.1007/978-981-15-3532-1_1

Weng, N., Akbar, A. N., & Goronzy, J. (2009). CD28− T cells: Their role in the age-associated decline of immune function. *Trends in Immunology*, *30*(7), 306–312. https://doi.org/10.1016/j.it.2009.03.013

Whitman, S. C., Ravisankar, P., Elam, H., & Daugherty, A. (2000). Exogenous Interferon-γ Enhances Atherosclerosis in Apolipoprotein E−/− Mice. *The American Journal of Pathology*, *157*(6), 1819–1824. https://doi.org/10.1016/S0002-9440(10)64820-1

WHO. (n.d.). *Cardiovascular diseases (CVDs)*. Retrieved July 2, 2024, from https://www.who.int/news-room/fact-sheets/detail/cardiovascular-diseases-(cvds)

Wigren, M. (2012). Low Levels of Circulating CD4+FoxP3+ T Cells Are Associated with an Increased Risk for Development of Myocardial Infarction but Not for Stroke. *Arterioscler. Thromb. Vasc. Biol*, *32*. https://doi.org/10.1161/ATVBAHA.112.251579.

Wigren, M. (2019). Lack of Ability to Present Antigens on Major Histocompatibility Complex Class II Molecules Aggravates Atherosclerosis in ApoE−/− Mice. *Circulation*, *139*. https://doi.org/10.1161/CIRCULATIONAHA.118.039288.

William Hollander, William Hollander, William Hollander, William Hollander, Marilyn Colombo, Marilyn Colombo, Barbara Kirkpatrick, Barbara Kirkpatrick, John Paddock, & John Paddock. (1979). Soluble proteins in the human atherosclerotic plaque. With spectral reference to immunoglobulins, C3-complement component, alpha 1-antitrypsin and alpha 2-macroglobulin. *Atherosclerosis*. https://doi.org/10.1016/0021-9150(79)90064-9

Winkels, H., & Wolf, D. (2021). Heterogeneity of T Cells in Atherosclerosis Defined by Single-Cell RNA-Sequencing and Cytometry by Time of Flight. *Arteriosclerosis, Thrombosis, and Vascular Biology*, *41*(2), 549–563. https://doi.org/10.1161/ATVBAHA.120.312137

Witztum, J. L., & Lichtman, A. H. (2014). The influence of innate and adaptive immune responses on atherosclerosis. *Annu Rev Pathol*, *9*, 73–102. https://doi.org/10.1146/annurev-pathol-020712-163936

Wong, J. B., Hewitt, S. L., Heltemes-Harris, L. M., Mandal, M., Johnson, K., & Rajewsky, K. (2019). B-1a cells acquire their unique characteristics by bypassing the pre-BCR selection stage. *Nat Commun*, *10*(4768). https://doi.org/10.1038/s41467-019-12824-z

Wu, H., Wu, H., Zhang, Y., Wu, H., & Zhang, Y. (2014). Reversing DNA Methylation: Mechanisms, Genomics, and Biological Functions. *Cell*. https://doi.org/10.1016/j.cell.2013.12.019

Wu, T., Hu, E., Xu, S., Chen, M., Guo, P., & Dai, Z. (2021). clusterProfiler 4.0: A universal enrichment tool for interpreting omics data. *Innovation (Camb*, *2*(100141). https://doi.org/10.1016/j.xinn.2021.100141

Xia, Q., Xiang, X., Patel, S., Puranik, R., Xie, Q., & Bao, S. (2012). Characterisation of IL-22 and interferon-gamma-inducible chemokines in human carotid plaque. *International Journal of Cardiology*, *154*(2), 187–189. https://doi.org/10.1016/j.ijcard.2011.10.093

Xie, J. J., Wang, J., Tang, T. T., Chen, J., Gao, X. L., & Yuan, J. (2010). The Th17/Treg functional imbalance during atherogenesis in ApoE(-/-) mice. *Cytokine*, *49*(2), 185–193.

Xu, J. L., & Davis, M. M. (2000). Diversity in the CDR3 region of VH is sufficient for most antibody specificities. *Immunity*, *13*, 37–45. https://doi.org/10.1016/S1074-7613(00)00006-6

Xu, Z., Butfiloski, E. J., Sobel, E. S., & Morel, L. (2004). Mechanisms of peritoneal B-1a cells accumulation induced by murine lupus susceptibility locus Sle2. *J Immunol*, *173*, 6050–6058. https://doi.org/10.4049/jimmunol.173.10.6050

Yang, Y., Wang, C., Yang, Q., Kantor, A. B., Chu, H., Ghosn, E. E., Qin, G., Mazmanian, S. K., Han, J., & Herzenberg, L. A. (2015). Distinct mechanisms define murine B cell lineage

immunoglobulin heavy chain (IgH) repertoires. *eLife*, *4*, e09083. https://doi.org/10.7554/eLife.09083

Yoshimoto, M. (2020). The ontogeny of murine B-1a cells. *Int J Hematol*, *111*, 622–627. https://doi.org/10.1007/s12185-019-02787-8

Zegeye, M. M., Lindkvist, M., Falker, K., Kumawat, A. K., Paramel, G., & Grenegard, M. (2018). Activation of the JAK/STAT3 and PI3K/AKT pathways are crucial for IL-6 trans-signaling-mediated pro-inflammatory response in human vascular endothelial cells. *Cell Commun Signal*, *16*(1).

Zhang, K., Huang, X. Z., Li, X. N., Feng, M., Li, L., & Cai, X. J. (2012). Interleukin 6 destabilizes atherosclerotic plaques by downregulating prolyl-4-hydroxylase alpha1 via a mitogen-activated protein kinase and c-Jun pathway. *Arch Biochem Biophys*, *528*(2), 127–133.

Zhang, L., Wang, T., Wang, X., Du, R., Zhang, K., Liu, X., Ma, D., Yu, S., Su, G., Li, Z., Guan, Y., & Du, N. (2013). Elevated Frequencies of Circulating Th22 Cell in Addition to Th17 Cell and Th17/Th1 Cell in Patients with Acute Coronary Syndrome. *PLoS ONE*, *8*(12), e71466. https://doi.org/10.1371/journal.pone.0071466

Zhang, W., Fu, R., Wang, H. Q., Li, L. J., Yue, L. Z., & Liu, H. (2012). TET2 and DLK1 gene expression and their clinical significance in bone marrow CD(3)(+) T cells of patients with myelodysplastic syndrome. *Zhonghua Nei Ke Za Zhi*, *51*, 543–546. https://doi.org/10.3760/cma.j.issn.0578-1426.2012.07.012

Zhang, W., Shao, Z., Fu, R., Wang, H., Li, L., & Liu, H. (2015). Down-regulation of TET2 in CD3(+) and CD34(+) cells of myelodysplastic syndromes and enhances CD34(+) cells proliferation. *Int J Clin Exp Pathol*, *8*, 10840–10846.

Zhang, W., Shao, Z. H., Fu, R., Wang, H. Q., Li, L. J., & Wang, J. (2012). TET2 expression in bone marrow mononuclear cells of patients with myelodysplastic syndromes and its clinical significances. *Cancer Biol Med*, *9*, 34–37. https://doi.org/10.3969/j.issn.2095-3941.2012.01.006

Zhang, W., Tang, T., Nie, D., Wen, S., Jia, C., Zhu, Z., Xia, N., Nie, S., Zhou, S., Jiao, J., Dong, W., Lv, B., Xu, T., Sun, B., Lu, Y., Li, Y., Cheng, L., Liao, Y., & Cheng, X. (2015). IL-9 aggravates the development of atherosclerosis in ApoE-/- mice. *Cardiovascular Research*, *106*(3), 453–464. https://doi.org/10.1093/cvr/cvv110

Zhang, X., Su, J., Jeong, M., Ko, M., Huang, Y., & Park, H. J. (2016). DNMT3A and TET2 compete and cooperate to repress lineage-specific transcription factors in hematopoietic stem cells. *Nat Genet*, *48*, 1014–1023. https://doi.org/10.1038/ng.3610

Zhang, Y., & Lee, T. Y. (2022). Revealing the immune heterogeneity between systemic lupus erythematosus and rheumatoid arthritis based on multi-omics data analysis. *Int J Mol Sci*, 23. https://doi.org/10.3390/ijms23095166

Zhao, H., Zhu, H., Huang, J., Zhu, Y., Hong, M., & Zhu, H. (2018). The synergy of Vitamin C with decitabine activates TET2 in leukemic cells and significantly improves overall survival in elderly patients with acute myeloid leukemia. *Leuk Res*, *66*, 1–7. https://doi.org/10.1016/j.leukres.2017.12.009

Zhao, Z., Chen, L., Dawlaty, M. M., Pan, F., Weeks, O., & Zhou, Y. (2015). Combined loss of tet1 and tet2 promotes B cell, but not myeloid Malignancies, in mice. *Cell Rep*, *13*, 1692–1704. https://doi.org/10.1016/j.celrep.2015.10.037

Zhao, Z., Chen, S., Zhu, X., Pan, F., Li, R., & Zhou, Y. (2016). The catalytic activity of TET2 is essential for its myeloid Malignancy-suppressive function in hematopoietic stem/progenitor cells. *Leukemia*, *30*, 1784–1788. https://doi.org/10.1038/leu.2016.56

Zhou, Y., Zhou, B., Pache, L., Chang, M., Khodabakhshi, A. H., Tanaseichuk, O., Benner, C., & Chanda, S. K. (2019). Metascape provides a biologist-oriented resource for the analysis of systems-level datasets. *Nature Communications*, *10*(1), 1523. https://doi.org/10.1038/s41467-019-09234-6

Zhu, Z. (2018). Function of T Regulatory Type 1 Cells Is Down-Regulated and Is Associated with the Clinical Presentation of Coronary Artery Disease. *Hum. Immunol*, *79*. https://doi.org/10.1016/j.humimm.2018.05.001.

Zunder, E. R., Finck, R., Behbehani, G. K., Amir, E. D., Krishnaswamy, S., Gonzalez, V. D., Lorang, C. G., Bjornson, Z., Spitzer, M. H., Bodenmiller, B., Fantl, W. J., Pe'er, D., & Nolan, G. P. (2015). Palladium-based mass tag cell barcoding with a doublet-filtering scheme and single-cell deconvolution algorithm. *Nature Protocols*, *10*(2), 316–333. https://doi.org/10.1038/nprot.2015.020